Synthesis and Evaluation of Novel Ratiometric Fluorescent Sensors for Cation and Anion Based on Calixarene

September 2011

Division of Energy and Material Science
Graduate School of Science and Engineering
Saga University

Xin-Long Ni

Synthesis and Evaluation of Novel Ratiometric Fluorescent Sensors for Cation and Anion Based on Calixarene

A dissertation presented to the Graduate School of Science and Engineering of Saga University in partial fulfillment of the requirements for the degree of Doctor of Philosophy

September 2011

By

Xin-long Ni

Supervisor:

Professor Dr. Takehiko Yamato

CERTIFICATE OF APPROVAL
Ph.D Dissertation

This is to certify that the Ph.D Dissertation of

Xin-Long Ni

has been approved by the Examining Committee for the dissertation requirement for the Doctor of Philosophy degree in Chemistry at the September, 2011 graduation.

Dissertation committee: _____

Supervisor: Prof. Takehiko Yamato

_____

Member, Prof. Tsugio Kitamura

_____

Member, Prof. Takeshi Hanamoto

_____

Member, Prof. Mishinori Takeshita

ACKNOWLEDGEMENTS

First, I would like to express my deepest gratitude to my supervisor, Professor Takehiko Yamato, for his kind support, invaluable guidance and limitless patience. Without his generous help, this dissertation would be nearly impossible.

I would like to express great appreciate to Professor Tsugio Kitamura, Professor Mishinori Takeshita, and Professor Takeshi Hanamoto and the rest of my thesis committee for their kind cooperation and suggestions. I also wish to convey my sincere thanks to Professor Xi Zeng, Professor Zhu Tao, Professor Sai-Feng Xue and others professor at Guizhou University, China, due to their inspiriting discussions and constant encouragement.

Deep gratitude is extend to all of the members in Yamato Lab. and the others Lab., especially to Dr. Sulfur Rahman, Dr. Jian-Yong Hu, Dr. Arjun Paudel, Dr. Dian Liu, Dr. Jing Jing Liu, Shi Wang, Liu Yi, Bigyan Sharma and Xing Feng, who made my research work more enjoyable. Also I am thankful to all my friends at Saga University for their constant supports in every respect. Special thanks are given to the staffs and faculty in the International Division of Saga University for their acting concerns.

Finally, I would like to express my deeply appreciation to my family for their endless encouragement, understanding and sacrifice. Without their careful assistance, it would not have been possible to complete my doctoral study. I would like to delicate this thesis to my family.

ABSTRACT

Currently, ion recognition and detection by artificial receptors has attracted increasing attention because of the important roles played by ions in both environment and biological systems. Among these detection approaches, fluorescence spectroscopy is widely used because of its high sensitivity, simple application, and low cost. Thus, against this background, several kinds of fluorescent chemosensors for heavy metal ions and anions were designed and synthesized based on calixarene in this dissertation. The sensitivity and selectivity properties of these receptors to the target analyte were carefully evaluated.

Fluorescent chemosensors with pyrenyl-appended triazole based on thiacalix[4]arene were first synthesized. The fluorescence spectra changes suggested that chemosensors fixed by thiacalix[4]arene are highly selective for Ag^{+} over other metal ions by enhancing the monomer emission of pyrene in neutral solution. Then, following the same interest, a new type of fluorescent chemosensor based on homooxacalix[3]arene was developed. The fluorescent sensor was highly selective for Pb^{2+} in comparison with other metal ions tested by enhancement of the monomer emission of pyrene by utilizing the C_3 symmetric structure of homooxacalix[3]arene. Meanwhile, this system exhibited an interesting ratiometric detection signal output for $H_2PO_4^{-}$ through switching the excimer emission of pyrene from the "on-off" to the "off-on" type in neutral organic solution. Fluorescence spectra and ^1H NMR titration results suggested that the Zn^{2+} center provided an excellent pathway of organizing anion binding groups for optimal host–guest interactions.

It is thus believed that the design strategy and the remarkable photophysical properties of these receptors in the present dissertation would have potential application in sensing, detection, and recognition of both cation and anion with different optical signals.

TABLE OF CONTENTS

Chapter 1

Development of Fluorescent Chemosensors Recently Based on Calixarene

In this chapter a shortly review of the recently development of fluorescent receptors for cations and anions based on calixarene are introduced

1.1 General Introduction

Cations and anions recognition by artificial receptors has attracted increasing attention because of the important roles played by ions in both environment and biological systems[1-2]. For example, Heavy metal ions are attracted great attention, not only for the fact that some heavy metal ions play important roles in living systems, but also due to they are very toxic and easy capable of causing serious environmental and health problems.[3-6] Some heavy metal ions, such as Zn(II), Cu(II), Fe(III), Mn(II), Co(II), and Mo(VI), are essential for the maintenance of human metabolism. However, high concentrations of these cations can lead to many adverse health effects.[3-6] It is also a fact that others such as Pb(II), Hg(II), Cd(II), and As(III) are among the most toxic ions known that lack any vital or beneficial effects. Accumulation of these over time in the bodies of humans and animals can lead to serious debilitating illnesses.[4] Therefore; the development of increasingly selective and sensitive methods for the determination of heavy metal ions is currently very important research topic. As a result, many approaches such as atomic absorption, ICP atomic emission, UV-vis absorption, and fluorescence spectroscopy have been employed to detect low limits.[7-10] Among these methods, fluorescence spectroscopy is widely used because of its high sensitivity, facile operation, and low cost.[10] Furthermore, the photophysical properties of a fluorophore can be easily tuned using a range of routes: charge transfer, electron transfer, energy transfer, the influence of the heavy metal ions, and the destabilization of nonemissive n-π^* excited states.[11]

Fluorescent chemosensors for anions and cations have proven efficiency, but those for many heavy metal ions such as Pb(II), Hg(II), Fe(III), Cu(II), and Ag(I) still retain some challenges because these cations often act as fluorescence quenchers. For example, Cu(II) is a typical ion that causes the chemosensor to decrease fluorescent emissions due to quenching of the fluorescence by mechanisms inherent to the paramagnetic species.[12-14] Such decreased emissions are impractical for analytical purposes because of their low signal outputs upon complexation. In addition, temporal separation of spectrally similar complexes by time-resolved fluorimetry is subsequently prevented.[15]

Calixarenes are one of the macrocyclic receptors known to date besides crown ethers, cyclodextrins, cryptands, and cucurbiturils,[16-22] which was introduced by Gustche[23] for cyclic oligomers, which were obtained from the condensation of formaldehyde with *p*-alkylphenols

under alkaline conditions. The use of this word "calix" means "beaker" in Latin and Greek, Figure 1, was suggested in particular by the shape of the tetramer, which can (and generally goes) adopt a bowl- or beaker-like conformation which indicates the possibility of the inclusion of "guest" molecules. Calixarenes are macrocyclic molecules, like crown ether and cyclodextrin.

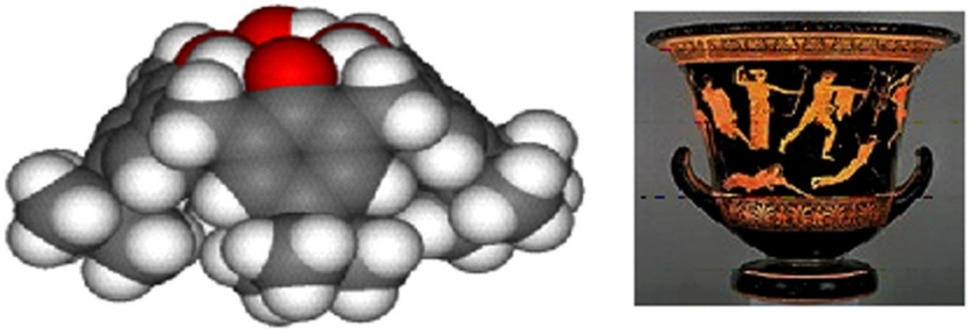

Figure 1. p-tert-Butyl-calix[4]arene resembles a calix crater vase in shape [23].

Calixarenes made up the phenol and methylene units have many conformational isomers because of two possible rotational modes of the phenol unit, shown in Figure 2, the oxygen-through-the annulus rotation and the para-substituent-through-the annulus rotation.

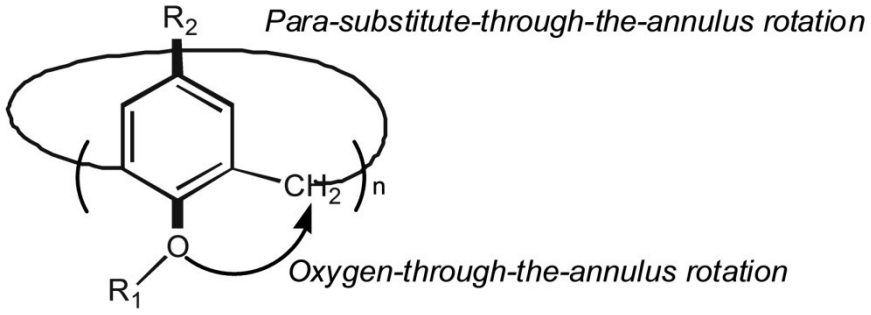

Figure 2. Two different modes for inversion of the phenyl units.

Two regions can be distinguished in calixarenes, *viz.* the phenolic OH groups and the *para* positions of the aromatic rings, which are called respectively the "lower rim" and the "upper

rim" of the calix (both rims can easily be selectively functionalized) as shown in Figure 3. In calix[4]arene, adjacent nuclei have been named "proximal" or (1,2) whereas the opposite ones are in "distal" or diametrical" (1,3) positions.

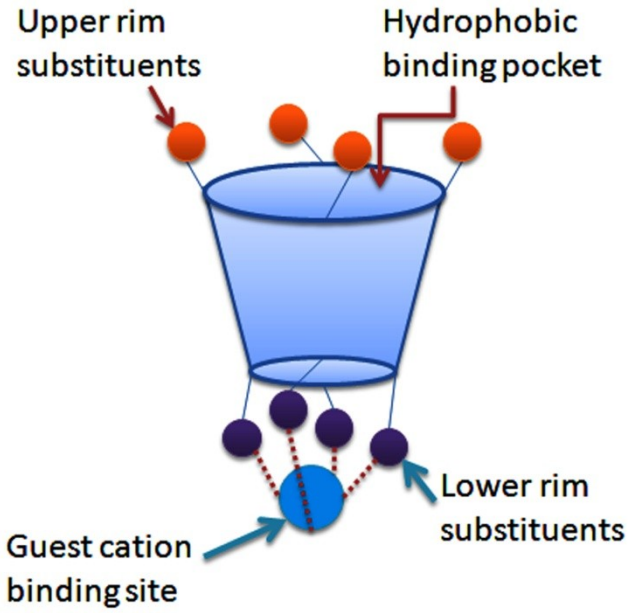

Figure 3. Anatomy of a calix[4]arene in the cone conformation.

One of the most fascinating aspects of calixarenes lies in the variety of conformations which results from the (more or less) free rotation about the σ bonds of Ar-C-Ar groups. In the case of calix[4]arenes, four relative orientations of the phenol units shown in Figure 4 can be assumed. Gustche has introduced the terms "cone", "partial cone", "1,2-*alternate*", and "1,3-*alternate*" which are generally accepted today, to these basis conformation. They differ with respect to the position of the phenolic OH groups (and the *p*-positions) with respect to the molecular plane (here easily define by the C, atoms of the methylene bridges). A reference of plane of the type is also clearly defined in the case of calix[5]arene, but not for larger oligomers: the conformation of the latter has been described in the literature in a correspondingly bewildering manner.

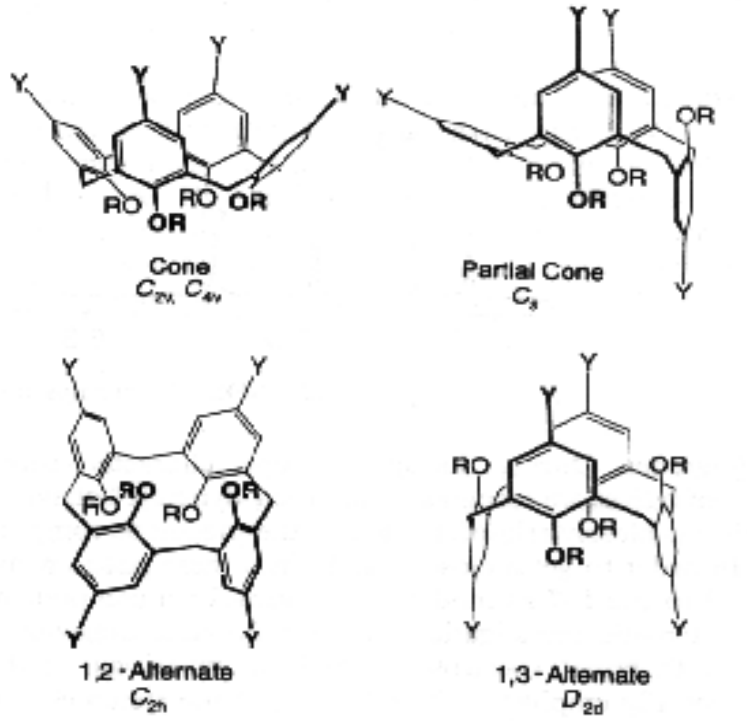

Figure 4. Four stable conformations of calix[4]arenes.

Although each phenol unit can rotate according to the oxygen-through-the annulus rotation mechanism, they favorably adopt a cone conformation because of the stabilization by intramolecular hydrogen-bonding interactions among OH groups.[24] Therefore, the *p-tert*-butylcalix[4]arene adopts C_{4v} symmetry and has a π-basic cavity in the upper rim. The conformation in which calix[4]arene is fixed upon derivation depends on the temperature, the solvent, the base, the *para* substituents of the calixarenes, and the reactivity of the electrophile.

Calixarenes are extremely versatile host framework and, depending on their degree of functionalization, may act as host for cations, anions and neutral molecules, are represented in Figure 5. Cation selectivity and ionophoric activity of calixarene-based receptors and carriers have been shown to depend on several factors, including the ring size of the calixarene skeleton, its conformation and conformation mobility, lipophilicity, the chemical nature (donor ability), spatial arrangement of binding functionalities, and the degree of preorganization of receptor.[25]

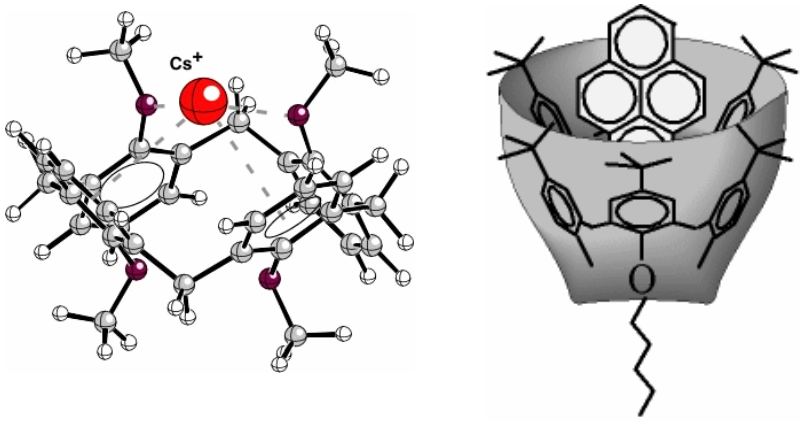

Figure 5. Examples of calixarene-guest complexes.

One of the most important properties of calixarenes is without doubt their ability to include smaller molecules and ions reversibly. Although the parent compounds form inclusion compounds in the solid state with such different guest as arenes(benzene, anisole, pyridine, toluene), acetone, chloroform, acetonitrile, methanol, and water, in solution their derivatives have become important as host molecules of ligands.[26] Chemical modification of calixarenes does not only permit the synthesis of new host molecules by the introduction of additional functional groups, it also allows control of the conformation of calixarenes and hindrance of conformation inversion. In this respect calixarenes are greatly superior to other macrocyclic molecules such as crown ether or cyclodextrins.

Calixarenes of the general structure was constituted with the phenol groups and the bridge methylene linkage. When the methylene groups of the bridge linkage were changed to other functional groups partially or totally, they are composed to the calixarene analogues as shown Figure 6. Homooxacalix[3]arenes represent a new class of macrocyclic receptors analogous to calixarenes[27-29] where small or all methylene bridges between the aromatic rings are resplaced by CH_2OCH_2 moieties. For example, the homocalixarenes with bridge linkage as CH_2CH_2[30] or $CH_2CH_2CH_2$,[31-32] and the hetero analogues as CH_2OCH_2,[33] CH_2SCH_2[34] or CH_2NRCH_2[35-37] as well as the newest cyclic analogues using the S as bridge linkage.[38-40] All of these calixarene analogues have the similar characteristic to that of calixarene. Furthermore, with different bridge linkage, they have special properties brought by these linkage substituents respectively.

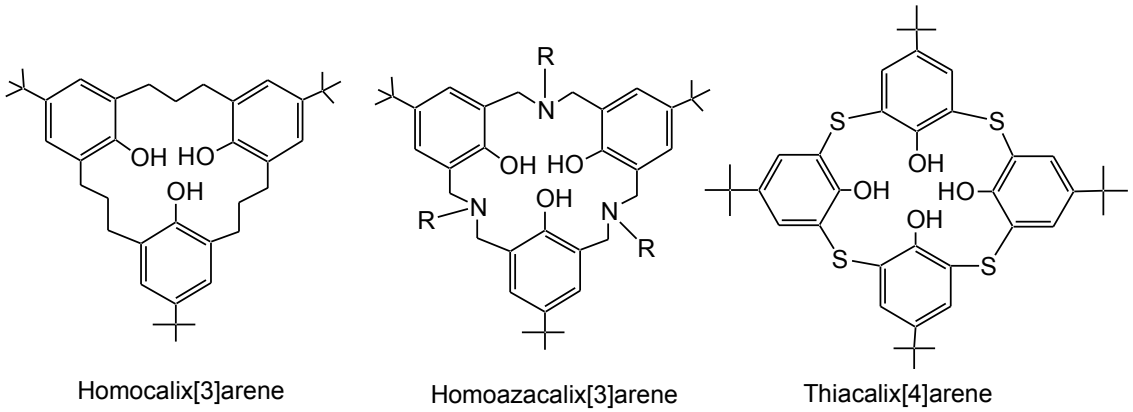

Homocalix[3]arene Homoazacalix[3]arene Thiacalix[4]arene

Figure 6. Calixarene analogues

In the case of oxygenated analogues, named homooxacalixarenes, the relation to calixarenes is not only a formal one, some of these compounds is actually formed together with true calixarenes upon heating of alkaline mixtures of phenols and formaldehyde. Three compounds in this series are relatively well-known materials are presented in Figure 7, while the isolation of a small sample of the pure compound only has been reported in the case of homooxacalix[4]arene.

In comparison with the structural characteristics of the calixarene family, homooxacalix[3]arene is more attractive for the following reasons: (1) Homooxacalix[3]arene has a cavity composed of an 18-membered ring, which is comparable with that of calix[4]arene composed of a 16-membered ring; (2) the rate of ring inversion for

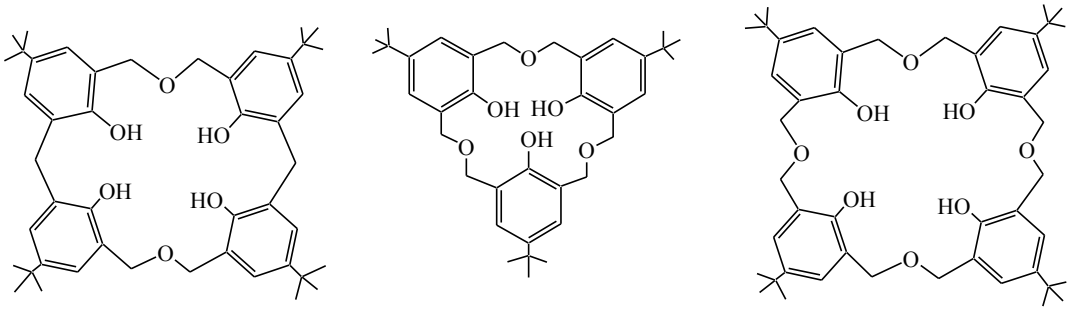

Figure 7. Homooxacalixarenes

homooxacalix[3]arene derivatives should be much faster than that for calix[4]arenes because of the flexibility of the ethereal linkages; (3) there are only two possible conformation, cone and partial-cone, in contrast to four possible conformations in calix[4]arenes, so that the conformational isomerism is much more simplified; (4) ethereal ring oxygens may act cooperatively with phenolic oxygens upon the binding of metal ions; and (5) the basic structure has C_3 symmetry which is expected to be particularly useful for the design of receptors for RNH_3^+.

In another case of sulfur analogues, thiacalix[4]arene Figure 6, the bridge linkage is S instead of the CH_2. In comparison to the structural characteristics of the calixarene family, it is also more attractive for the following reasons: (1) although both thiacalix[4]arene and calix[4]arene are composed of a 16-membered ring, the ring size of thiacalix[4]arene is larger than that of calix[4]arene because of the longer covalent bond length C-S than C-C; (2) because of the larger electron density of covalent bond C-S than that of C-C and the electron lone pairs on S, thiacalix[4]arene has the cavity composed by calix benzene ring with higher π electron density contributed by C-S than calix[4]arene; (3) ring linkage containing sulfurs may act cooperatively with phenolic oxygen upon the binding of metal ions; and (4) because of the potential oxidation of S of the bridge linkage to SO and SO_2, it is possible to modify the linkage and change the properties of cavity formed by calix benzene rings, which is superior to any other calixarenes.

1.2 Photophysics of Fluorescent chemosensors

1.2.1 Principle of fluorescent chemosensor

The Perrin–Jablonski diagram (Figure 8) is convenient for visualizing in a simple way the possible processes: photon absorption, internal conversion, fluorescence, intersystem crossing, phosphorescence, delayed fluorescence and triplet–triplet transitions. The singlet electronic states are denoted S_0 (fundamental electronic state), S_1, S_2,…… and the triplet states, T_1, T_2,……Vibrational levels are associated with each electronic state. Thus, Emission of photons accompanying the $S_1 \rightarrow S_0$ relaxation is called fluorescence. As a consequence of the strong influence of the surrounding medium on fluorescence emission, fluorescent molecules are currently used as probes for the investigation of physicochemical, biochemical

and biological systems, so-called fluorescent probes.

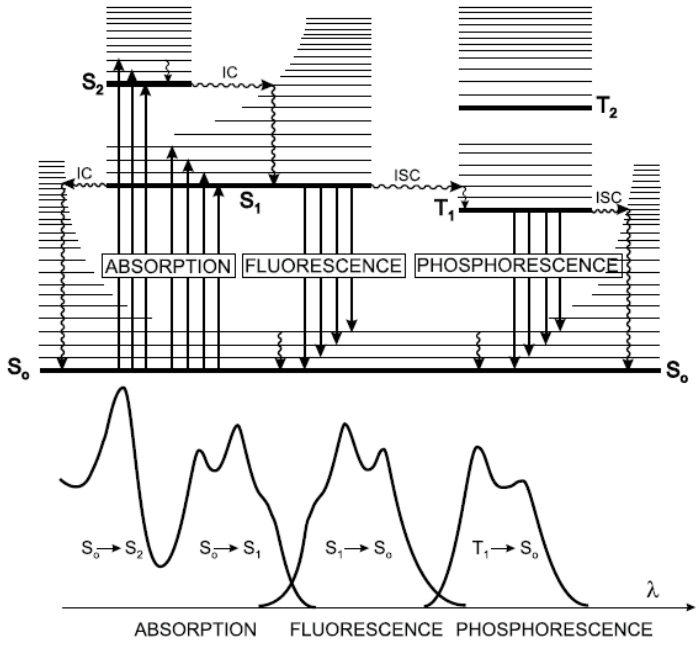

Figure 8. Perrin–Jablonski diagram and illustration of the relative positions of absorption, fluorescence and phosphorescence spectra.

The main issue in the design of any effective chemosensor is the association of a selective molecular recognition event with a physical signal highly sensitive to its occurrence. As shown in Figure 9, an effective fluorescent chemosensor includes an ion recognition unit (ionophore) and a fluorogenic unit (fluorophore), both moieties generally can be independent species or covalently linked by a spacer.[41-42] The ionophore is required for selective binding of the substrate, while the fluorophore provides the means of or inhibition. Mechanisms which control the response of a fluorophore to substrate binding include photoinduced electron transfer (PET),[43-49] photoinduced charge transfer (PCT),[50-58] excimer/exciplex formation or extinction,[59-60] and Fluorescence (FoÖrster) resonance energy transfer (FRET).[61-63]

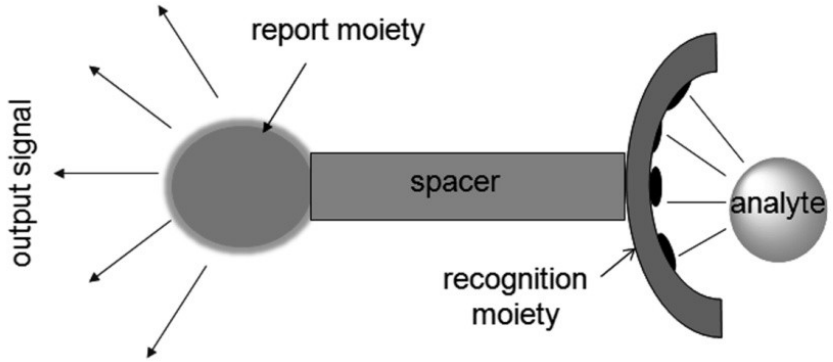

Figure 9. Diagram of an effective fluorescent chemosensor

In that case, Changes in both the absorption and emission of light can be utilized as signals provided appropriate chromophores or fluorophores are available, and two important classes of sensors are those of the optical and fluorimetric types. While spectrophotometry and fluorimetry are both relatively simple techniques which are rapidly performed, nondestructive and suited to multicomponent analysis, fluorimetry is commonly considered superior, principally because of its greater sensitivity.[64-71] Whereas absorbance measurements can at best determine concentrations down to 0.1 μM, fluorescence techniques can accurately measure concentrations 1 million times smaller. An additional advantage of fluorimetry is that discrimination between analytes is possible by timeresolved measurements.[72]

1.2.2 Photoinduced Electron Transfer (PET)

In the simplest cases, emission of a photon, fluorescence, follows HOMO to LUMO excitation of an electron in a molecule. Where this emission is efficient, the molecule may be termed a fluorophore. Vibrational deactivation of the excited state prior to emission usually gives rise to a “Stokes shift” in that the wavelength of the emitted radiation is less than that of the exciting radiation.[73] Various other interactions may also modify the emission process, and these are of considerable importance in regard to analytical applications of fluorescence. Thus, when a lone electron pair is located in an orbital of the fluorophore itself or an adjacent

molecule and the energy of this orbital lies between those of the HOMO and LUMO, efficient electron transfer of one electron of the pair to the hole in the HOMO created by light absorption may occur, followed by transfer of the initially excited electron to the lone pair orbital. Such PET provides a mechanism for nonradiative deactivation of the excited state (Figure 10), leading to a decrease in emission intensity or "quenching" of fluorescence.[43-49]

Fluorescence lost as a result of PET may be recovered if it is possible to involve the lone pair in a bonding interaction. Thus, protonation or binding of a metal ion effectively places the electron pair in an orbital of lower energy and inhibits the electron-transfer process. The excited-state energy may then again be lost by radiative emission. In the case of metal ion binding, this effect is referred to as chelation-enhanced fluorescence (CHEF).[74-75]

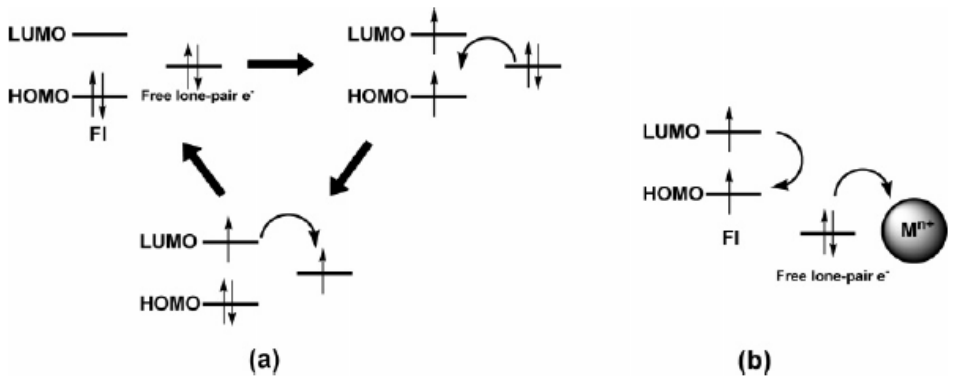

Figure 10. Mechanisms for PET (a) and CHEF (b) systems.

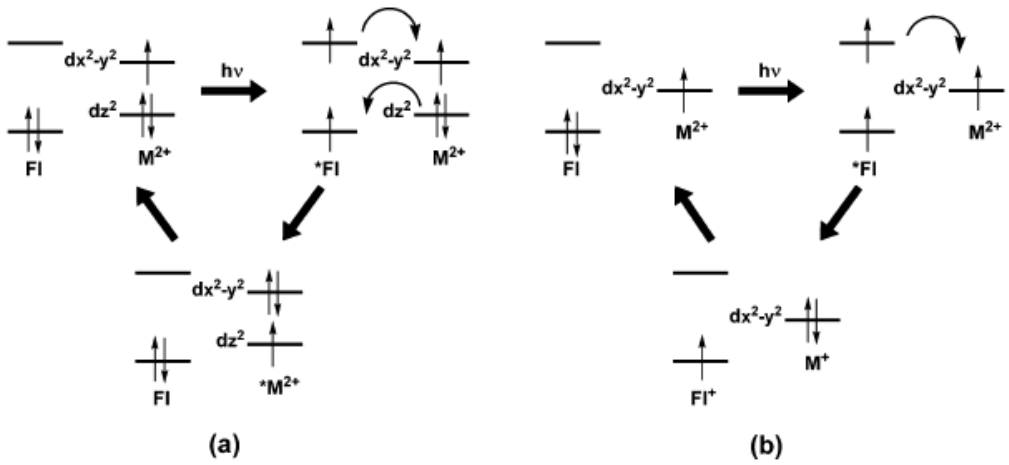

Figure 11. Mechanisms for (a) ET and (b) ET in systems containing an excited fluorophore and a d^9 metal ion.

In some cases, complexation of metal ions, Cu(II) and Ni(II), for example,[76-79] does not induce CHEF but causes the fluorescence to be quenched via two well-defined mechanisms, electron transfer (ET) and energy transfer (ET) to the metal ion, that lead to rapid nonradiative decay. While the ET process (Figure 11) involves no formal charge transfer, the ET process does and must therefore be associated with some spatial reorganization of solvating molecules, so that inhibition of their motions should cause inhibition of ET. Thus, the two processes can be distinguished by comparing the luminescence of liquid and frozen solutions, enhancement of luminescence in the latter indicating that ET must be responsible for quenching in the liquid solution. It has been shown that ET has a weaker dependence on the donor acceptor separation than ET, so that ET tends to dominate for longer separations and ET for shorter.[80-81]

1.2.3 Photoinduced Charge Transfer(PCT)

Electronic excitation necessarily involves some degree of charge transfer, but in fluorophores containing both electronwithdrawing and electron-donating substituents, this charge transfer may occur over long distances and be associated with major dipole moment changes, making the process particularly sensitive to the microenvironment of the fluorophore. Thus, it can be expected that cations or anions in close interaction with the donor or the acceptor moiety will change the photophysical properties of the fluorophore.[82]

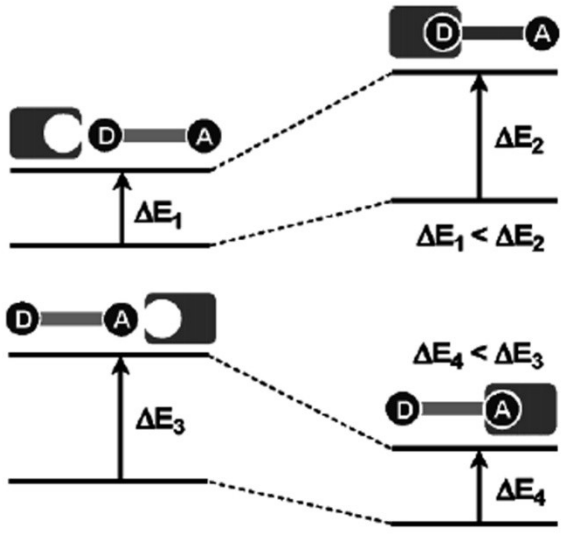

Figure 12. PCT system.

Upon, for example, cation complexation of an electron donor group within a fluorophore, the electron-donating character of the donor group will be reduced. The resulting reduction of conjugation causes a blue shift of the absorption spectrum together with a decrease of the molar absorptive. In contrast, metal ion binding to the acceptor group enhances its electron-withdrawing character, and the absorption spectrum is thus red-shifted with an increase in molar absorptive (Figure 12).[83] The fluorescence spectra should be shifted in the same direction as the absorption spectra, and in addition to these shifts, changes in the quantum yields and lifetimes can be observed. All these photophysical effects are obviously dependent on the charge and the size of the cation, and therefore, some selectivity is expected.

1.2.4 Excimer Formation

Where aromatic rings are involved in weak interactions (such as π-stacking) which bring them within van der Waals contact distances, electronic excitation of one ring can cause an enhanced interaction with its neighbor, leading to what is termed an excited-state dimer or "excimer".[84-85] In other words, an excimer is a complex formed by the interaction of an excited fluorophore with another fluorophore in its ground state. Excimer emission typically provides a broad fluorescence band without vibrational structure, with the maximum shifted, in the case of most aromatic molecules,[86] by about 6000 cm^{-1} to lower energies compared to that of the uncomplexed ("monomer") fluorophore emission. An excimer may also form from an excited monomer if the interaction develops within the lifetime of the latter. Thus, it is expected that excimers are more likely to be produced by relatively long-lived monomer excited states.[87-90] Rates of fluorophore diffusion, especially in viscous solvents, are therefore another limit on excimer formation.[91-94] Importantly, the separation and relative orientation of multiple fluorophore units attached to ligands can be controlled by metal ion coordination, so that recognition of a cation can be monitored by the monomer:excimer fluorescence intensity ratio.

1.2.5 Fluorescence Resonance Energy Transfer (FRET)

FRET arises from an interaction between a pair of dissimilar fluorophores in which one acts as a donor of excited-state energy to the other (acceptor). This returns the donor to its electronic ground state, and emission may then occur from the acceptor center (Figure 13).

FRET is influenced by three factors: the distance between the donor and the acceptor, the extent of spectral overlap between the donor emission and acceptor absorption spectrum (Figure 14), and the relative orientation of the donor emission dipole moment and acceptor absorption moment.[95]

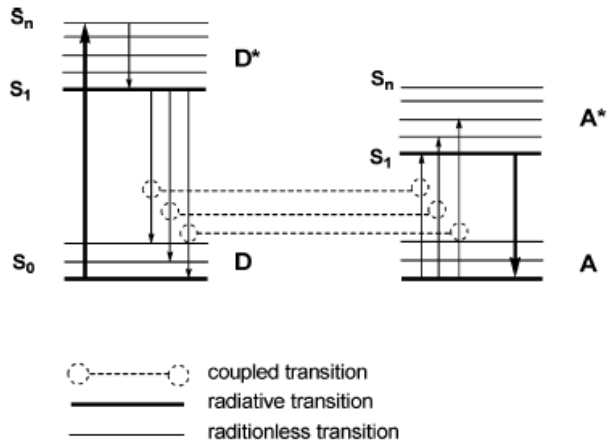

Figure 13. Fluorescence (FÖrster) resonance energy transfer system

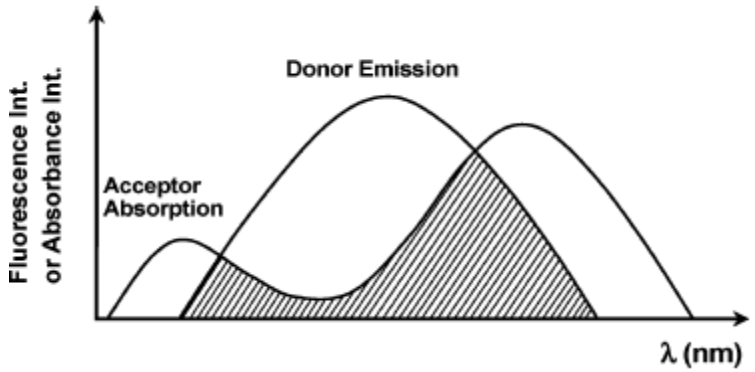

Figure 14. Spectral overlap for FRET.

1.3 Fluorescent probes based on calixarene

1.3.1Calixarene-derived sensors for cations

1.3.1.1 Cu^{2+} recognition

Most of the Cu^{2+} recognitions are generally observed as "turn off" as a result of their paramagnetic nature except in some cases where turn-on fluorescence has been observed as a result of blocking the PET.

Calix[4]azacrown **1**,[74] bearing an anthracenyl unit, was reported to have a pronounced CHEF effect with Cs^+, Rb^+, and K^+ ions, In this case, the anthracenyl fluorophore is bound to the crown site, The addition of Cu^{2+} to an C_2H_5OH/CH_2Cl_2 solution containing the complex **1**•Cs^+ causes fluorescence quenching due to binding of Cu^{2+} to the azacrown ether, which causes ejection of Cs^+ and thus facilitates PET between the proximate crown oxygen atoms and the excited anthracenyl.

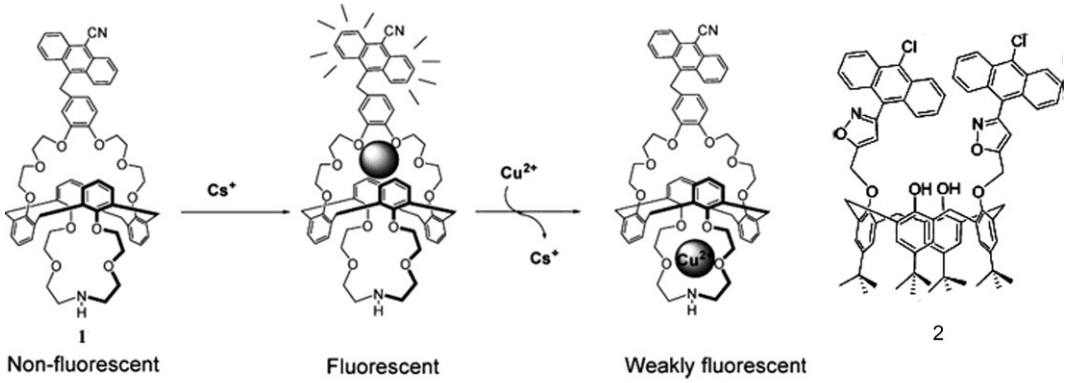

Figure 15. Schematic structures of **1** and **2**

Similarly, Chung et al reported a calix[4]arene appended with arylisoxazole unit at the lower rim **2**[96] shows Cu^{2+} receptor property by fluorescence quenching wherein the 10-chloroanthracenyl moiety has been integrated into this for monitoring the fluorescence changes (Figure 15). Receptor **2** forms a 1:1 complex with K_a = 1.58 $\times 10^4$ M^{-1} in $CH_3CN/CHCl_3$ (v/v = 1000:4). The Cu^{2+} undergoes autoreduction by the phenol, and the oxidized product can accommodate Cu^{2+} as evidenced from the sharp NMR spectrum observed.

Host compound **3**[97] can be used as a fluorescent chemosensor for Cu^{2+} and Zn^{2+} in CH_3OH/H_2O (9:1, v/v) with pH control. When excited at 340 nm, free **3** (Figure 16) shows a weak emission at 408 nm due to the PET between the imidazoles and the fluorophore. When protonated, the PET process is suppressed to give an increased fluorescence. While Cu(II)

coordination could be expected to produce a CHEF effect, in its complex with **3** there is an ET between Cu^{2+} and the excited fluorophore which dominates and leads to quenching. As expected, the ET pathway is not available for Zn(II), so the CHEF effect operates and the emission intensity is greater. Other cations tested gave negligible effects due to their weak complexation. The fluorescence changes induced by Cu^{2+} and Zn^{2+} are most apparent in a medium of pH 10.

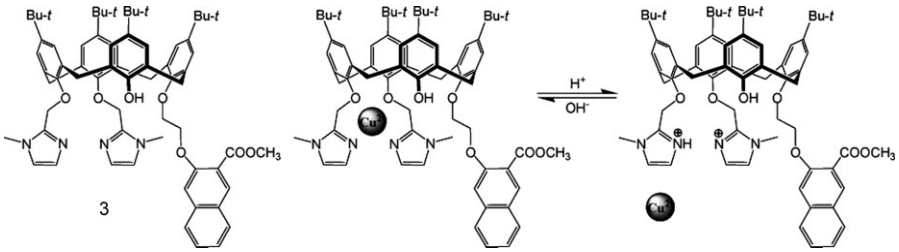

Figure 16. Schematic structure of **3**

Kim et al reported a calixarene-based fluorescent sensors showing PCT sensor.[98] Compound **4** (Figure 17) containing two cation recognition sites, a crown ether ring and two facing pyrene amide moieties, shows a drastic change in the fluorescence and absorption spectra in CH_3CN upon complexation of Pb^{2+}, Cu^{2+}, or K^+ with different binding modes. N…Cu^{2+}…N chelation makes the distance between the two pyrenes shorter, resulting in a static excimer evidenced by a red shift in the excitation spectrum of its complex. Conversely, C=O…Pb^{2+}…O=C coordination forces the two pyrenes apart, allowing no static excimer formation at all. Complexation of both Cu^{2+} and Pb^{2+} reduces the emission intensity. The addition of K^+, however, makes the excimer emission increase, presumably because the polyether ring of calix[4]crown-5 is more suitable for complexation of K^+. Only Cu^{2+} induces shifts in both the fluorescence and absorption maxima, and these are attributed to a PCT process.

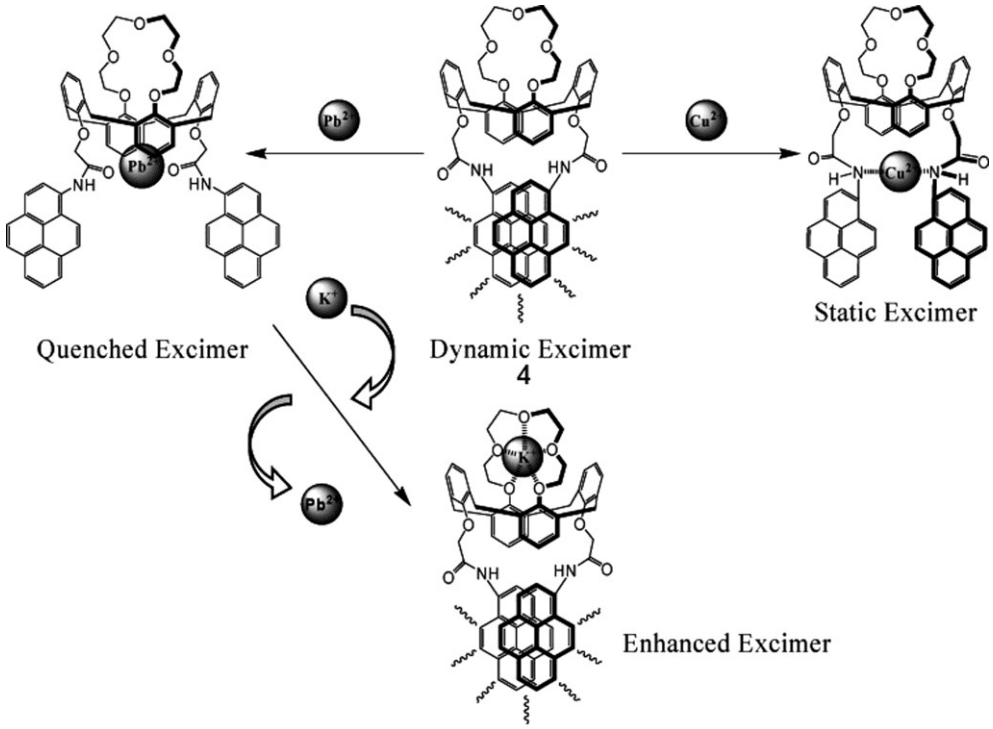

Figure17. Schematic structure of **4**

A derivative of β-amino-R,β-unsaturated ketone (**6**) and its isoxazole precursor (**5**) (Figure 18) were found to be selective toward Cu^{2+} by fluorescence enhancement and quenching, respectively.[99] In both cases, Cu^{2+} undergoes autoreduction by phenolic-OH groups of the lower rim (Figure 18). The K_a values observed for Cu^{2+}were 17 200 and 2080 M^{-1}, for receptor **6** and **5** in CH_3CN, respectively.

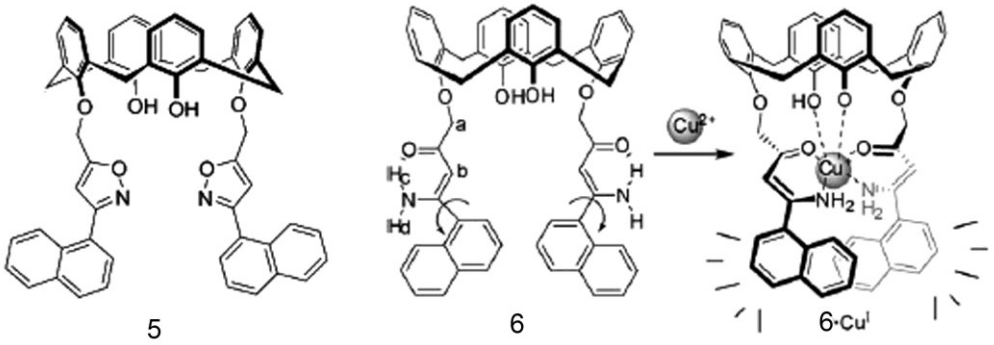

Figure18. Schematic structures of **5** and **6**

A bishydroxamate derivative connected to pyrene as signaling moiety, receptor **7**[100] exhibits sensitivity toward Cu^{2+} and Ni^{2+} in aqueous methanol depending upon the pH of the medium among other transition metal ions, Fe^{2+}, Co^{2+}, and Zn^{2+}, studied by the fluorescence quenching of both the excimer and the monomer emissions (Figure 19). Receptor **7** shows response to Cu^{2+} in HEPES medium, while Ni^{2+} requires a pH of 8 to exhibit ON/OFF fluorescence behavior with **7**.

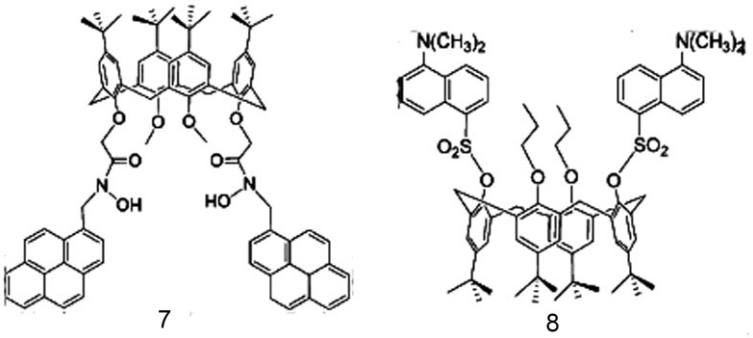

Figure 19. Schematic structures of **7** and **8**

Calix[4]arene bearing two dansyl groups at 1,3-positions and two propyl groups at 2,4-positions (**8**)[101] exhibited a fluorescence quenching of 98% and 70% with Cu^{2+} and Hg^{2+}, respectively (Figure 19). Receptor **8** forms a 1:2 (**8**•Cu^{2+}) complex with Cu^{2+} and exhibited $\ln(K_a)$ of 4.19 and a lowest detection of 4×10^{-6} M in CH_3CN. The receptor **8** selectively forms complexes with Cu^{2+} even in the presence of other ions, which is evident from the competitive titration studies.

Kumar et al developed new fluorescent chemosensor for Cu^{2+} based on thiacalix[4]arene, for example, A series chemosensor based on the thiacalix[4]arene of 1,3-*alternate* conformation (**9,10** and **11**)[102] have been designed and synthesized. The binding behavior of this chemosensor has been studied toward different metal ions and anions by fluorescence spectroscopy, and it was observed that receptor **9** has a chemosensor selectively senses Cu^{2+} ions by quenching the fluorescence and 16% enhancement in the fluorescence intensity in the case of fluoride ions in THF/H_2O.

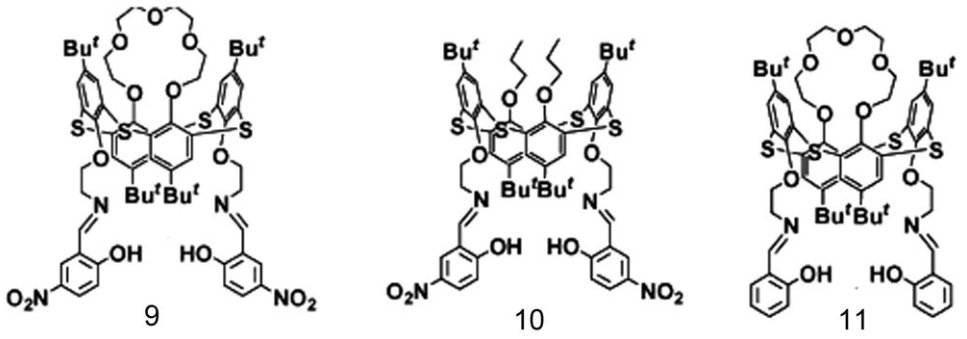

Figure 20. Schematic structures of **9, 10** and **11**

Based on the same conformation of thiacalix[4]arene scaffold, receptor **12**[103] with two different types of cation binding sites has been synthesized by the same group. Two pyrene moieties linked to a cation recognition unit composed of two imine groups form a strong excimer in CH_3CN/CH_2Cl_2 solution. Of the metal ions tested, the fluorescence of **2** was strongly quenched by Hg^{2+}, Pb^{2+} and Cu^{2+} ions. The fluorescence was revived by the addition of only K^+ to the Cu^{2+} ligand complex. Thus, metal-ion exchange triggers an "on–off" switchable fluorescent chemosensor.

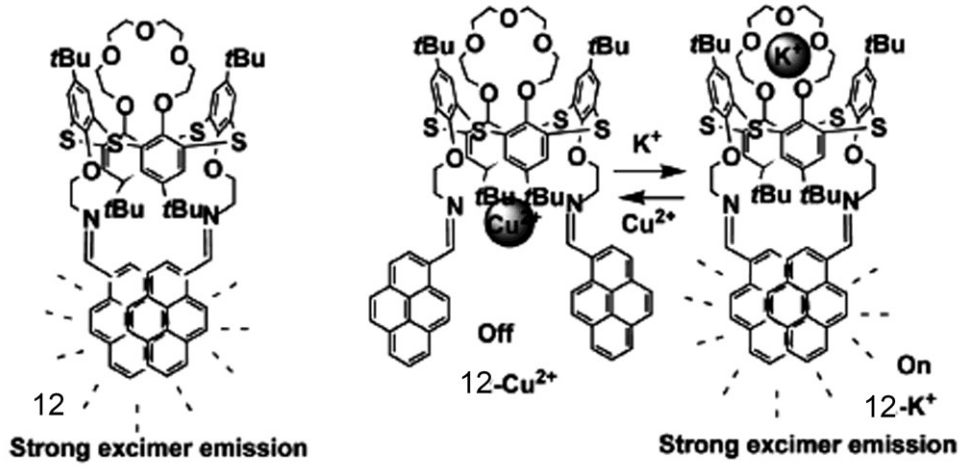

Figure 21. Schematic structure of **12**

Furthermore, Three new ditopic receptors (**13**, **14** and **15**)[104] based on thiacalix[4]arene of

1,3-*alternate* conformation possessing two different complexation sites have been designed and synthesized for both soft and hard metal ions. The imino nitrogens bind soft metal ion (Ag^+, Pb^{2+} and Cu^{2+}) and the crown moiety binds K^+ ion. The preliminary investigations show that **13-15** behave as ditopic receptors for Ag^+/K^+, Pb^{2+}/K^+, and Cu^{2+}/K^+ ions, respectively. In all the three receptors it was observed that the formation of **13**•Ag^+/**14**•Pb^{2+}/**15**•Cu^{2+} complex triggers the decomplexation of K^+ ion from crown moiety and acts as a gateway, which regulates the binding of alkali metal to crown moiety. Thus, allosteric binding between metal ions "switch off" the recognition ability of crown ether ring.

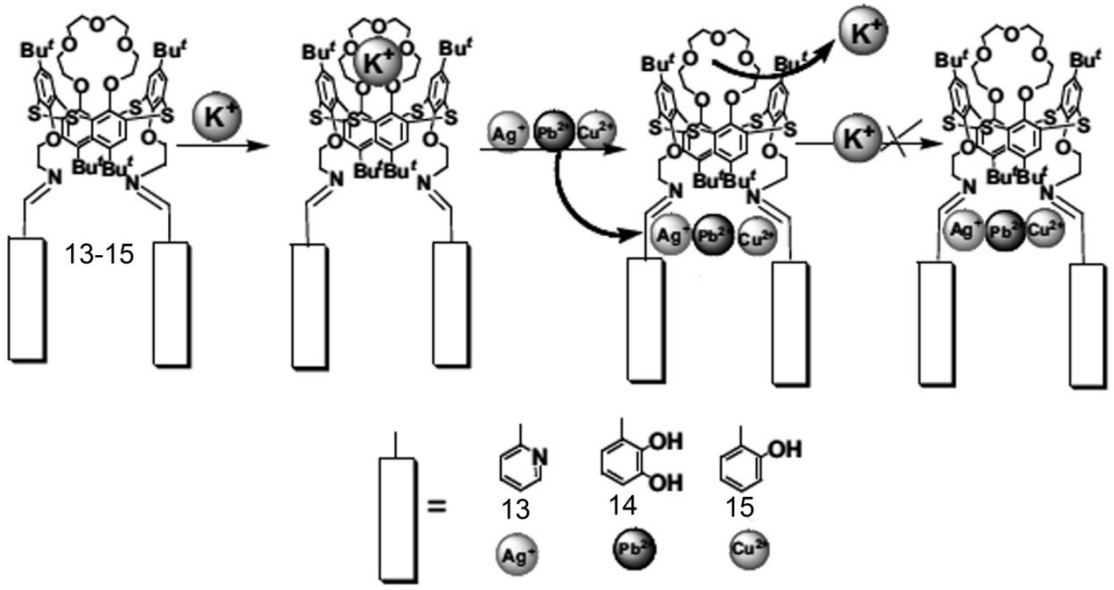

Figure 22. Schematic structures of **13, 14** and **15**

1.3.1.2 Pb^{2+} recognition

Receptor compounds **16** and **17**[105] (Figure 23), containing two pyrene moieties and a pendent primary alkylamine, provide systems where both monomer and excimer emissions may be affected by PET. That their weak emission is a consequence of PET is confirmed by a comparison with **17**, a calixarene having the same structure as **16** but without an attached amine group, where strong monomer and excimer emissions are seen. In the presence of Pb^{2+}, both **16** and **17** in CH_3CN exhibit an enhanced monomer emission and diminished excimer emission. This CHEF effect can be attributed to a conformational change due to the metal

binding as well as to the coordination of the electron-donor N center. However, upon addition of alkali-metal ions to **16** and **17**, both monomer and excimer emissions are enhanced, suggesting that there is no conformational change involved. A competitive metal ion exchange experiment shows that the binding ability of **16** for Pb^{2+} is much greater than that for Li^{+}.

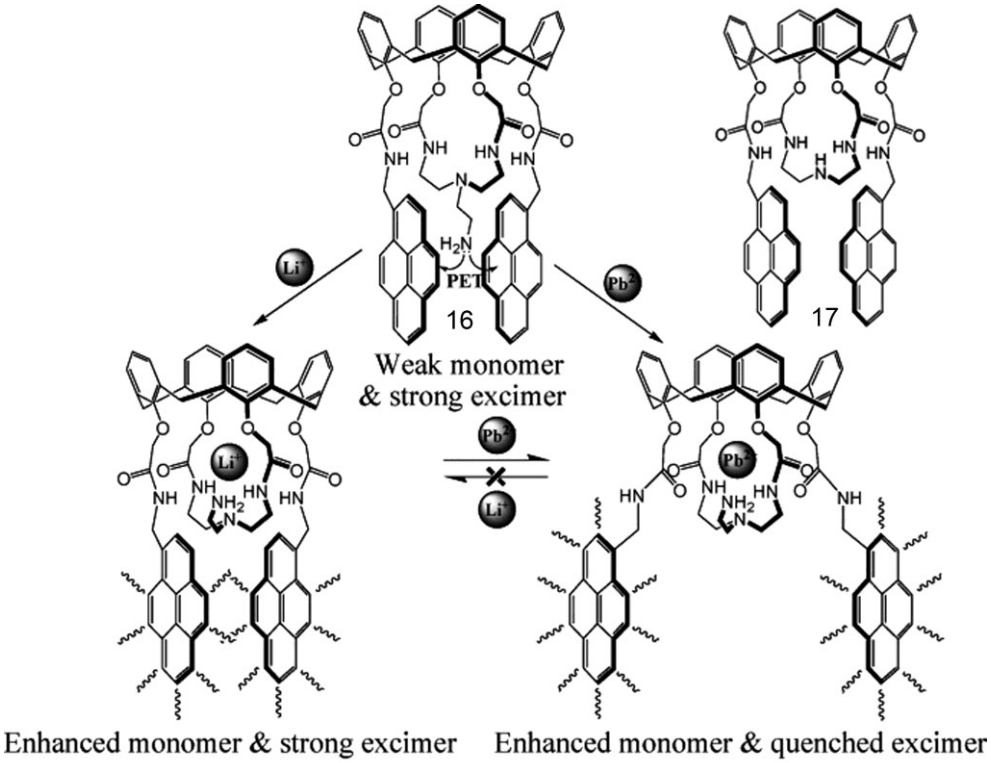

Figure 23. Schematic structures of **16** and **17**

A new fluorescent chemosensor with two different types of cation binding sites on the lower rims of a 1,3-alternate calix[4]arene (**18**)[87] is synthesized by the same group. Two pyrene moieties linked to a cation recognition unit composed of two amide groups form a strong excimer in CH_3CN solution. For **18**, the excimer fluorescence is quenched by Pb^{2+}, but revived by addition of K^{+} to the Pb^{2+} ligand complex. Thus, metal ion exchange produces an on-off switchable, fluorescent chemosensor. Computational results show that the highest occupied molecular orbital (HOMO) and the lowest unoccupied molecular orbitals (LUMO)

of the two pyrene moieties interact under UV irradiation of **1** and its K^+ complex, while such HOMO-LUMO interactions are absent in the Pb^{2+} complex.

Very similar behavior was also observed by Chung and co-workers; in that case, receptor **19** was constructed by click chemistry.[106] Compound **19** was synthesized by clicking anthracene units onto a calix[4]crown scaffold to create two potential metal binding sites: between the triazoles below the calixarene ring, and in the crown ether above the ring. Limited selectivity was observed in $CH_3CN/CHCl_3$: the fluorescence of the anthracene groups was quenched by Hg^{2+}, Cu^{2+}, Cr^{3+} and Pb^{2+}, and enhanced by K^+, Ba^{2+} and Zn^{2+}. Interestingly, addition of K^+ to the Pb^{2+} complex resulted in almost complete revival of

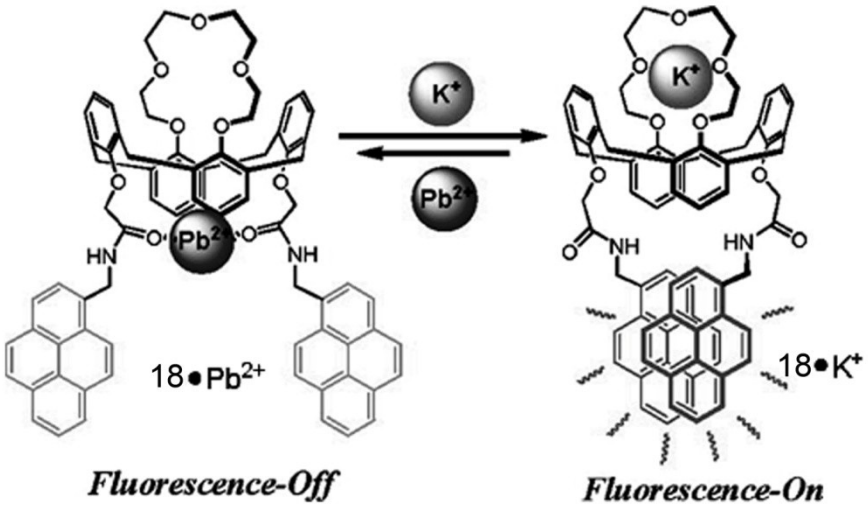

Figure 24. Schematic structure of **18**

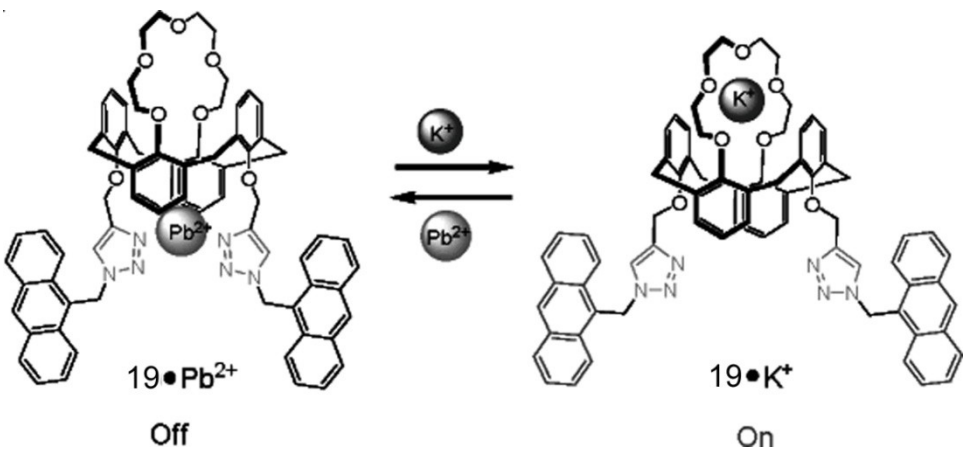

Figure 25. Schematic structure of **19**

fluorescence emission, whilst quenching occurred when Pb^{2+} was added to the K^+ complex. Therefore **19** is a metal-ion switchable chemosensor, with K^+ and Pb^{2+} as the on and off switches respectively. ^1H NMR studies indicated that K^+ binds to the crown ether and Pb^{2+} to the triazole binding pocket, with the metal exchange attributed to electrostatic repulsion and uncharacterised allosteric effects.

Fluorescence quenching commonly occurs by the PET mechanism in which the excited state acts as an oxidant, although the inverse phenomenon, termed reverse PET, is also sometimes observed. Thus, **20** (figure 26)[107] exhibits a strong emission at *ca*. 400 nm when excited at 344 nm.114 Addition of Pb^{2+} to **20** in $CH_3CN/CHCl_3$ (1:1, v/v) causes a marked decrease in fluorescence intensity, attributed to reverse PET involving electron donation from the excited pyrene unit to the carbonyl groups, the electron density of which is decreased by Pb^{2+} complexation. A "heavy metal effect" due to the redox activity of the metal ion cannot, however, be excluded.

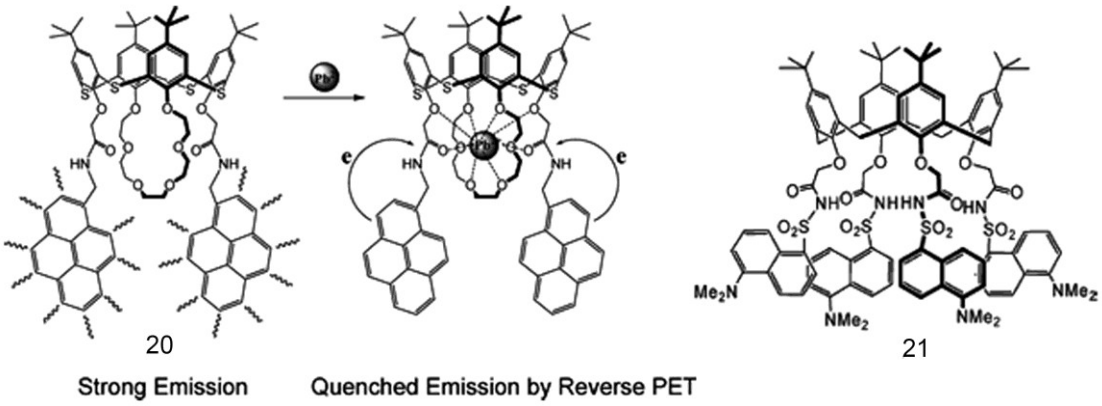

Figure 26. Schematic structures of **20** and **21**

For compound **21**,[108] the optimum pH for observation of the effects of Pb^{2+} binding is 5.2, at which point **57** is mainly in its neutral form (Figure 26). There, addition of Pb^{2+} causes a 52 nm blue shift of the fluorescence peak and a 1.7-fold enhancement of the fluorescence quantum yield. The absorption spectra are also shifted to higher energy (11 nm) upon Pb^{2+} binding. The blue shift is rationalized by the deprotonation of the sulfonamide group upon cation binding.

Pb^{2+} extraction and the detection were mainly observed with receptors bearing hard donormoieties such as oxygen in addition to the participation of phenolic-OH's, amide oxygen, or nitrogen centers. Pb^{2+} easily forms higher coordinations with the help of oxygen atoms of crown ether, phenolic-OH's, etc. Nitrogen containing triazole units also prefer transition metal ions as is evident from this parts. It is also important to note that the pH of the medium has some role in the efficiency of extraction of Pb^{2+}. Attaching a fluorophore helps the derivatives to monitor the ion recognition by fluorescence spectroscopy.

1.3.1.3 Hg^{2+} recognition

A calix[4]arene receptor appended with pyrenylacetamide, receptor **22**[109] (Figure 27), detects Hg^{2+} through fluorescence quenching after a 100 equiv addition of the ion even in the presence of other ions such as alkali, alkaline earth, transition, and heavy metal ions, with an association constant of 4.5×10^4 M^{-1} in methanol. The fluorescence emission of **22** mainly originates from the monomer and weak excimer in methanol, while it is the reverse in 50% aqueous methanol. Upon interaction with Hg^{2+}, both the monomer and the excimer emissions

of **22** have been quenched, indicating an ON–OFF type receptor. A series of aza crown derivatives of calix[4]arene with an anthrancene fluorophore have been studied for their ability to detect Hg^{2+}.[110] The receptor **24** shows highest fluorescence enhancement toward Hg^{2+} as compared to **23** and **25** (Figure 27). The fluorescence of **24** enhances in the presence of Cu^{2+} and Pb^{2+}, although this enhancement is much less than that of Hg^{2+} in a mixture of methanol/tetrahydrofuran. The nonselectivity of **25** toward all of the ions is mainly due to the presence of more number of nitrogen donor centers in the system, indicating that only the presence of requisite number of ligating nitrogen centers is necessary for optimal binding. However, the selectivity is lost when the number of ligating centers is lower or higher than this. The higher selectivity of **24** is attributable to the flexibility of the spacer unit present in **24** as compared to **23** that brings better coordination between Hg^{2+} and the nitrogen donor centers in the former.

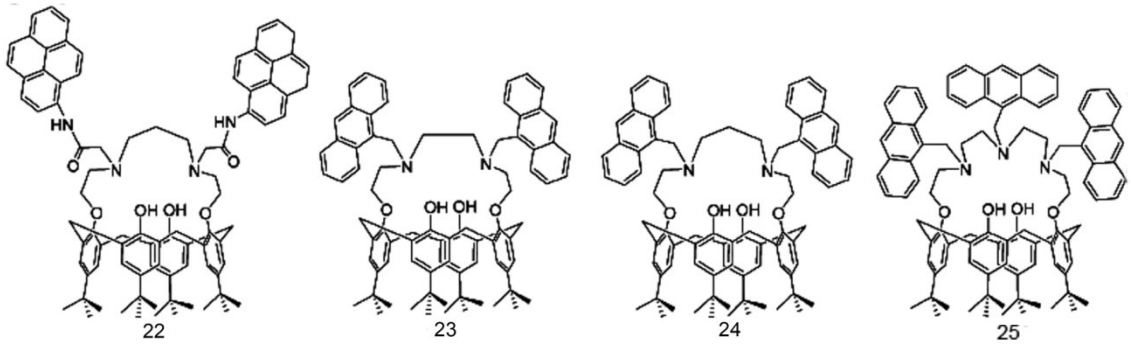

Figure 27. Schematic structures of **22-25**

An amido-dansyl conjugate (**26**)[111] exhibit good extraction ability toward Hg^{2+} and found that Pd^{2+} is only the competitor for Hg^{2+} (Figure 28). The receptor **26** also showed Hg^{2+} selectivity by fluorescence quenching as a result of electron transfer among the other ions studied, Na^+, K^+, Ca^{2+}, Cu^{2+}, Zn^{2+}, Cd^{2+}, and Pb^{2+}, in aqueous acetonitrile at pH = 4. It forms a 1:1 stoichiometric complex with Hg^{2+} with an association constant of 1.5×10^7 M^{-1} in CH_3CN/H_2O (60:40 v/v). **26** showed response toward Hg^{2+} even in the presence of other ions but for Pb^{2+}, which interferes to some extent. ^1H NMR spectral titration of this derivative with Hg^{2+} indicates that, upon complexation, calix[4]arene exists in the cone conformation.

Time-resolved fluorescence titration has also been carried out to get more insight into the mercury complexation. The alkali and transition metal ion interactions of a series of calix[4]arenes possessing dansyl fluorophore (**27**, **28** and tetramethyl ammonium salt of **26**, Figure 28) have been studied by absorption and fluorescence spectroscopy.[112] The metal ions, Fe^{3+}, Hg^{2+}, and Pb^{2+}, exhibit strong interaction with these conjugates by quenching the original fluorescence by 97%. A calix[4]arene functionalized with two dansyl fluorophores and two long alkyl chains of triethoxysilane groups (**29**) that was placed in mesoporous silica showed the ability to sense Hg^{2+} in water by forming a 1:1 complex (Figure 28). Also A cyclicamido-dansyl conjugate receptor **30**[113] forms a 1:1 complex by exhibiting high fluorescence sensitivity with Hg^{2+} through the formation of N_4 binding core (Figure 28); the heavy metal ions, such as Pb^{2+},Cu^{2+}, Cd^{2+}, and Zn^{2+}, compete for Hg^{2+}.

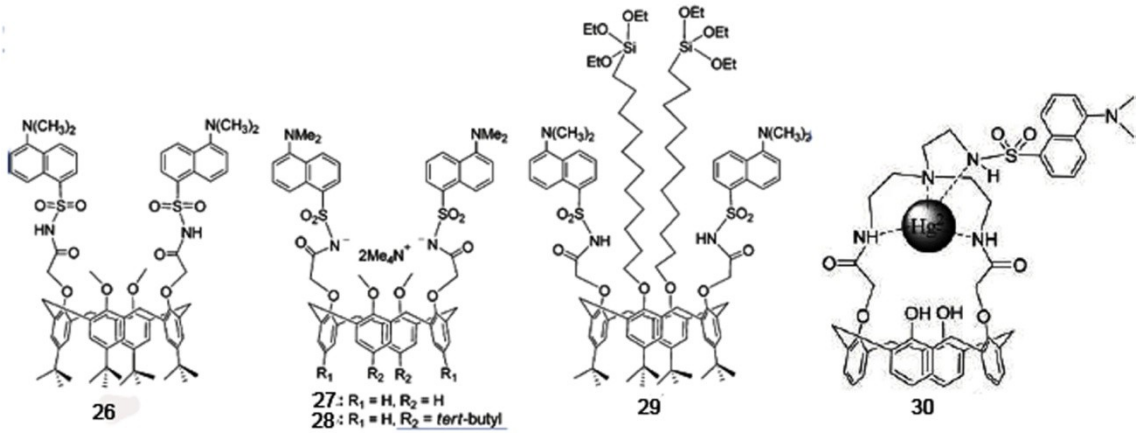

Figure 28. Schematic structures of **26-30**

A triazole linked 8-oxyquinoline conjugate (**31**)[114] exhibits selectivity toward Hg^{2+} by fluorescence quenching at a low pH (Figure 29). While the K_a for the 1:1 complex is 8.5×10^3 M^{-1} in case of Hg^{2+}, these are 1.2×10^3 and 4.4×10^3 M^{-1}, respectively, for Cu^{2+} and Fe^{2+} showing no greater selectivity in CH_3CN:H_2O (v/v 3:1). A NOR logic gate property has been proposed using the fluorescence intensity of **31** in the presence of Hg^{2+} as a function of pH.

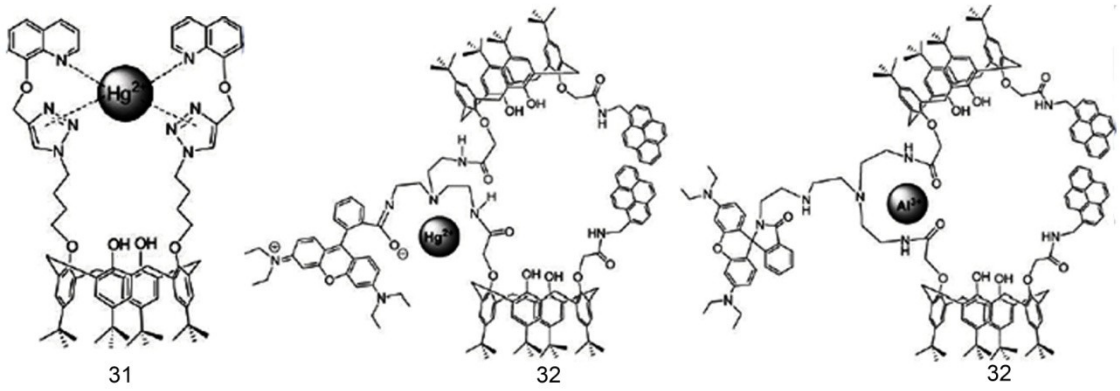

Figure 29. Schematic structures of **31** and **32**

The receptor **32**[115] (Figure 29), a double branched calixarene conjugate bearing one amidopyrenylmethyl moiety and a rhodamine B unit, acts as 1:1 stoichiometric chemosensor for Hg^{2+} and Al^{3+}. While Hg^{2+} opens the spirolactam ring of rhodamine to bind (trenspirolactum), Al^{3+} binds unopened. Although this paper demonstrates the role of FRET, the role of calixarene moiety has not been addressed adequately.

1.3.1.4 Zn^{2+} recognition

A simple O-methylanthracenyl derivative **33**[116] (Figure 30), exhibits a low fluorescence enhancement toward some transition metal ions. When an imine moiety is introduced into this to result in **34**, this starts exhibiting some selectivity by showing significant fluorescence enhancement toward a few transition ions over the others in the order, $Fe^{2+} \approx Cu^{2+} > Zn^{2+} >$ other 3d ions, and hence is poorly selective. Further, when the arms were derivatized with 2-hydroxy naphthalidene moiety, **35** exhibits selectivity toward Zn^{2+} over a number of other ions studied , by showing a large fluorescence enhancement that is sufficient enough to detect Zn^{2+} even at ≤60 ppb n methanol.[117] fluorescence enhancement is attributable to the reversal of PET when Zn^{2+} orms a 1:1 chelate complex with **35**, its imine and phenolic-OH moieties present on both of the arms wherein the association constant has been found to be 2.3×10^5 M^{-1} in methanol.

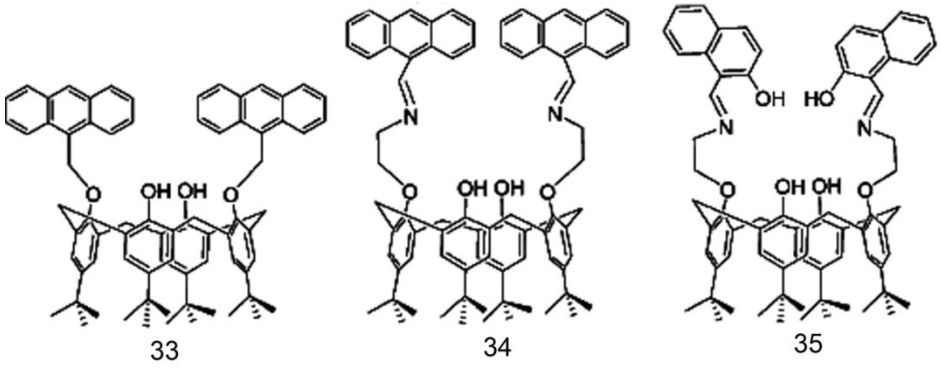

Figure 30. Schematic structures of **33-35**

Receptor **36** (Figure 31) was synthesised independently by two groups[118-119] by clicking two fluorescent pyrene subunits to a calix[4]arene framework. Upon addition of Zn^{2+} or Cd^{2+} in MeCN, **36** exhibits a ratiometric response, with increased pyrene monomer emission and quenching of excimer emission. ^{1}H NMR experiments suggest that the pyrene subunits of **36** are initially involved in π–π stacking, but their separation is forced by the introduction of the metal ion into the triazole binding pocket. To test the effectiveness of **36** as a chemosensor, the fluorescence response was recorded in the presence of other metal ions.[118] Only Cu^{2+} and Hg^{2+} were found to disrupt the sensor by quenching fluorescence completely. It was suggested that the different fluorescence responses to Zn^{2+} and Cu^{2+} could be employed as 'inhibition' (INH) and 'not or' (NOR) logic gates.[119]

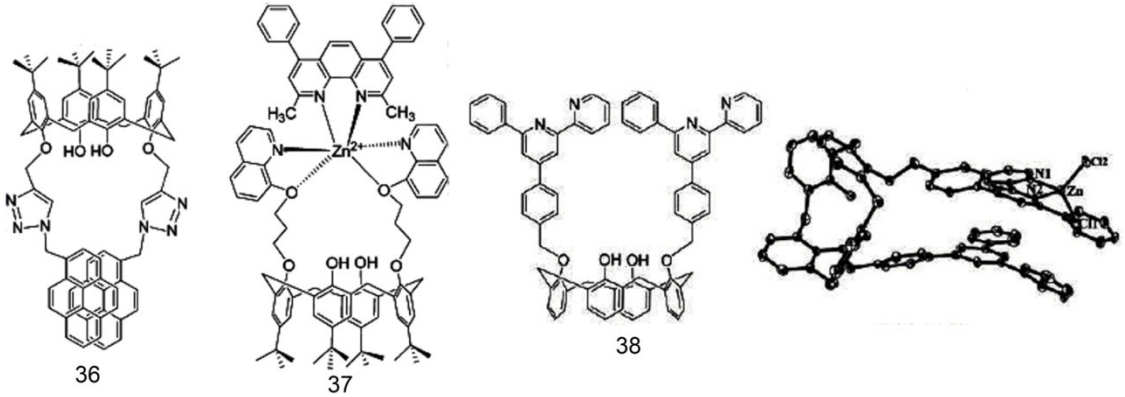

Figure 31. Schematic structures of **36-38**

An oxyquinoline derivative of calix[4]arene (**37**)[120] exhibits 1:1 and 1:2 complexes when titrated with Zn^{2+} through fluorescence quenching. When the two solvent molecules present in this complex were replaced by 2,9-dimethyl-4,7-diphenyl-1, 10-phenanthroline as bidentate ligand (Figure 31), it exhibits enhancement in the fluorescence as a result of the interaction of phenanthroline with Zn^{2+} followed by energy transfer. The interaction has also been proven by ^1H NMR spectroscopy. The receptor **38** possessing two bipyridyl cores (Figure 31) that exhibits 1:2 binding with Zn^{2+} in solution, however, resulted in an 1:1 complex when in solid, even when the reactions were carried out under 2 equiv of zinc salt.[121] Zn^{2+} is bound to only the bipyridyl core of one of the arms where the four-coordination is being filled by the bipyridyl and two chloride ions, keeping the second bipyridyl moiety of the other arm unoccupied (Figure 31).

Last but not least, Shinkai et al reported that **39**[122] (Figure 32) can be used to selectively recognize guanidinium ion in $CHCl_3$ in the presence of primary ammonium ions. When excited at 346 nm, **39** showed monomer and excimer emissions at 396 and 487 nm, respectively. As the guanidinium ion concentration increased, the excimer emission intensity decreased while that of monomer emission increased, suggesting that guanidinium ion bound to the ionophoric $OCH_2C{=}O$ cavity prevents intramolecular contact of the pyrene moieties. These changes are almost unaffected in the presence of *tert*-butylammonium, protonated L-alanine methyl ester or *n*-hexylammonium ions. Compound **40**[123] was also reported to be capable of binding guanidinium ion and inducing fluorescence changes, but the binding is competitively inhibited by primary ammonium ions.

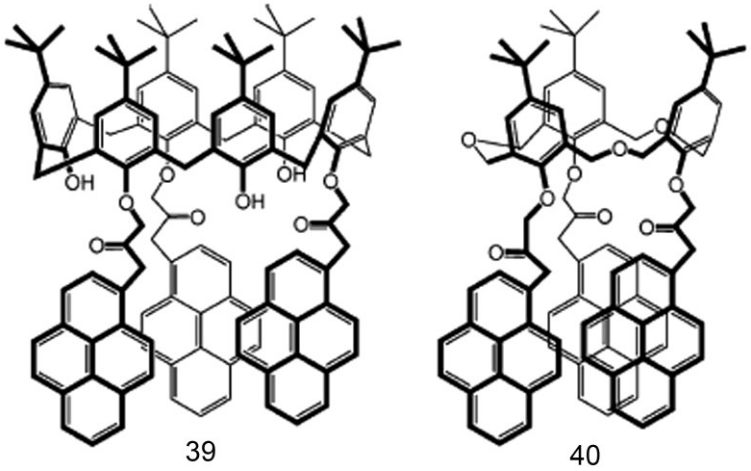

Figure 32. Schematic structures of **39** and **40**

1.3.2 Calixarene-derived sensors for anions

Calixarene-based anion receptors are synthesized by introducing functionalities such as amide, urea, or thiourea, which can interact with anions through hydrogen bonding. Incorporation of fluorophores into such binding cores would be of great use in monitoring the binding aspects.

When receptor **41**[124] was excited at 335 nm, it exhibited an emission band at 420 nm, which is quenched upon complexation of F^- in CH_3CN to give rise to a weak band at 508 nm. The addition of F^- to **41** causes a decrease in emission intensity together with a red shift, which results from H-bonding followed by protonation.

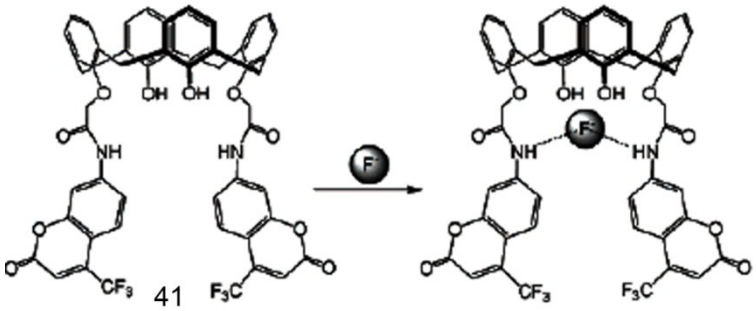

Figure 33. Schematic structure of **41**

Kim et al. reported an amide-based calix[4]arene derivative bearing pyrene and nitrophenylazo moieties (**42** and **43**)[125] exhibited F^- recognition as studied by UV_vis and fluorescence spectroscopy. The interaction of F^- with **42**, **43** has been found to be through the amide and the phenolic protons, respectively, Addition of F^- to **42** in CH_3CN produces a bimodal response in which initially the excimer emission is quenched but then a new species with emission bands at 385 and 460 nm appears. This behavior has been rationalized in terms of static pyrene dimer formation in the ground state influenced by H-bonding between F^- and the amide proton. The fluorescence of **43** also changes upon addition of F^- but in a different manner. In this case, the presence of a methylene spacer between the pyrene moiety and amide N probably forces the two pyrenes to be orthogonal to each other, as in a similar

compound, thus preventing the interaction which might give a dynamic excimer.

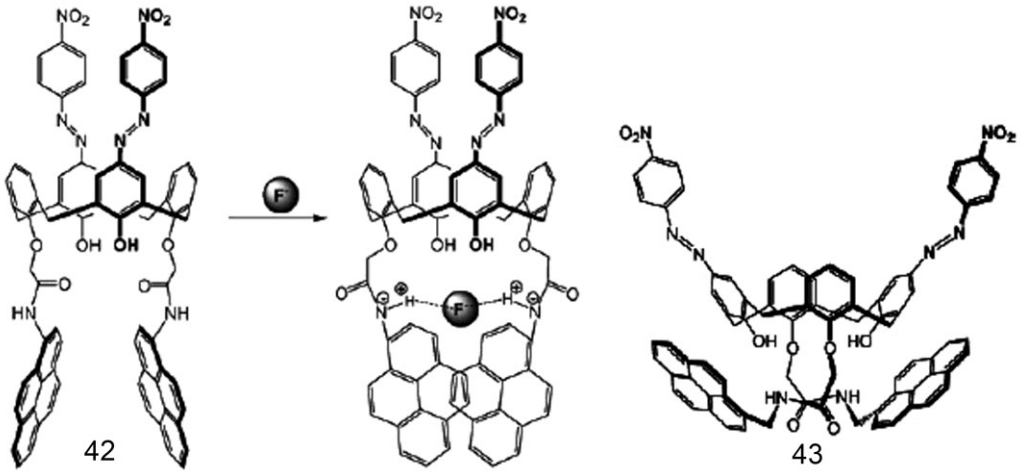

Figure 34. Schematic structures of **42** and **43**

1,3-alternate calix[4]arene **44**[126] (Figure 35) with bis(pyrenylurea) groups on the lower rim, when excited, shows monomer and much broader (intramolecular) excimer emissions at 398 and 452 nm, respectively. The *I*E/*I*M ratio remains unchanged at 4.4 in the concentration range from 10^{-7} to 10^{-5} M, as expected for intra- and not intermolecular excimer formation. Four urea groups providing eight possible H-bonds for anion binding are in close proximity to pyrene moieties, the relative orientation of which is thought to change upon anion complexation. Anion binding can thus be monitored by ratiometric changes in the emission spectrum (*I*E/*I*M ratio) of **44**. Of the anions tested, Cl^- causes the most marked changes in the emission spectrum of **44**. There is a strong quenching of the excimer emission with a corresponding enhancement in monomer emission. These observations suggest that the chloride anion may selectively coordinate with the urea protons in the cavity of **44** so as to "unstack"or lever apart the facing π-π stacked pyrenes.

A conjugate in which anthracene connected to both of the arms through triazole moiety, receptor **45** [127] (Figure 35), exhibits anion recognition in methanol as studied by fluorescence spectroscopy. The fluorescence intensity of this derivative in various solvents follows the order $CH_3OH<CH_3CN<THF=CHCl_3$. While TBABr, TBAI, LiBr, and LiI exhibit fluorescence enhancement, the TBAHS (tetrabutylammonium hydrogen sulfate) exhibits

fluorescence quenching. Maximum fluorescence intensity was observed upon the addition of iodide salts.

A tetraamide derivative of calix[4]arene (**46**), showed fluorescence enhancement with $H_2PO_4^-$ with K_a of 5.48×10^9 M^{-2} by forming a 1:2 (**46**•$H_2PO_4^-$) complex in CH_3CN (Figure 35).[128] However, F^- shows fluorescence quenching through the formation of a 1:2 complex and yields a K_a of 2.02×10^6 M^{-2}. The ^1H NMR spectral titrations explain the multiple hydrogen-bonding interaction of $H_2PO_4^-$ with the amide, sulfonamide groups, OH, and several CH protons of **46**, and that resulted in the high selectivity of this guest species.

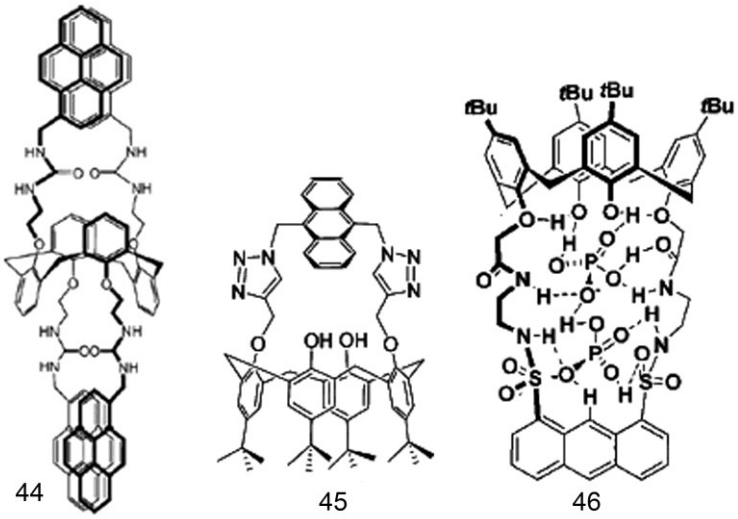

Figure 35. Schematic structures of **44-46**

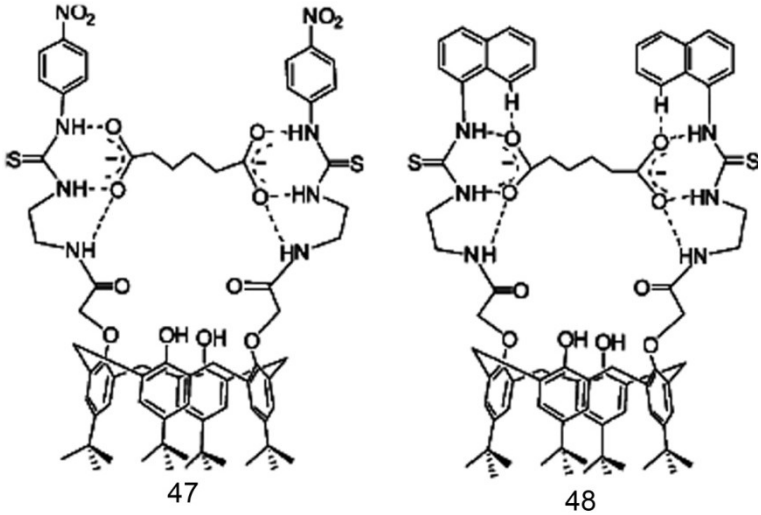

Figure 36. Schematic structures of **47** and **48**

Calix[4]arene conjugate bearing thiourea and amide (**47** and **48**)[129] (Figure 36) selectively and adipate over AcO^-, $H_2PO_4^-$, Cl^-, Br^-, and I^- in DMSO as studied by UV-visible, fluorescence, and ^1H NMR spectral titrations. Both of the conjugates form stoichiometric complexes with all of the dicarboxylates through multiple hydrogen bonding, and the sensitivity of the recognition depends on the chain length, and the selectivity follows an order adipate>glutarate>succinate>malonate, based on their K_a values. The conjugate **47** undergoes color change from yellow to red when it interacts with dicarboxylate anions.

1.4 Conclusions

According to the above review of recently development of fluorescent chemosensor for cations and anions based on calixarene scaffold. The synthesis, characterization, and ions selectivity recognition properties of receptor focused on calixarene would exhibit further interests and challenges to the supramolecular chemists, because such scaffold not only provide requisite binding cores but also are flexible enough to accommodate various ions and molecular species with demand diverse features of interactions and geometry. Thus, against this background, several kinds of fluorescent chemosensors for heavy metal ions and anions were designed and synthesized based on calixarene in this dissertation.

1.5 References

1. Schmidtchen, F. P.; Berger, M. *Chem. Rev.* **1997**, *97*, 1609.
2. Beer, P. D.; Gale, P. A. *Angew. Chem., Int. Ed.* **2001**, *40*, 486.
3. Orvig, C.; Abrams, M. J. *Chem. Rev.* **1999**, *99*, 2201.
4. McRae, R.; Bagchi, P.; Sumalekshmy, S.; Fahrni, C. J. *Chem. Rev.* **2009**, *109*, 4780.
5. Que, E. L.; Domaille, D. W.; Chang, C. J. *Chem. Rev.* **2008**, *108*, 1517
6. Bargossi, C.; Fiorini, M. C.; Montalti, M.; Prodi, L.; Zaccheroni, N. *Coord. Chem. Rev.* **2000**, *208*, 17.
7. Butler, O. T.; Cook, J. M.; Harrington, C. F.; Hill, S. J.; Rieuwerts, J.; Miles, D. L. *J. Anal. At. Spectrom.* **2006**, *21*, 217.
8. Li, Y.; Chen, C.; Li, B.; Sun, J.; Wang, J.; Gao, Y.; Zhao, Y.; Chai, Z. *J. Anal. At. Spectrom.* **2006**, *21*, 94.

9. Leermakers, M.; Baeyens, W.; Quevauviller, P.; Horvat, M. *Trends Anal. Chem.* **2005**, *24*, 383.
10. Valeur, B. *Molecular Fluorescence: Principles and Applications*; Wiley-VCH: Weinheim, Germany, 2002.
11. Prodi, L.; Bolletta, F.; Montalti, M.; Zaccheroni, N. *Coord. Chem. Rev.* **2000**, *205*, 59.
12. Fabbrizzi, L.; Licchelli, M.; Pallavicini, P.; Perotti, A.; Taglietti, A.; Sacchi, D. *Chem. Eur. J.* **1996**, *2*, 75.
13. Fabbrizzi, L.; Licchelli, M.; Pallavicini, P.; Perotti, A.; Sacchi, D. *Angew. Chem.* **1994**, *106*, 2051.
14. Kim, H. J.; Park, S. Y.; Yoon, S.; Kim, J. S. *Tetrahedron* **2008**, *64*, 1230.
15. Zhang, H.; Xie, L.; Yan, W.; He, C.; Cao, X.; Duan, C. *New J. Chem.* **2009**, *33*, 1478.
16. J. Vicens, V. Böhmer Eds., *Calixarenes:* A *Versatile Class of Macrocyclic Compounds*, Kluwer Academic: Dordrecht, 1991.
17. Ikeda, A.; Shinkai, S. *Chem. Rev*. **1997**, *97*, 1713.
18. C. D. Gutsche, *Calixarenes, An Introduction*, Royal Society of Chemistry: Cambridge, U.K., 2008.
19. Z. Asfari, V. Böhmer, J. Harrowfield, J. Vicens Eds., *Calixarenes 2001*, Kluwer Academic: Dordrecht, 2001.
20. N. Morohashi, F. Narumi, N. Iki, T. Hattori and S. Miyano, *Chem. Rev*. **2006**, *106*, 5291.
21. (J. S. Kim and D. T. Quang, *Chem. Rev*. **2007**, *107*, 3780.
22. D. Coquière, S. Le Gac, U. Darbost, O. Sénèque, I. Jabin and O. Reinaud, *Org. Biomol. Chem.* **2009**, *7*, 2485.
23. Gutsche, C. D. In Calixarenes Revisited, Royal Society of Chemistry, Cambridge, 1998.
24. Gutsche, C. D. *Acc. Chem. Res.* **1993**, *16*, 161.
25. Vicens, J.; Böhmer, V. In Calixarenes: A Versatile Class of Macrocyclic Compounds, Kluwer Academic Publishers, Cambridge, 1990.
26. Andreetti, G. D.; Ungaro, R.; Pochini, A. *J. Chem. Soc., Chem. Commun.* **1979***, 22*, 1005.
27. Gutsche, C. D. *Calixarenes, Monographs in Supramolecular Chemistry;* Stoddart, J. F. Ed. The Royal Society of Chemistry: London, 1989, Vol. *1*.
28. Vicens, J.; Böihmer, V. *Calixarenes:* A *Versatile Class of Macrocyclic Compounds*; Topics in Inclusion Science; Kluwer Academic Press: Dordrecht, 1991; Vol. *3*.

29. Gutsche, C. D. *Calixarenes Revisited, Monographs in Supramolecular Chemistry;* Stoddart, J. F., Ed. The Royal Society of Chemistry: London, 1998.
30. Vögtle, F.; Schmitz, J.; Nieger, M. *Chem. Ber.* **1992**, *125*, 2523. (b) Brodesser, G.; Vögtle, F. *J. Incl. Phenom.* **1994**, *19*, 111.
31. Yamato, T.; Sakaue, N.; Tanaka, K.; Tsuzuki, H. *New. J. Chem.* **2001**, *25,* 434. (b) Yamato, T.; Saruwatari, Y.; Yasumatsu, M. *J. Chem. Soc. Perkin Trans. 1* **1997**, 1731.
32. Bates, R. B.; Gangwar, S.; Kane, V. K.; Suvannachut, K.; Taylor, S. R. *J. Org. Chem.* **1991**, *56*, 1696. (b) Burns, D. H.; Miller, J. D.; Santana, J. *J. Org. Chem.* **1993**, *58*, 6526.
33. Gutsche, C. D.; Dhawan, B. *J. Org. Chem.* **1983***, 48*, 1536.
34. Tashiro, M.; Tsuge, A.; Savada, T.; Makishima, T.; Horie, S.; Arimura, T.; Matake, S.; Yamato, T. *J. Org. Chem.* **1990**, *55*, 2404.
35. Khan, I. U.; Takemura, H.; Suenaga, M.; Shinmyozu, T.; Inazu, T. *J. Org. Chem.* **1993**, *58*, 3158.
36. Takemura, H.; Shinmyozu, T.; Miura, H.; Khan, I. U. *J. Incl. Phenom.* **1994**, *19*, 193-206.
37. Hampton, P. D.; Tong, W.; Wu, S.; Duesler, E. N. *J. Chem. Soc. Perkin Trans. 2*, **1996**, 1127.
38. Sone, T. Ohba, Y.; Moriya, K.; Kumada, H.; Ito, K. *Tetrahedron* **1997**, *53*, 10689.
39. Akdas, H.; Bringel, L.; Graf, E.; Hosseini, M. W.; Mislin, G.; Pansanel, J.; Cian,A. D.; Fischer, J. *Tetrahedron Lett.* **1998***,* 2311.
40. Lhoták, P.; Himl, M.; Pakhomova, S.; Stibor, I. *Tetrahedron Lett.* **1998***,* 8915.
41. Bissell, R. A.; de Silva, A. P.; Gunaratne, H. Q. N.; Lynch, P. L. M.; Maguire, G. E. M.; Sandanayake, K. R. A. S. *Chem. Soc. Rev.* **1992**, 187.
42. Wiskur, S. L.; Ait-Haddou, H.; Lavigne, J. J.; Anslyn, E. V. *Acc. Chem. Res.* **2001**, *34*, 963.
43. Jin, T.; Ichikawa, K.; Koyama, T. *J. Chem. Soc., Chem. Commun.* **1992**, 499.
44. Aoki, I.; Kawabata, H.; Nakashima, K.; Shinkai, S. *J. Chem. Soc., Chem. Commun.* **1991**, 1771.
45. Aoki, I.; Sakaki, T.; Shinkai, S. *J. Chem. Soc., Chem. Commun.* **1992**, 730.
46. Ji, H.-F.; Dabestani, R.; Brown, G. M.; Sachleben, R. A. *Chem. Commun.* **2000**, 833.
47. Ji, H.-F.; Dabestani, R.; Brown, G. M.; Hettich, R. L. *J. Chem. Soc*., *Perkin Trans. 2* **2001**, 585.

48. Ji, H.-F.; Brown, G. M.; Dabestani, R. *Chem. Commun.* **1999**, 609.
49. Leray, I.; O'Reilly, F.; Jiwan, J.-L. H.; Soumillion, J.-Ph.; Valeur, B. *Chem. Commun.* **1999**, 795
50. Gutsche, C. D. In *Calixarene: Monographs in Supramolecular Chemistry*; Stoddart, J. F., Ed.; Royal Society of Chemistry:Cambridge, U.K., 1989; Vol. 1.
51. Gutsche, C. D. In *Synthesis of Macrocycles: Design of Selecti*Ve *Complexing Agents*; Izatt, R. M., Christensen, J. J., Eds.; Wiley: New York, 1987; p 93.
52. Vicens, J., Bo¨hmer, V., Eds. *Calixarenes*: *A Versatile Class of Macrocyclic Compounds*;
53. Kluwer: Dordrecht, The Netherlands, 1991 Bo¨hmer, V.; McKervey, M. A. *Chem. Unserer Zeit* **1991**, *25*, 195
54. Gutsche, C. D. In *Inclusion Compounds*; Atwood, J. L., Davies, J. E. D., MacNicol, D. D., Eds.; Oxford University Press: New York, 1991; Vol. 4, p 27.
55. Van Loon, J.-D.; Verboom, W.; Reinhoudt, D. N. *Org. Prep. Proced. Int.* **1992**, *24*, 437.
56. Ungaro, R.; Pochini, A. In *Frontiers in Supramolecular Organic Chemistry and Photochemistry*; Schneider, H.-J., Ed.; VCH: Weinheim, Germany, 1991; p 57
57. Asfari, Z., Bo¨hmer, V., Harrowfield, J., Vicens, J., Eds. *Calixarenes2001*.
58. Kluwer Academic Publishers: Dordrecht, The Netherlands, 2001.
59. Jin, T.; Ichikawa, K.; Koyama, T. *J. Chem. Soc., Chem. Commun.* **1992**, 499.
60. Nishizawa, S.; Kaneda, H.; Uchida, T.; Teramae, N. *J. Chem. Soc., Perkin Trans. 2* **1998**, 2325.
61. Hossain, M. A.; Mihara, H.; Ueno, A. *J. Am. Chem. Soc.* **2003**, *125*, 11178.
62. Takakusa, H.; Kikuchi, K.; Urano, Y.; Higuchi, T.; Nagano, T. *Anal. Chem.* **2001**, *73*, 939
63. Arduini, M.; Felluga, F.; Mancin, F.; Rossi, P.; Tecilla, P.; Tonellato, U.; Valentinuzzi, N. *Chem. Commun*. **2003**, 1606.
64. de Silva, A. P.; Gunaratne, H. Q. N.; Gunnlaugsson, T.; Huxley, A. J. M; McCoy, C. P.; Rademacher, J. T.; Rice, T. E. *Chem. Rev.* **1997**, *97*, 1515.
65. Valeur, B.; Leray, I. *Inorg. Chim. Acta* **2007**, *360*, 765.
66. Kim, S. H.; Kim, H. J.; Yoon, J.; Kim, J. S. In *Calixarenes in the Nanoworld*; Vicens, J., Harrowfield, J., Eds.; Springer: Dordrecht, The Netherlands, 2007; Chapter 15.
67. Fabbrizzi, L.; Poggi, A. *Chem. Soc. Rev.* **1995**, 197.

68. Valeur, B.; Bourson, J.; Pouget, J.; Czarnik, A. W. *Fluorescent Chemosensors for Ion and Molecule Recognition*; ACS Symposium Series 538; American Chemical Society: Washington, DC, 1993; p25.
69. Dixon, A. J.; Benham, G. S. *Int. Lab*. **1988**, *4*, 38.
70. Tan, W.; Shi, Z. Y.; Kopelman, R. *Anal. Chem.* **1992**, *64*, 2985.
71. Sharp, S. L.; Warmack, R. J.; Goudonnet, J. P.; Lee, I.; Ferrell, T. L. *Acc. Chem. Res.* **1993**, *26*, 377.
72. Valeur, B. *Molecular fluorescence*; Wiley-VCH: Weinheim, Germany, 2001.
73. Lakowicz, J. R., Ed. *Principles of Fluorescence Spectroscopy*; Plenum Publishers Corp.: New York, 1999.
74. Kim, J. S.; Noh, K. H.; Lee, S. H.; Kim, S. K.; Kim, S. K.; Yoon. J. *J. Org. Chem.* **2003**, *68*, 597.
75. Kim, J. S.; Shon, O. J.; Rim, J. A.; Kim, S. K.; Yoon, J. *J. Org. Chem.* **2002**, *67*, 2348.
76. Unob, F.; Asfari, Z.; Vicens, J. *Tetrahedron Lett.* **1998**, *39*, 2951.
77. Fabbrizzi, L.; Licchelli, M.; Pallavicini, P.; Perotti, A.; Taglietti, A.; Sacchi, D. *Chem. Eur. J.* **1996**, *2*, 75.
78. De Santis, G.; Fabbrizzi, L.; Licchelli, M.; Mangano, C.; Sacchi, D. *Inorg. Chem.* **1995**, *34*, 3581.
79. De Santis, G.; Fabbrizzi, L.; Licchelli, M.; Sardone, N.; Velders, A. H. *Chem. Eur. J.* **1996**, *2*, 1243.
80. Bergonzi, R.; Fabbrizzi, L.; Licchelli, M.; Mangano, C. *Coord. Chem. Rev.* **1998**, *170*, 31.
81. Suppan, P. *Chemistry and Light*; The Royal Society of Chemistry: Cambridge, U.K., 1994.
82. Rettig, W.; Lapouyade, R. In *Probe design and chemical sensing*; Lakowicz, J. R., Ed.; Topics in Fluorescence Spectroscopy; Plenum: New York, 1994; Vol. 4, p 109.
83. Lo¨hr, H.-G.; Vo¨gtle, F. *Acc. Chem. Res*. **1985**, *18*, 65.
84. Birks, J. B. *Photophysics of Aromatic Molecules*; John Wiley: New York, 1970; Chapter 7.
85. Klopffer, W. In *Organic Molecular Photophysics*; Birks, J. B., Ed.; Wiley: New York, 1973; Vol. 1, Chaper 7.
86. Birks, J. B.; Lumb, M. D.; Munro, I. H. *Proc. R. Soc. London* **1964**, *A280*, 289.

87. Kim, S. K.; Lee, S. H.; Lee, J. Y.; Lee, J. Y.; Bartsch, R. A.; Kim, J. S. *J. Am. Chem. Soc.* **2004**, *126*, 16499.
88. Winnik, F. M. *Chem. Rev.* **1993**, *93*, 587.
89. Lee, S. H.; Kim, S. H.; Kim, S. K.; Jung, J. H.; Kim, J. S. *J. Org. Chem.* **2005**, *70*, 9288.
90. Lee, J. Y.; Kim, S. K.; Jung, J. H.; Kim, J. S. *J. Org. Chem.* **2005**, *70*, 1463.
91. Winnik, M. A. *Chem. Rev.* **1981**, *81*, 491.
92. Wang, Y. C.; Morawetz, H. *J. Am. Chem. Soc*. **1976**, *98*, 3611.
93. Morawetz, H. *J. Lumin.* **1989**, *43*, 59.
94. Goldenberg, M.; Emert, J.; Morawetz, H. *J. Am. Chem. Soc*. **1978**, *100*, 7171.
95. Stryer, L.; Haugland, R. P. *Proc. Natl. Acad. Sci. U.S.A.* **1967**, *58*,719.
96. Chang, K.-C.; Luo, L.-Y.; Diau, E. W.-G.; Chung, W.-S. *Tetrahedron Lett*. **2008**, *49*, 5013.
97. Cao, Y.-D.; Zheng, Q.-Y.; Chen, C.-F.; Huang, Z.-T. *Tetrahedron Lett.* **2003**, *44*, 4751.
98. Choi, J. K.; Kim, S. H.; Yoon, J.; Lee, K.-H.; Bartsch, R. A.; Kim, J. S. *J. Org. Chem.* **2006**, *71*, 8011.
99. Senthilvelan, A.; Ho, I.-T.; Chang, K.-C.; Lee, G.-H.; Liu, Y.-H.; Chung, W.-S. *Chem. Eur. J*. **2009**, *15*, 6152.
100. Bodenant, B.; Weil, T.; Businelli-Pourcel, M.; Fages, F.; Barbe, B.; Pianet, I.; Laguerre, M. *J. Org. Chem*. **1999**, *64*, 7034.
101. Gruber, T.; Fischer, C.; Felsmann, M.; Seichter, W.; Weber, E. *Org. Biomol. Chem*. **2009**, *7*, 4904.
102. Kumar, M.; Dhir, A.; Bhalla, V. *Org. Lett.* **2009**, *11*, 2567.
103. Kumar, M.; Dhir, A.; Bhalla, V. *Eur. J. Org. Chem.* **2009**, 4534.
104. Kumar, M.; Dhir, A.; Bhalla, V. *Tetrahedron* **2009**, *65*, 7510.
105. Lee, S. H.; Kim, S. H.; Kim, S. K.; Jung, J. H.; Kim, J. S. *J. Org. Chem.* **2005**, *70*, 9288.
106. Chang, K.-C.; Su, I.-H.; Senthilvelan, A.; Chung, W-S. *Org. Lett*. **2007**, 9, 3363.
107. Kim, S. K.; Lee, J. K.; Lim, J. M.; Kim, J. W.; Kim, J. S. *Bull. Korean Chem. Soc*. **2004**, *25*, 1247.
108. Métivier, R.; Leray, I.; Valeur, B. *Chem. Commun.* **2003**, 996.
109. Kim, J. H.; Hwang, A.-R.; Chang, S.-K. *Tetrahedron Lett*. **2004**, *45*, 7557.

110. Cha, N. R.; Kim, M. Y.; Kim, Y. H.; Choe, J.-I.; Chang, S.-K. *J. Chem. Soc., Perkin Trans. 2* **2002**, 1193.

111. (a) Talanova, G. G.; Elkarim, N. S. A.; Talanov, V. S.; Bartsch, R. A. *Anal. Chem*. **1999**, *71*, 3106. (b) M_etivier, R.; Leray, I.; Valeur, B. *Chem.-Eur. J*. **2004**, *10*, 4480.

112. Ocak, U.; Ocak, M.; Surowiec, K.; Bartsch, R. A.; Gorbunova, M. G.; Tu, C.; Surowiec, M. A. J. *Inclusion Phenom. Macrocyclic Chem*. **2009**, *63*, 131.

113. Chen, Q.-Y.; Chen, C.-F. *Tetrahedron Lett*. **2005**, *46*, 165.

114. Tian, D.; Yan, H.; Li, H. *Supramol. Chem*. **2010**, *22*, 249.

115. Othman, A. B.; Lee, J. W.; Wu, J.-S.; Kim, J. S.; Abidi, R.; Thuery, P.; Strub, J. M.; Van Dorsselaer, A.; Vicens, J. *J. Org. Chem*. **2007**, *72*, 7634.

116. Kumar, A.; Ali, A.; Rao, C. P. J. *Photochem. Photobiol., A* **2006**, *177*, 164.

117. Dessingou, J.; Joseph, R.; Rao, C. P. *Tetrahedron Lett*. **2005**, *46*, 7967.

118. Park, S-Y.; Yoon, J-H.; Hong, C-S.; Souane, R.; Kim, J.-S. Matthews, S. E., Vicens, J. *J. Org. Chem.* **2008**, *73*, 8212.

119. Zhu, L.-N.; Gong, S.-L.; Gong, S.-L.; Yang, C.-L.; Qin, J.-G. *Chin. J. Chem*., **2008**, *26*, 1424.

120. Bagatin, I. A.; de Souza, E. S.; Ito, A. S.; Toma, H. E. *Inorg. Chem. Commun*. **2003**, *6*, 288.

121. Zhang, J. F.; Bhuniya, S.; Lee, Y. H.; Bae, C.; Lee, J. H.; Kim, J. S. *Tetrahedron Lett*. **2010**, *51*, 3719.

122. Takeshita, M.; Shinkai, S. *Chem. Lett.* **1994**, 1349.

123. Takeshita, M.; Shinkai, S. *Chem. Lett.* **1994**, 125.

124. Lee, S. H.; Kim, H. J.; Lee, Y. O.; Vicens, J.; Kim, J. S. *Tetrahedron Lett*. **2006**, *47*, 4373.

125. Kim, H. J.; Kim, S. K.; Lee, J. Y.; Kim, J. S. *J. Org. Chem*. **2006**, *71*, 6611.

126. Schazmann, B.; Alhashimy, N.; Diamond, D. *J. Am. Chem. Soc.* **2006**, *128*, 8607.

127. Morales-Sanfrutos, J.; Ortega-Muñoz, M.; Lopez-Jaramillo, J.; Hernandez-Mateo, F.; Santoyo-Gonzalez, F. *J. Org. Chem*. **2008**, *73*, 7768.

128. Chen, Q.-Y.; Chen, C.-F. *Eur. J. Org. Chem*. **2005**, 2468.

129. Liu, S.-Y.; He, Y.-B.; Wu, J.-L.; Wei, L.-H.; Qin, H.-J.; Meng, L.-Z.; Hu, L. *Org. Biomol. Chem*. **2004**, *2*, 1582.

Chapter 2

Synthesis, Crystal Structure and Complexation Behaviour of A Thiacalix[4]arene Bearing 1,2,3-Triazole Groups

*This chapter focused on the structure and complexation behavior of 1,3-alternate-1,2,3-triazole based on thiacalix-[4]arene, 1,3-alternate-**1** and **2**, which have been determined by means of X-ray analysis, fluorescence and ^{1}H NMR spectroscopy. The X-ray results suggested that the nitrogen atom N3 on triazole ring can act as hydrogen bond acceptors in the self-assembly of a supramolecular structure.*

2.1 Introduction

Recently, there has been intense interest in the design and synthesis of receptors and sensors based on 1,2,3-triazole derivatives, which has resulted primarily from the work of Meldal[1] and Sharpless[2] on the Cu(I) catalysis of 1,3-dipolar cycloaddition of alkynes and azides. Such 1,2,3-triazoles find potential application in organic synthesis,[3] biological molecular systems,[4,5] medical[6,7] and materials chemistry.[8–10] The properties of the 1,2,3-triazole moiety as a linker in multivalent derivatives can be exploited for the binding of cations, typified by the accelerated catalysis of the "click" reaction by *in situ* formation of copper complexes.[11] The coordination chemistry of the triazole group has also been investigated through the formation of transition metal complexes of a range of bis-triazoles.[12,13] Cation binding properties of triazoles have been shown to have potential in the radiolabeling of biomolecules.[14] At the same time, it has been shown that the polarity of neutral 1,4-disubstituted aryl-1,2,3-triazoles and of the C5-H bond can create an electropositive site that can function as an effective hydrogen bond donor for anion binding. For example, Li *et al* have synthesized a macrocyclic receptor that is devoid of conventional X-H hydrogen-bond donors but interacts exclusively *via* C-H···chloride contacts.[15–18]

In calixarene chemistry, a copper catalyzed 1,2,3-triazole has previously been exploited by Zhao and co-workers for the functionalization of a calixarene scaffold.[19] More relevant to this work have been investigations by others on the selective binding of various metal cations *via* the use of calixarene scaffolds suitably functionalized with triazoles.[20–25] For example, Chung and co-workers have developed Ca^{2+} and Pb^{2+} chromogenic selective sensors through the introduction of triazole binding sites at the lower rim of calix[4]arene,[20] resulting in on-off switchable fluorescent sensors.[21]

Similarly, thiacalix[4]arenes[26–29] have received growing interest since their discovery in 1997, due to their novel features; their use as platforms is an emerging area. Di- or poly-topic receptors, constructed with two or more binding subunits in a single molecule, have been reported.[30] Such systems are suitable candidates for the allosteric regulation of host–guest interactions with metal cations. In particular, the so-called 1,3-*alternate* conformation of calix[4]arene, which has D_{2h} symmetry (tube-shaped),[31–34] can be suitably adapted for the formation of 1:1 as well as 1:2 complexes owing to its symmetrical ditopic arrangement.

In this chapter, we report on the synthesis, crystal structures and complexation properties of 1,3-*alternate*-**1** and **2** based on thiacalix[4]arene scaffold.

2.2 Results and Discussion

2.2.1 Syntheses of compounds 1,3-alternate-1 and 2

The syntheses of 1,3-*alternate*-**1** and **2** are shown in Scheme 1. In our previous work, we regioselective synthesis of the controlled conformation of thiacalix[4]arene derivatives by a protection-deprotection method using benzyl groups as a protecting group, and the result demonstrated that solid superacid (Nafion-H) is a good catalyst for the present deprotection of benzyl group.[28] Hence, the *O*-alkylation of thiacalix[4]arene

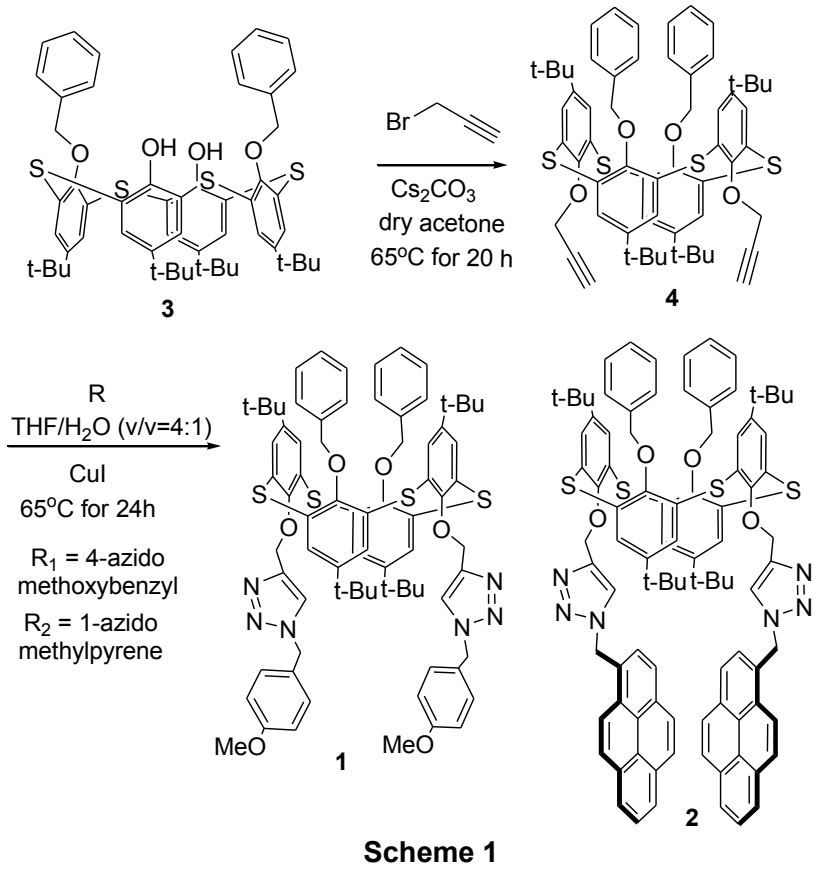

Scheme 1. The synthetic route of receptors 1,3-*alternate*-**1** and **2**.

was carried out with 10 equiv. of benzyl bromide in the presence of 10 equiv. of Na_2CO_3 according to the reported procedure[28] to afford *distal*-**3** in 93% yield. Compound **4** was prepared by the reaction of *distal*-**3** with propargyl bromide in the presence of 10 equiv. of Cs_2CO_3 in dry acetone in 81% yield. The Cu(I)-catalyzed 1,3-dipolar-cycloaddition reaction of 1,3-*alternate*-**4** with 4-azidomethoxybenzyl under Click conditions afforded 1,3-*alternate*-**1** in a yield of 74%. The latter procedure was also employed in the synthesis of 1,3-*alternate*-**2** from the reaction with 1-azidomethylpyrene with a yield of 51%. The product structures were supported by their spectroscopic and analytical data. For example, The ^{1}H NMR spectrum of 1,3-*alternate*-**1** shows two singlets for the *tert*-butyl protons at δ 0.79 and 1.13 ppm; the former peak is observed at a higher field due to the ring current effect arising from the two inverted benzene ring of benzyl groups. Other signals in the ^{1}H NMR spectrum may correspond to either the *cone* or 1,3-*alternate* conformer which differ only slightly in their observed chemical shifts.[35] Fortunately, the 1,3-*alternate* conformation of compound 1,3-*alternate*-**1** was also confirmed by a single-crystal X-ray diffraction study, and the structure is shown in Figure 1.

2.2.2 Crystal Structures of 1,3-alternate-1

Compound 1,3-*alternate*-**1** adopts a ‘‘1,3-*alternate* conformation’’, with the four sulfur atoms forming an almost square plane (S_4 plane) (Figure 1); the dihedral angles between the S_4 plane and substituted phenyl rings are 76.45(3) and 79.19(3)° (1,2,3-triazole substituted) and 87.50(3) and 72.61(3)° (benzyl substituted), respectively. The distances between the centres of opposite calix benzene rings of the calixarene are 6.013 Å and 5.733 Å, respectively.

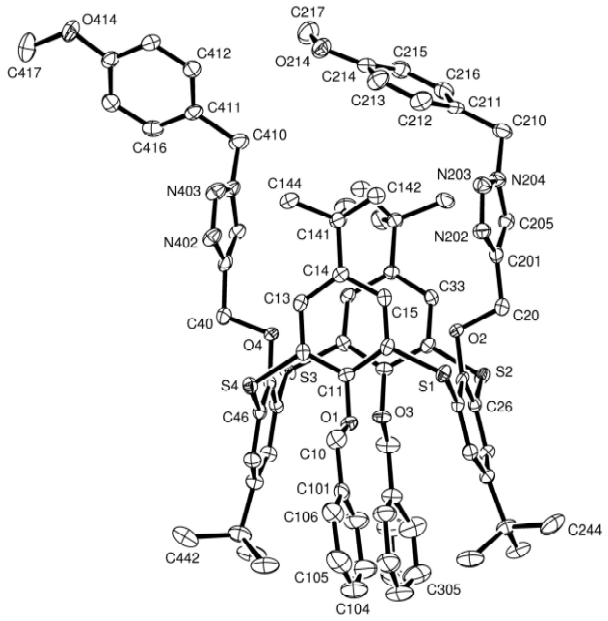

Figure 1. X-ray structure of 1,3-*alternate*-**1**. The thermal ellipsoids are drawn at 50% probability; hydrogen atoms are omitted for clarity.

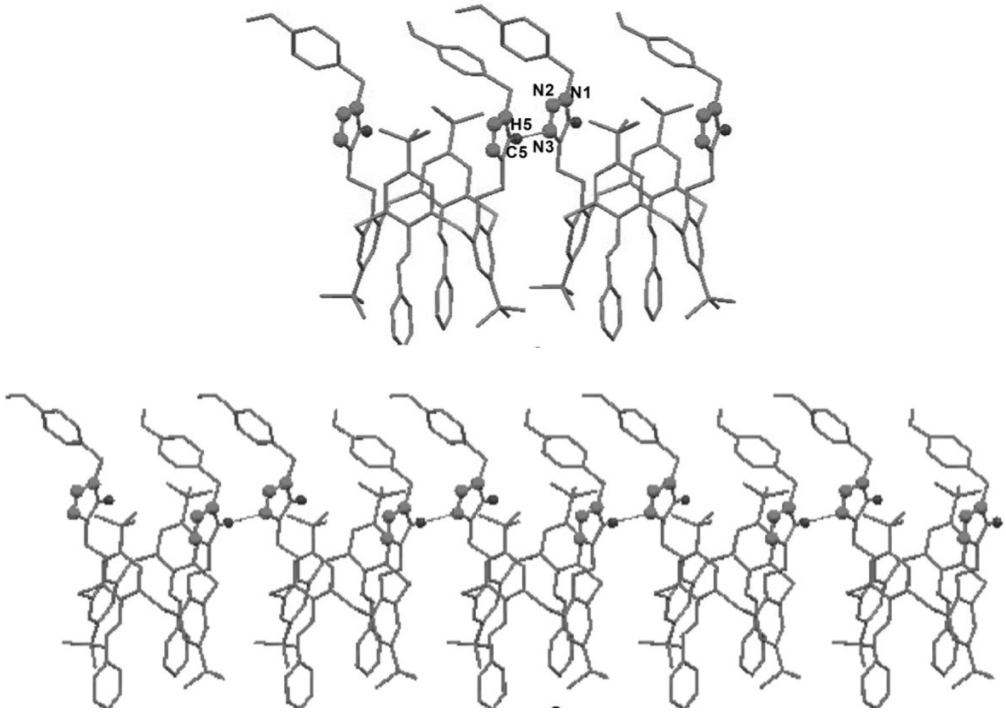

Figure 2. C-H···N hydrogen bonding: between N3 and C5-H in 1,3-*alternate*-**1** and 1D supramolecular chains constructed through C-H···N interactions in 1,3-*alternate*- **1**. Others hydrogen atoms are omitted for clarity**.**

Ghadiri and co-workers have shown that triazole units can act as amide mimics enabling protein folding by virtue of the strongly polarized C5-H bond of the triazole ring acting as a hydrogen bond donor[36] and the N3 atom acting as a hydrogen bond acceptor: an amide/peptide bond mimic. This result demonstrated the unique properties of the 1,4-disubstituted 1,2,3-triazole ring in terms of its ability to participate in hydrogen bonding and dipole-dipole interactions. As shown in Figure 1, in the crystal structure of 1,3-*alternate*-**1**, the thiacalix[4]arene unit contains two nearly parallel 1,2,3-triazole groups functionalized with the 4-methoxybenzene moiety. It is clearly shown, Figure 2, that the N3 atom, N(402), of one 1,2,3-triazole tethered to a thiacalix[4]arene also acts as acceptor of an intermolecular hydrogen bond from the C5-H, C(205)-H(205) group of an adjacent molecule, with an H···N distance of 2.40 Å; thus, molecules are linked in chains.

2.2.3 Fluorescence Spectroscopy Studies

In order to better evaluation the recognition properties of 1,2,3 triazole groups based on thiacalix[4]arene, 1,3-*alternate*-**2** has been synthesized(*37*), in which the methoxybenzyl unit of 1,3-*alternate*-**1** was replaced by the pyrene moiety as a fluorophore(*38–41*). Consequently, the binding behaviour of 1,2,3 triazole moieties based on thiacalix[4]arene toward different metal cations can be facile investigated by fluorescence spectroscopy. As shown in Figure 3, the fluorescence spectra of 1,3-*alternate*-**2** displayed a typical excimer emission around 485 nm and monomer emissions around 378 and 396 nm in CH_3CN/CH_2Cl_2 (1000:1, v/v) with excitation wavelength at 343 nm. On addition of various metal ions such as Li^+, Na^+, K^+, Cs^+, Zn^{2+}, Pb^{2+}, Ag^+, Cu^{2+}, Hg^{2+}, Cd^{2+}, Ni^{2+}, Co^{2+}, and Cr^{3+} as their perchlorates salts in aqueous

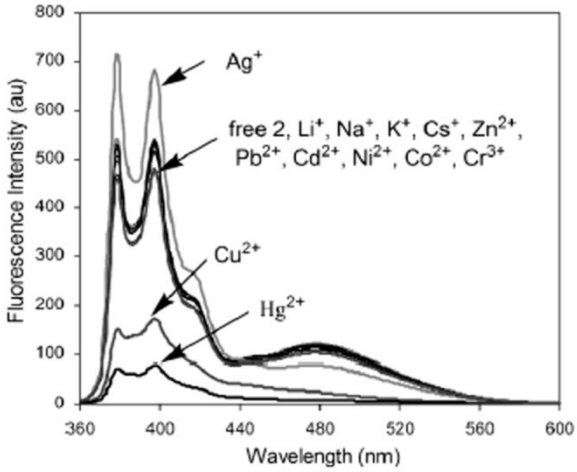

Figure 3. Fluorescence spectra of the receptor **2** (5.0 μM) in CH_3CN/CH_2Cl_2 (1000:1, v/v) at 298 K upon addition of various metal ions (100 μM) as their aqueous solution.

solution. As can be seen, when upon addition of Ag^+ ion into the solution of receptor **2**, an obviously enhancement of the monomer emission was occurred, whilst the accompanying excimer emission decreased. On the other hand, both the excimer and monomer emissions of 1,3-*alternate*-**2** were acutely quenched by Cu^{2+}, and Hg^{2+}, and much weaker fluorescence quenching were observed by addition of Pb^{2+}, Ni^{2+}, Co^{2+}, and Cr^{3+} ions compared to Cu^{2+}, and Hg^{2+}. No significant fluorescence intensity changes were given upon addition of alkali metal ions. Basically, the quenching in excimer emission of receptor **2** is due to a conformational change that occurred during the complexation of related metal ions with the nitrogen atoms on the triazole rings, which make it is not possible for the pyrene moieties to stack together for excimer emission, whereas the quenching in monomer emission of receptor **2** is may be attributed to reverse PET from pyrene groups to the nitrogen atom of the triazole units[42] or a heavy atom effect.[43]

Figure 4 shows the fluorescence spectra of receptor **2** at various concentrations of Ag^+ ion, upon addition of increasing amounts of Ag^+ as its perchlorate salt from 1 to 100 μM to the solution of receptor **2**, there was a significant enhancing monomer emission at 378 nm and a companying excimer emission decreasing at 485 nm observed. On the basis of the titration experiments data, the association constant (K_a) for **2**•Ag^+ was thus calculated to be 5.40×10^4 M^{-1} by a Benesi–Hilderbrand plot (Figure 5).[44] In the job pot (inset of Figure 4),[45] a

maximum fluorescence intensity change was appeared at 0.5 in the molar fraction of receptor **2** vs Ag^+ ion, which clearly indicated a 1:1 complex of receptor **2** with Ag^+ ion.

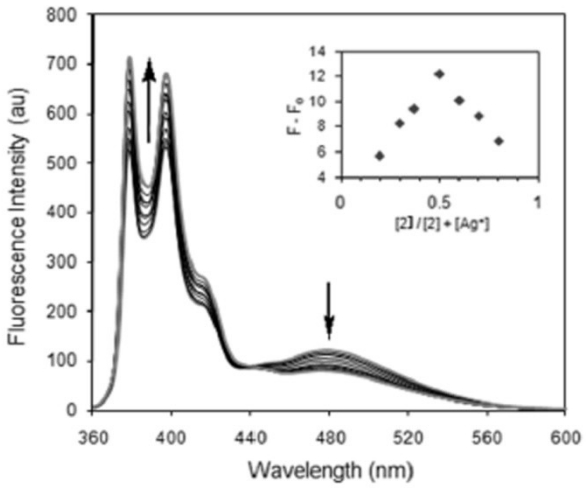

Figure 4. Fluorescence intensity changes of **2** (5.0 μM) upon addition of increasing concentrations of Ag^+ ion in aqueous solution (0-100 μM) at 298 K in CH_3CN/CH_2Cl_2 (1000:1, v/v) with an excitation at 343 nm. Inset: Job's plot showing a 1:1 stoichiometry.

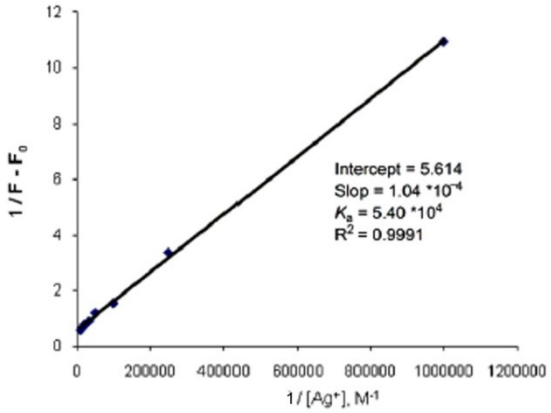

Figure 5. Benesi-Hilderbrand plot of **2** with $AgClO_4$.

The practical applicability of receptor **2** as a selective chemosensor to Ag^+ ion was evaluated by competitive experiment. As shown in Figure 6, the fluorescence intensity was almost identical of that obtained in the absence of other cations suggested that no obviously

interference to the selective response of receptor **2** to Ag^+ ion at the presence of most competitive metal ions, except for Hg^{2+} interference with the detection signal by abolished the ratiometric effect on complexation of Ag^+ ion.

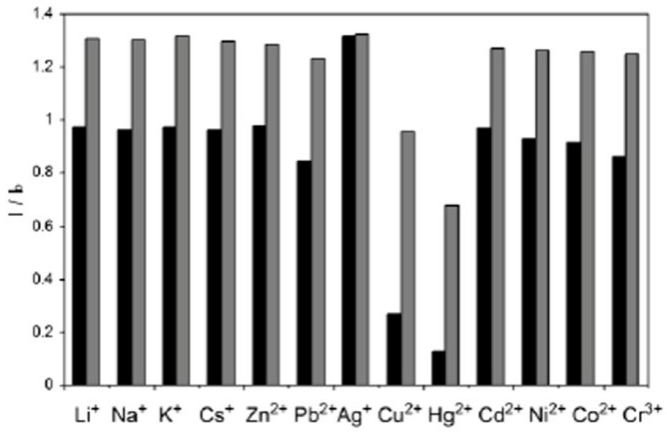

Figure 6. Fluorescence response of **2** (5.0 μM) in CH_3CN/CH_2Cl_2 (1000:1, v/v) to 100 μM various tested metal ions (black bar) and to the mixture of 100 μM tested metal ions with 100 μM Ag^+ ion (gray bar) at 298K. I_0 is the fluorescence intensity at 378 nm for free **2**, and I is the fluorescence intensity after adding metal ions with an excitation at 343 nm.

2.2.4 Proton NMR Studies

The complexation modes of receptor **2** with silver ion also investigated by ^{1}H NMR spectroscopy. **Figure 7** shows the partial ^{1}H NMR spectra of receptor **2** in the absence and presence of Ag^+ ion in a mixture solution of $CDCl_3/CD_3CN$ (10:1, v/v). Upon addition of 1.0 equiv of Ag^+ ion to the solution of receptor **2**, some significant chemical shifts changes are observed in the ^{1}H NMR spectra. For example, the proton H_b on the triazole ring undergoes a significant downfield chemical shift from δ 7.47 to 7.79 ppm (Δδ = 0.32), and the proton H_c on the O-*CH*$_2$-triazole also moves downfield shift from δ 4.61 ppm to δ 5.01 ppm, whereas the peak of protons H_a and H_d are not undergo an obviously changes in the presence of Ag^+ cation. These results strongly suggested that silver cation can be selectivity bound by the nitrogen atoms of the triazole rings. On the other hand, the chemical shift changes of protons on the phenol of thiacalix[4]arene scaffold indicated that the ionophoricity cavity, which

formed by the two inverted benzene rings with the sulfur atoms framework based on thiacalix[4]arene, are also involved in binding with the silver ion.[46–48]

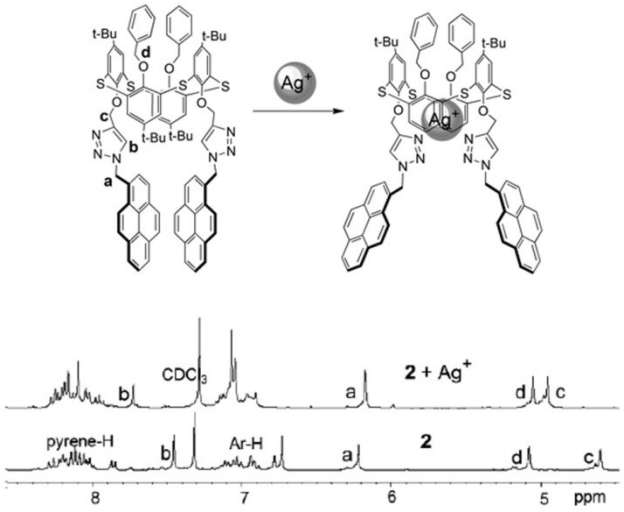

Figure 7. Proposed structure for 1,3-*alternate*-**2** on complexation with silver cation, and ^{1}H NMR spectra of 1,3-*alternate*-**2** in $CDCl_3/CD_3CN$ (10:1) and in the presence of 1.0 equiv of $AgClO_4$ at 298 K ; (partial *tert*-Butyl moieties are omitted for clarity).

2.3 Conclusions

In summary, the synthesis, structure and complexation behaviour of 1,2,3-triazole ring based on 1,3-*alternate*-thiacalix[4]arene, has been investigated by X-ray analysis, fluorescence and ^{1}H NMR spectroscopy. These experimental results suggested that the nitrogen atoms on the triazole moiety of a thiacalix[4]arene have a strong binding affinity for Ag^+ ion. We expect the novel electronic properties of triazole ring; such as the large dipole moment and electropositive C5–H group will lead to their increasing use as valuable design tools for self-assembly of supramolecular chemistry and cation binding sites of receptors. Further investigation of 1,2,3-triazole-based calixarenes is currently on going.

2.4 Experimental Section

2.4.1 General

All melting points (Yanagimoto MP-S1) are uncorrected. ^{1}H NMR spectra were recorded at 300 MHz with a Nippon Denshi JEOL FT-300 NMR spectrometer with $SiMe_4$ as an internal reference: J-values are given in Hz. Mass spectra were obtained on a Nippon Denshi JMS-01SA-2 spectrometer at 75 eV using a direct-inlet system through GLC. Elemental analysis: Yanaco MT-5.

2.4.2 Materials.

5,11,17,23-Tetra-*tert*-butyl-25,27-dibenzyloxy-26,28-dihydroxy-2,8,14,20-tetrathia-calix[4]arene **3** was prepared according to the reported procedure.[28]

2.4.2.1. 5,11,17,23-Tetra-tert-butyl-25,27-dibenzyloxy-26,28-[bis-(propargyloxy)]-2,8,14,20- tetrathiacalix[4]arene (4)

A suspension of *distal*-**3** (300 mg, 0.333 mmol) and Cs_2CO_3 (1.085 g, 3.33 mmol) was refluxed for 1 h in dry acetone (15 ml). A solution of 3-bromo-1-propyne [propargyl bromide (396 mg, 3.33 mmol)] in dry acetone (10 ml) was added and the mixture refluxed for 20 h. The solvents were evaporated and the residue partitioned between 10% HCl and CH_2Cl_2. The organic layer was dried ($MgSO_4$) and evaporated. The residue was recrystallized from $CHCl_3$/hexane (1:3, v/v) to afford the desired product **4** as colourless prisms with a yield of 81% (263.5 mg). Mp 180–182°C. ^{1}H NMR (300 MHz, $CDCl_3$) δ 0.60, 0.85, 0.98, 1.11, 1.31 (each s, 36H, *t*Bu), 2.20–2.51, 4,41–5.08 (m, 10H, acetylene-*H,* ArO-*CH*$_2$-acetylene and ArO-*CH*$_2$-Ph) and 7.0–8.8 (18H, m, Ar*H*). FABMS: *m/z* 977.4 (M^+). Anal. calcd for $C_{60}H_{64}O_4S_4$ (977.42): C, 73.74; H, 6.61. found: C, 74.10; H, 6.67. The splitting pattern in ^{1}H NMR shows that the isolated compound is a mixture of *cone*- and *partial-cone*-**4**. Compoun **4** was not further isolated and directly used for next reaction.

2.4.2.2. 5,11,17,23-Tetra-tert-butyl-25,27-dibenzyloxy-26,28-bis{[1H-(4-methoxybenzyl)-(1,2,3-triazolyl)]-4-methoxy}-2,8,14,20-tetrathiacalix[4]-arene(1,3-alternate-1)

Copper iodide (5 mg) was added to compound **4** (112 mg, 0.12 mmol) and 4-methoxybenzyl azide (58 mg, 0.36 mmol) in 40 ml mixture of THF/H_2O (v/v = 4:1) and the mixture was heated at 65°C for 24 h. The resulting solution was cooled and extracted thrice with $CHCl_3$. The organic layer was separated and dried ($MgSO_4$) and evaporated to give the

solid crude product. The residue was eluted from a chromatographic column of silica gel with hexane/ethyl acetate (v/v = 1:1) to give the desired product 1,3-*alternate*-**1** (112 mg, 74%). Recrystallization from $CHCl_3$ /hexane afforded X-ray quality colourless crystals. Mp 180–182°C. ^{1}H NMR (300 MHz, $CDCl_3$) δ 0.79 (s, 18H, *t*Bu), 1.13 (s, 18H, *t*Bu), 3.78 (s, 6H, OMe), 4.89 (s, 4H, CH_2), 5.16 (s, 4H, CH_2), 5.46 (s, 4H, CH_2), 6.82 (s, 4H, ArH), 6.85 (d, *J*= 8.4 Hz, 4H, ArH), 7.23–7.02 (m, 14H, ArH), 7.34 (s, 4H, ArH) and 7.40 (s, 2H, Triazole-H). ^{13}C NMR (75 MHz, $CDCl_3$) δ 30.69, 30.76, 33.74, 34.09, 53.37, 55.23, 62.93, 72.10, 114.26, 122.84, 126.83, 127.25, 127.98, 128.02, 129.41, 129.47, 129.62, 131.56, 137.82, 144.04, 145.94, 146.18, 155.67, 157.61 and 159.68. FABMS: *m*/*z* 1303.50 (M^+). Anal. calcd for $C_{76}H_{82}N_6O_6S_4$ (1303.76): C, 70.01; H, 6.34; N, 6.45. found: C, 69.71; H, 6.35; N, 6.37.

2.4.2.3. 5,11,17,23-Tetra-tert-butyl-25,27-bisbenzyl-26,28-bis[1H-(1-pyrenylmethyl- (1,2,3-triazolyl)-4-methoxy)]-tetrathiacalix[4]arene (1,3-alternate-2)

Copper iodide (20 mg) was added to compound **4** (112 mg, 0.12 mmol) and 1-azidomethylpyrene (92 mg, 0.36 mmol) in 20 mL THF/H_2O (4:1) and the mixture was heated at 65 °C for 24 h. The resulting solution was cooled and diluted with water and extracted trice with CH_2Cl_2. The organic layer was separated and dried ($MgSO_4$) and evaporated to give the solid crude product. The residue eluted from a column chromatography of silica gel with hexane/CH_2Cl_2 (1:1, v/v) to give the desired product (92 mg, 51%). Mp 134–136°C. ^{1}H NMR (300 MHz, $CDCl_3$) δ 0.46 (18H, s, tBu), 1.14 (18H, s, tBu), 4.64 (4H, s, CH_2-Triazole), 5.08 (4H, s, CH_2Ph), 6.24 (4H, CH_2-Pyrene), 6.74 (4H, s, ArH), 7.11- 6.9 (14H, m, Ph-H), 7.45 (2H, s, Triazole-H) 7.86-8.28 (18H, m, Pyrene-H). ^{13}C NMR (75 MHz, $CDCl_3$) δ 30.38, 31.25, 33.41, 34.15, 52.26, 63.93, 72.69, 122.29, 123.29, 124.52, 124.84, 125.01, 125.75, 125.79, 126.29, 126.83, 126.97, 127.23, 127.29, 127.34, 127.41, 127.85, 127.99, 128.16, 128.98, 129.24, 129.69, 129.76, 130.62, 131.22, 131.98, 132.98, 137.86, 143.99, 145.58. 146.01, 155.56, 158.09. FABMS: m/z 1491.23 (M^+). Anal. Calcd for $C_{94}H_{86}N_6O_4S_4$ (1491.99): C, 75.67; H, 5.81; N, 5.63. Found: C, 75.35; H, 5.67; N, 5.54.

2.4.3 Crystallography

Crystallographic Data for 1,3-*alternate*-1: Recrystallized from $CHCl_3$/Hexane (1:3). Crystal data: $C_{76}H_{82}O_6N_6S_4$; *M* = 1303.7; crystal system: triclinic; space group: P–1; *a* =

10.5587(2) Å, b =11.2767(2) Å, c =29.5518(5) Å; α =90.906(2)°, β = 93.0121(14)°, γ =101.166(2)°, V =3446.06 (11) Å^3; Z =2; D_c = 1.256 g cm^{-3}; R_{int} = 0.060, R [I > 2σ(I)][a] = 0.038, wR [I > 2σ(I)][b] = 0.078 for 15794 unique reflections. The intensity data of the compound 1,3-*alternate*-**1** were measured on an Oxford Diffraction Xcalibur-3/Sapphire 3 CCD diffractometer. Structural solution was by direct methods in the SHELXS program, and refinement was by full-matrix least-squares methods on F^2 in the SHELXL program.[49] All the non-hydrogen atoms in structure were refined anisotropically. The hydrogen atoms were generated geometrically. Crystallographic data (excluding structure factors) for the structure reported in this paper have been deposited with the Cambridge Crystallographic Data Centre as supplementary publication No. CCDC–786359. Copies of the data can be obtained free of charge on application to CCDC, 12 Union Road, Cambridge CB2 1EZ, UK (fax: +44 1223/336 033; deposit@ccdc.cam.ac.uk).

2.5 References

1 Tornoe, C. M.; Christensen, C; Meldal, M. P. *J. Org. Chem.* **2002**, *67*, 3057–3064.

2 Rostovtsev, V. V.; Green, L. G.; Fokin, V. V.; Sharpless, K. B. *Angew. Chem., Int. Ed.* **2002**, *41*, 2596–2599.

3 Moses, J. E.; Moorhouse, A. D. *Chem. Soc. Rev.* **2007**, *36*, 1249–1262.

4 Bock, V. D.; Hiemstra, H.; van Maarseveen, J. H. *Eur. J. Org. Chem.* **2006**, 51–68.

5 Lutz, J.-F. *Angew. Chem., Int. Ed.* **2007**, *46*, 1018–1025.

6 Angell, Y. L.; Burgess, K. *Chem. Soc. Rev*. **2007**, *36*, 1674–1689.

7 Whiting, M.; Tripp, J. C.; Lin, Y.-C.; Lindstrom, W.; Olson, A. J.; Elder, J. H.; Sharpless, K. B.; Fokin, V. V. *J. Med. Chem.* **2006**, *49*, 7697–7710.

8 Gao, H.; Matyjaszewski, K. *Macromolecules* **2006**, *39*, 4960–4965.

9 Wu, P.; Feldman, A. K.; Nugent, A. K.; Hawker, C. J.; Scheel, A.; Voit, B.; Pyun, J.; Frechet, J. M. J.; Sharpless, K. B.; Fokin, V. V. *Angew. Chem., Int. Ed.* **2004**, *43*, 3928–3932.

10 Fournier, D.; Hoogenboom, R.; Schubert, U. S. *Chem. Soc. Rev.* **2007**, *36*, 1369–1380.

11 Chan, T. R.; Hilgraf, R.; Sharpless, K. B.; Fokin, V. V. *Org. Lett.* **2004**, *6*, 2853–2855.

12 Bronisz, R. *Inorg. Chem.* **2005**, *13*, 4463–4465.

13 Meudtner, R. M.; Ostermeier, M.; Goddard, R.; Limberg, C.; Hecht, S. *Chem. Eur. J.*

2007, *13*, 9834–9840.

14 Mindt, T. L. Struthers, H., Brans, L., Anguelov, T., Schweinsberg, C., Maes, V., Tourwe, D., Schibili, R. *J. Am. Chem. Soc.* **2006**, *128*, 15096–15097.

15 Li, Y.; Flood, A. H. *Angew. Chem., Int. Ed.* **2008**, *47*, 2649–2652.

16 Li, Y.; Flood, A. H. *J. Am. Chem. Soc.* **2008**, *130*, 12111–12122.

17 Juwarker, H.; Lenhardt, J. M.; Pham, D. M.; Craig, S. L. *Angew. Chem., Int. Ed.* **2008**, *47*, 3740–3743.

18 Meudtner, R. M.; Hecht, S. *Angew. Chem., Int. Ed.* **2008**, *47*, 4926–4930.

19 Ryu, E.-H.; Zhao, Y. *Org. Lett.* **2005**, **7**, 1035–1037.

20 Chang, K-C.; Su, I-H.; Lee, G-H.; Chung, W-S. *Tetrahedron Lett.* **2007**, *48*, 7274–7278.

21 Chang, K.-C.; Su, I.-H.; Senthilvelan, A.; Chung, W.-S. *Org. Lett.* **2007**, *9*, 3363–3366.

22 Park, S-Y.; Yoon, J-H.; Hong, C-S.; Souane, R.; Kim, J.-S. Matthews, S. E., Vicens, J. *J. Org. Chem.* **2008**, *73*, 8212–8218.

23 Colasson, B.; Save, M.; Milko, P.; Roithová, J.; Schröder, D.; Reinaud, O. *Org. Lett.* **2007**, *9*, 4987–4990.

24 Zhan, J.; Tian, D.; Li, H. *New J. Chem.* **2009**, *33*, 725–728.

25 Tzadka (Bulkhatsev), E.; Goldberg, I.; Vigalok, A. *Chem. Comm.* **2009**, 2041–2043.

26 Lhoták, P. *Eur. J. Org. Chem.* **2004**, 1675–1692.

27 Morohashi, N.; Narumi, F.; Iki, N.; Hattori, T.; Miyano, S. *Chem. Rev*. **2006**, *106*, 5291–5316.

28 Ni, X.-L.; Tomiyasu, H.; Shimizu, T.; Pérez-Casas, C.; Zeng, X.; Yamato, T. *J. Incl. Phenom. Macrocyclic Chem*. **2010**, *68*, 99–108.

29 Iki, N.; Kabuto, C.; Fukushima, T.; Kumagai, H.; Takeya, H.; Miyanari, S.; Miyashi, T.; Miyano, S. *Tetrahedron* **2000**, *56*, 1437–1443.

30 Lehn, J. M. Supramolecular Chemistry: Concepts and Perspectives.VCH, Weinheim, Germany (1995).

31 Koh, K. N.; Araki, K.; Shinkai, S.; Asfari, Z.; Vicens, J. *Tetrahedron Lett.* **1995**, *36*, 6095–6098.

32 Csokai, V.; Grün, A .; Balázs, B.; Simon, A .; Tóth, G.; Bitter, I. *Tetrahedron* **2006**, *62*, 10215–10222.

33 Stoikov, I. I.; Yushkova, E. A.; Zhukov, A. Y.; Zharov, I.; Antipin, I. S.; Konovalov, A. I.

Tetrahedron **2008**, *64*, 7489–7497.

34 Kumar, M.; Dhir, A.; Bhalla, V. *Tetrahedron* **2009**, *65*, 7510–7497.

35 Pérez-Casas, C.; Yamato, T. *J. Incl. Phenom. Macrocycl. Chem.* **2005**, *53*, 1–8.

36 Horne, W. S.; Yadav, M. K.; Stout, C. D.; Ghadiri, M. R. *J. Am. Chem. Soc.* **2004**, *126*, 15366–15367.

37 Ni, X.-L.; Zeng, X.; Redshaw, C. Yamato, T. *Tetrahedron* **2011**, *67*, 3248–3253.

38 Kim, S. K.; Lee, S. H.; Lee, J. Y.; Lee, J. Y.; Bartsch, R. A.; Kim, J. S. *J. Am. Chem. Soc*. **2004**, *126*, 16499–16506.

39 Kim, S. K.; Bok, J. H.; Bartsch, R. A.; Lee, J. Y.; Kim, J. S. *Org. Lett*. **2005**, *7*, 4839–4842.

40 Kim, S. K.; Kim, S. H.; Kim, H. J.; Lee, S. H.; Lee, S. W.; Ko, J.; Bartsch, R. A.; Kim, J. S. *Inorg. Chem*. **2005**, *44*, 7866–7875.

41 Kim, J. S.; Quang, D. T. *Chem. Rev*. **2007**, *107*, 3780–3799.

42 Ojida, A.; Mito-oka, Y.; Inoue, M.-A.; Hamachi, I. *J. Am. Chem. Soc*. **2002**, *124*, 6256–6258.

43 Chae, M.-Y.; Cherian, X. M.; Czarnik, A. W. *J. Org. Chem*. **1993**, *58*, 5797–5801.

44 Benesi, H. A.; Hildebrand, J. H. *J. Am. Chem. Soc.* **1949**, *71*, 2703–2707.

45 Job, P. *Ann. Chim*. **1928**, *9*, 113–203.

46 Kumar, M.; Kumar, R.; Bhalla, V. *Org. Lett.* **2011**, *13*, 366–369.

47 Sýkona, J.; Himl, M.; Stibor, I.; Císařová, I.; Lhoták, P. *Tetrahedron* **2007**, *63*, 2244–2248.

48 Iki, N. *J. Incl. Phenom. Macrocyclic Chem*. **2009**, *64*, 1–13.

49 Sheldrick, G.M. SHELX-97 – Programs for the determination (SHELXS) and refinement (SHELXL) of crystal structures, *Acta Crystallogr.* **2008**, A*64*, 112.

Chapter 3

Synthesis and Evaluation of A Novel Pyrenyl-Appended Triazole-Based Thiacalix[4]arene As Fluorescent Sensor for Ag^+ Ion

*This chapter described New fluorescent chemosensors 1,3-alternate-**3** and mono-triazole ligand **4** with pyrenyl-appended. The fluorescence spectra changes indicated that the fluorescent sensitive and selective binding of Ag^+ ion requires the coordination of two triazole rings of receptors which fixed by thiacalix[4]arenes.*

3.1 Introduction

Owing to their simplicity, high sensitivity, and high detection limits for trace chemicals in chemistry, biology and the environment,[1] fluorescent chemosensors have received much attention in the field of supramolecular chemistry. Generally, an effective fluorescent chemosensor includes an ion recognition unit (ionophore) and a fluorogenic unit (fluorophore), that effectively converts the information of binding recognition from the ionophore unit into an easily monitored and a highly sensitive light signal from the fluorophore. Amongst the different fluorogenic units, pyrene is one of the most useful tools due to its relatively efficient monomer and excimer emissions. The sensing mechanism of pyrene is attributable to the intensity ratio of the excimer-to-monomer emission, which is very sensitive to conformational change.[2] On the other hand, the simple, effective and versatile chemical modifications possible for calixarenes, together with their unique topology, offer a wide range of scaffolds enabling them to be selective for many different metal ions.[3–5]

Thiacalix[4]arenes, which have received growing interest since their discovery in 1997;[6] possess additional coordination sites and have shown a more flexible structure and strong affinity for both soft and transition metal ions.[7] Acetates are amongst the most versatile compounds in calixarene chemistry, because the acetate group is easily converted to carboxylic acids, amides, and other esters.[7c] Given this, one of the most interesting features of thiacalix[4]arenes is that the conformation can be controlled by the reaction with ethyl bromoacetate in the presence of alkali carbonate as base. Additionally, with the development of the electronics industry and photographic and imaging industry, more attention has been paid to the negative effect of silver ions on the environment. For example, it is believed that silver ions can bind to various metabolites and enzymes, such as in the inactivation of sulphydryl enzyme,[8] and as a consequence, many methods have been utilized to measure trace amounts of silver ion; including atomic absorption, ICP atomic emission, UV-vis absorption, and fluorescence spectroscopy. Among these approaches, fluorescence spectroscopy is widely used because of its high sensitivity and facile operation. However, due to silver belonging to heavy transition-metal ions, which usually quench fluorescence emission via enhanced spin-orbital coupling,[9] energy or electron transfer,[10] only a few fluorescent “turn on” chemosensor for detecting silver ion have been reported at present.[11] Fluorescence quenching is not only disadvantageous for a high signal output during detection

but is also undesirable for analytical purposes.[12] As a result, the development of highly selective chemosensors for the Ag^+ ion still remains a challenge

With these observations in mind, we continue our studies into the design and synthesis of chemosensors for heavy metal ions.[13] Herein, we have designed a new fluorescent sensor through pyrene-appended triazole-based thiacalix[4]arene with 1,3-*alternate* conformation. Such chemosensors display high affinity for silver ion by changing the monomer and excimer emission of the pyrene moieties.

3.2 Results and Discussion

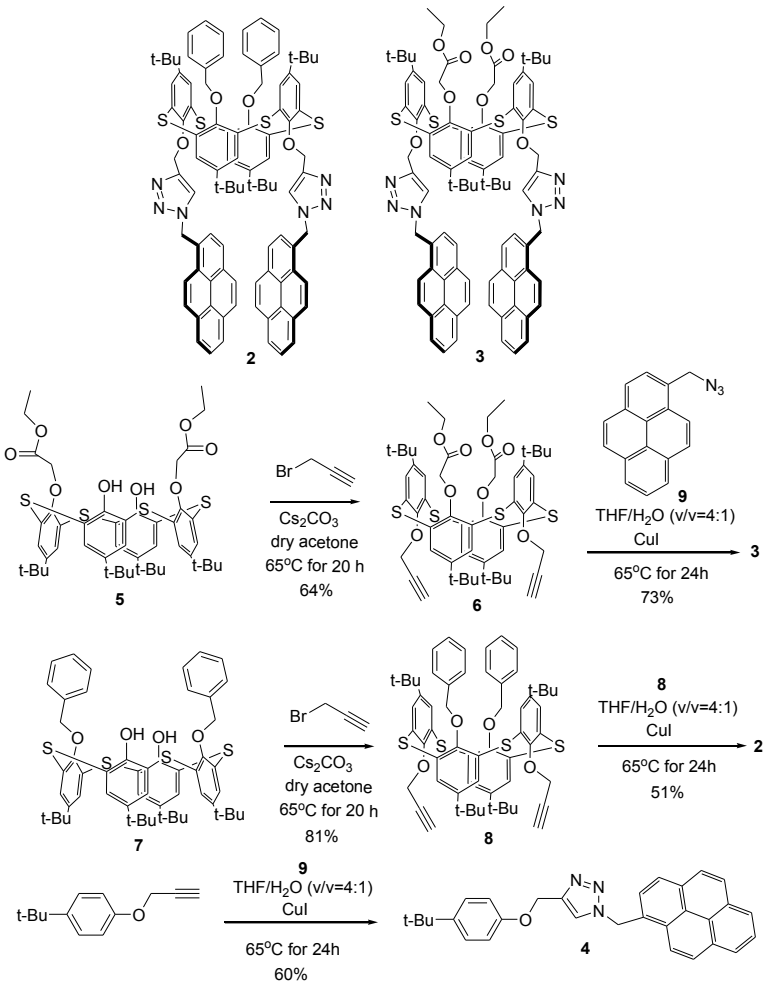

Scheme 1

As shown in Scheme 1, compound *cone*-**5** can be obtained following the reported precedures.[14] Thus, compound 1,3-*alternate*-**6** was prepared in 64% yield by the reaction of compound *cone*-**5** with propargyl bromide in the presence of Cs_2CO_3 in dry acetone. Cu(I)-catalyzed *1,3*-dipolar cycloaddition reaction of compound 1,3-*alternate*-**6** with 1-azidomethylpyrene **9** under Click conditions afforded the 1,2,3-triazole thiacalix[4]arene 1,3-*alternate*-**3** in 73% yield. A similar procedure was employed in the synthesis of receptor 1,3-*alternate*-**2** with 51% yield. The reference compound **4** was prepared by *O*-propargyl *t*-Bu phenyl reactions with azide **9** through Click chemistry in a yield of 60%.

The fluorescence spectra of 1,3-*alternate*-**2** and **3** appeared with a typical intramolecular excimer emission around 485 nm and monomer emissions around 378 and 396 nm in organic solution, and a typical monomer emission appeared for reference compound **4** (excitation at 343 nm) in CH_3CN/CH_2Cl_2 (1000:1, v/v) (Figure 1). The excimer emission band was attributed to the interaction of two pyrene units forming an intramolecular $\pi\ldots\pi$ stacking, which was fixed by the thiacalix[4]arene scaffold.[15] The cation-binding properties of receptors **2**-**4** were then investigated by fluorescence spectroscopy.

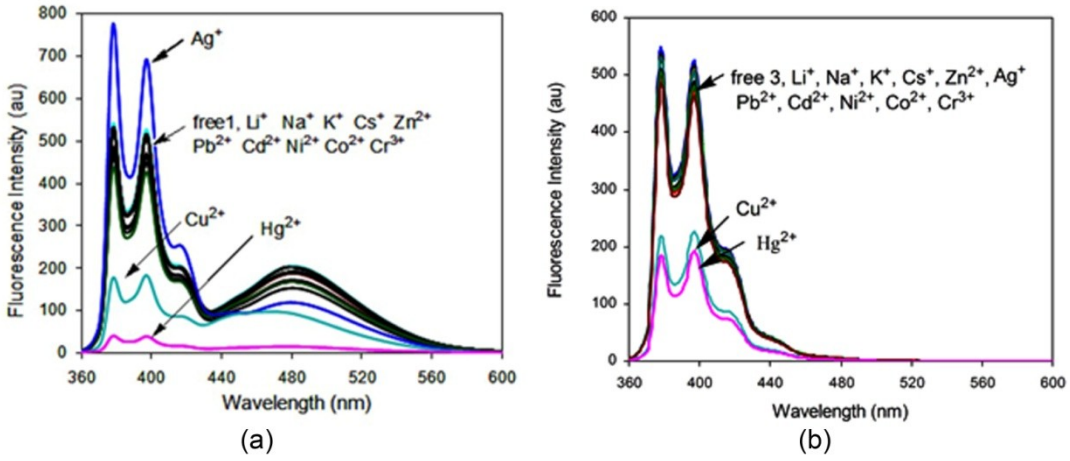

Figure 1. Fluorescence spectra of receptor **3** (a) and **4** (b) (5.0 μM) in CH_3CN/CH_2Cl_2 (1000:1, v/v) at 298 K upon addition of various metal ions. λ_{ex} = 343 nm.

The fluorescence intensity changes upon addition of various perchlorate salts such as Li^+, Na^+, K^+, Cs^+, Zn^{2+}, Pb^{2+}, Ag^+, Cu^{2+}, Hg^{2+}, Cd^{2+}, Ni^{2+}, Co^{2+}, and Cr^{3+} in aqueous solution, are

depicted in Figure 1. It was observed that both the excimer and monomer emissions of receptor 1,3-*alternate*-**3** were strongly quenched by Hg^{2+}, and Cu^{2+}. By contrast, when upon

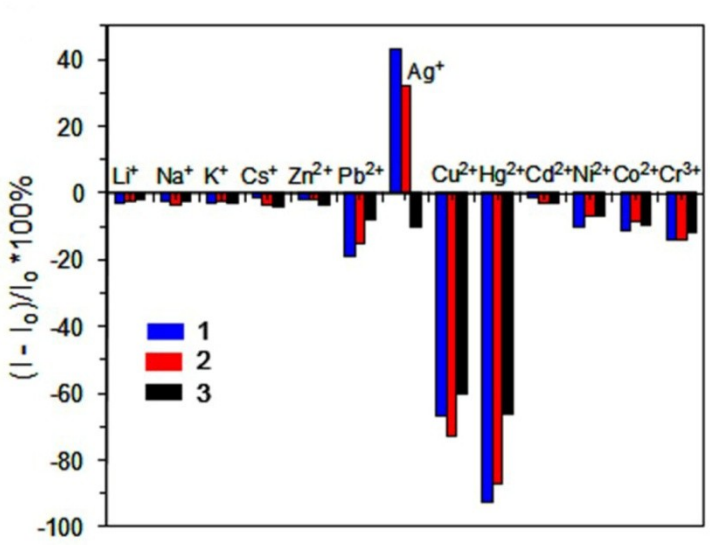

Figure 2. Fluorescence spectra of the receptors **2-4** (each of 5.0 μM) in CH_3CN/CH_2Cl_2 (1000:1, v/v) at 298 K upon addition of various metal ions (100 μM) as their aqueous solution. I_o is fluorescent emission intensity at 378 nm for free receptors, and I is the fluorescent intensity after adding metal cations with an excitation at 343 nm.

addition of Ag^+ ion into the solution of receptor **3**, an obviously enhancement of the monomer emission occurred, whilst the accompanying excimer emission declined (Figure 1 and figure 2). Much weaker responses for fluorescence emissions of the monomer and excimer quenching were given by addition of Pb^{2+}, Ni^{2+}, Co^{2+}, and Cr^{3+} ions, and no significant fluorescence intensity changes were observed upon addition of alkali metal ions. Similar selective fluorescent behavior caused by metal ions was also observed for receptor **2** (Figure 2). However, under the same analytical conditions, the fluorescent intensity of compound **4** (Figure 1b and Figure 2) was not obviously changed upon addition of Ag^+ ion and other metal ions, except in the cases of Hg^{2+}, and Cu^{2+} ions, where acute quenching was observed. These results indicated that the fluorescent sensitive and selective binding of Ag^+ ion requires the coordination of two triazole rings of receptors **2** and **3**. Generally, the fluorescence of monomer emission quenching by heavy atoms, such as Hg^{2+}, and Cu^{2+} in the

chemosensors **2**-**4** can be attributed to the reverse PET (photon electron transfer)[16] from the pyrene unit to the nitrogen atoms of triazole ring or a heavy atom effect.[17] The excimer quenching is a result of a conformational change, which occurs during the binding of the targeted metal ions with the nitrogen atoms on the triazole ring. In this procedure, the coordination force make the pyrene groups move far away from each other and inhibits the π-π stacking for generating excimer emission.

The fluorescence spectra of 1,3-*alternate*-**3** at various concentrations of Ag^+ ion are shown in Figure 3a. As can be seen, the fluorescence intensity of the monomer emission of receptor **3** gradually increased on increasing concentrations of Ag^+ ion from 0 to 100 μM and was accompanied by a concomitant decrease in the excimer emission. A discernible isomessive point appeared at 430 nm. On the basis of the fluorescence titration experiments, the association constant (K_a)[18] for **3**•Ag^+ was determined to be 1.33×10^5 M^{-1}, and a job plot[19] for the complexation showed a 1:1 stoichiometry (Figure 3a).

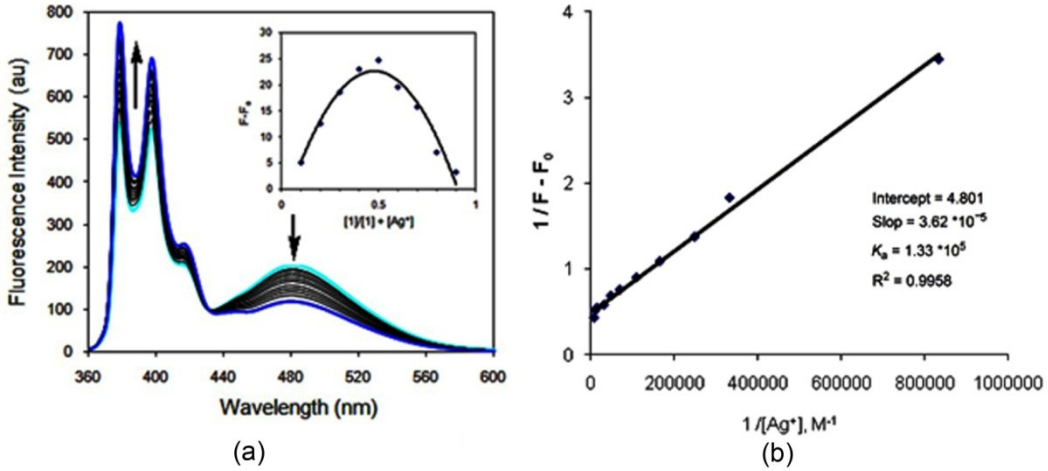

Figure 3. (a) Changes in the fluorescence emission spectra of **3** (5.0 μM) upon addition of increasing concentrations of Ag^+ ion in aqueous solution (0-100 μM) at 298 K in CH_3CN/CH_2Cl_2 (1000:1, v/v) with an excitation at 343 nm. Inset: Job's plot showing a 1:1 stoichiometry; (b) Benesi-Hilderbrand plot of **3** with $AgClO_4$.

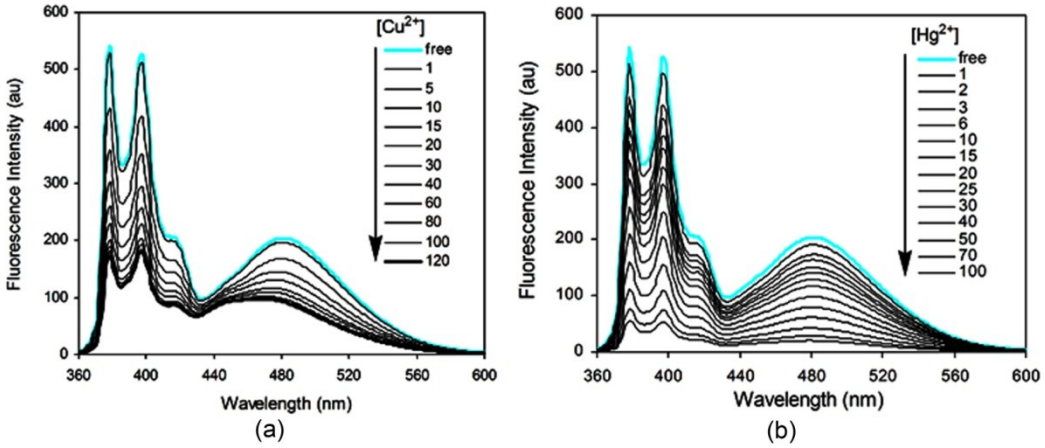

Figure 4. Changes in the fluorescence emission spectra of **3** (5.0 μM) upon addition of increasing concentrations of Cu^{2+} (a) and Hg^{2+} (b) ion aqueous solution at 298 K in CH_3CN/CH_2Cl_2 (1000:1, v/v) with an excitation at 343 nm.

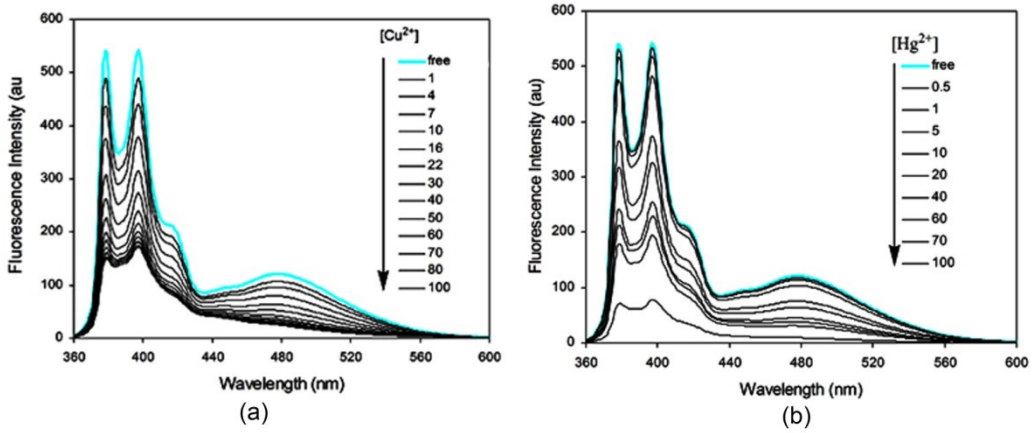

Figure 5. Changes in the fluorescence emission spectra of **2** (5.0 μM) upon addition of increasing concentrations of Cu^{2+} (a) and Hg^{2+} (b) ion aqueous solution at 298 K in CH_3CN/CH_2Cl_2 (1000:1, v/v) with an excitation at 343 nm.

Similar fluorescence titration behavior was also evaluated in the case of receptors **3** and **2** with related metal ions (Figure 4 and Figure 5). From these observations, the association constants for complexation were calculated to be: **3**•Hg^{2+} = 4.24 × 10^4 M^{-1}, **3**•Cu^{2+} = 3.97 × 10^4 M^{-1}, **2**•Ag^{+} = 5.40 × 10^4 M^{-1}, **2**•Hg^{2+} = 2.46 × 10^4 M^{-1}, **2**•Cu^{2+} = 5.39 × 10^4 M^{-1}, respectively.

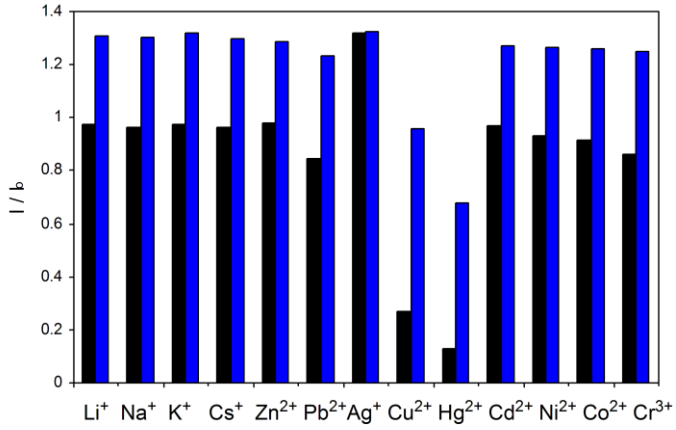

Figure 6. Fluorescence response of **3** (5.0 μM) in CH_3CN/CH_2Cl_2 (1000:1, v/v) to 100 μM various tested metal ions (black bar) and to the mixture of 100 μM tested metal ions with 100 μM Ag^+ ion (blue bar) at 298K. I_0 is the fluorescence intensity at 378 nm for free **3**, and I is the fluorescence intensity after adding metal ions with an excitation at 343 nm.

To better investigate the practical applicability of the receptors **3** and **2** as Ag^+ ion selective fluorescent sensor, competitive experiments were carried out in the presence of Ag^+ ion (100 μM) mixed with Li^+, Na^+, K^+, Cs^+, Zn^{2+}, Pb^{2+}, Cu^{2+}, Hg^{2+}, Cd^{2+}, Ni^{2+}, Co^{2+}, and Cr^{3+} at 100 μM; as shown in Figure 6 and Figure S8, no significant interference in detection of Ag^+ with receptors **3** and **2** was observed in the presence of most other competitive metal ions except for the Hg^{2+} ion, for which interference with the detection signal by abolished the ratiometric effect on binding of Ag^+ ion. Accordingly, these observations suggested that receptors **3** and **2** can be used as selective fluorescent sensor for Ag^+ ion in the presence of most completive metal ions.

In order to obtain detailed information on the complexation structure of receptors **3** and **2** with Ag^+ ion, ^1H NMR titration experiments in $CDCl_3/CD_3CN$ (10:1, v/v) were carried out. The partial spectral changes are shown in Figure 7. Upon addition of 1.0 equiv of Ag^+ ion to the solution of 1,3-*alternate*-**3**, as expected, the chemical shift of proton H_b on the triazole ring exhibited significant downfield shift by $\Delta\delta$ 0.45 ppm from δ 7.29 ppm. The peak of H_c on the O*CH*$_2$-triazole unit and H_f also demonstrated a similar but weak downfield shift from δ 4.87 to 5.06 ppm and δ 4.42 to 4.58 ppm, respectively, whereas the peaks of the proton on the ester moieties were little affected

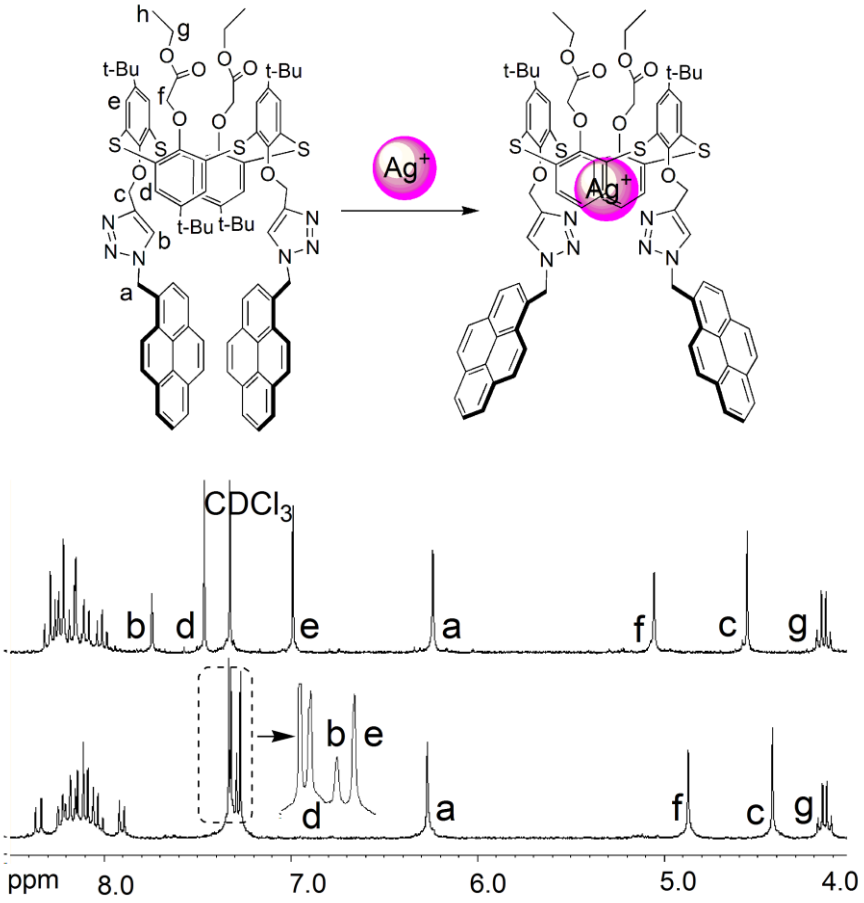

Figure 7. Plausible complexation structure of receptor **3** for Ag^+ ion, and partial ^1H NMR spectra of 1 (5.0 mM) in $CDCl_3/CD_3CN$ (10:1, v/v) upon addition of 1.0 equiv Ag^+ ion at 298K; (partial *tert*-butyl moieties are omitted for clarity).

. Additionally, a similar coordination behavior was observed for complexation **2**•Ag^+ (Chapter2). These spectral changes suggested that Ag^+ ion can be selectively bound by the nitrogen atoms on the triazole rings. On the other hand, it should be noted that the protons of H_d and H_e on the phenol of 1,3-*alternate* thiacalix[4]arene also experienced downfield shift from δ 7.32 to 7.50 ppm and upfield shift from δ 7.26 to 6.98 ppm. These data further indicated that there must be a conformation change of receptor **3** in the presence of Ag^+ ion. As a matter of fact, it is believed that the conformation of thiacalix[4]arene can be preorganized for the binding of Ag^+ ion in solution in a manner that is similar to an example described by Shinkai and co-workers.[20] In that case, the X-ray structure clearly demonstrated that Ag^+ ion was included in the π-basic benzene cavity at the lower rim, where the two distal benzene rings were being flattened and the residual two benzene rings were standing upright

for binding Ag^+ ion. Thus, we conclude that the two triazole groups and the ionophoricity cavity, formed by the two inverted benzene rings with the sulfur atoms framework based on thiacalix[4]arene, are all involved in the complexation with the Ag^+ ion.[21]

3.3 Conclusions

In conclusion, we have synthesized a new type of fluorescent sensor having triazole rings as cation binding sites on the lower rim of a thiacalix[4]arene scaffold with 1,3-*alternate* conformation. The selective binding behavior of receptors **3** and **2** has been evaluated by fluorescence spectra and ^1H NMR analysis. All the results suggested that the triazole moieties on the receptors **3** and **2** are highly sensitive and selective for Ag^+. This is due to cooperative coordination by the ionophoricity cavity, formed by the two inverted benzene rings and the sulfur atoms of the thiacalix[4]arene, by enhancement of the monomer emission of pyrene.

3.4 Experimental Section

3.4.1 General

All melting points (Yanagimoto MP-S1) are uncorrected. NMR spectra were determined at 300 MHz with a Nippon Denshi JEOL FT-300 spectrometer with Me_4Si as an internal reference: *J* values are given in Hz. IR spectra were measured for samples as KBr pellets in a JASCO FT/IR 4200. All the fluorescence spectra were recorded on a JASCO FP-6200 spectrometer. Mass spectra were obtained on a Nippon Denshi JMS-01SG-2 mass spectrometer at ionization energy of 70 eV using a direct inlet system through GLC. Elemental analyses were performed by Yanaco MT-5.

3.4.2 Materials

Compounds **5**,[14] **7**,[22] and **9**[15b] were prepared following the reported procedure.

3.4.2.1. 5,11,17,23-Tetra-tert-butyl-25,27-bis(ethoxycarbonylmethoxy)-26,28-[bis(propergyloxy)]-tetrathiacalix[4]arene (1,3-alternate-6)

Cone-**5** (300 mg, 0.34 mmol) and Cs_2CO_3 (1.085 g, 3.33 mmol) were refluxed for 1 h in dry acetone (15 mL). 3-bromo-1-propyne (propargyl bromide (396 mg, 3.33 mmol) and dry acetone (10 mL) was added and the mixture refluxed for 20 h. The solvents were evaporated and the residue partitioned between 10% HCl and CH_2Cl_2. The organic layer was separated and dried ($MgSO_4$) and the solvents were evaporated. The residue was recrystallized from $CHCl_3$/hexane (3:1) to afford 1,3-*alternate*-**5** (210 mg, 64%) as prisms. Mp 223–225°C. ^{1}H NMR (300 MHz, $CDCl_3$) δ 1.06 (18H, s, tBu), 1.28 (6H, m, CH_2CH_3), 1.40 (18H, s, tBu), 2.10 (1H, t, *J*=3.0 Hz, acetylene-H), 2.44 (1H, m, acetylene-H), 4.25 (4H, q, *J*=7.1 Hz, CH_2CH_3), 4.61 (4H, s, CH_2), 4.83 (4H, s, CH_2), 7.46 (4H, s, ArH), 7.59 (4H, s, ArH). IR: ν_{max} (KBr)/cm^{-1} 3309, 2958, 1768, 1575, 1440, 1367, 1268, 1193, 1085, 1010. FABMS: *m/z* 969.39 (M^+). Anal. calcd for $C_{54}H_{64}O_8S_4$ (969.35): C, 66.91; H, 6.66. Found: C, 67.09; H, 6.70.

3.4.2.2. 5,11,17,23-Tetra-tert-butyl-25,27-bis(ethoxycarbonylmethoxy)-26,28-bis[1H- (1-pyrenylmethyl-(1,2,3-triazolyl)-4-methoxy)]-tetrathiacalix[4]arene (1,3-alternate-3)

Copper iodide (20 mg) was added to a solution of 1,3-*alternate*-**6** (174 mg, 0.18 mmol) and 1-(azidemethyl)pyrene **9** (139 mg, 0.54 mmol) in 20 mL THF/H_2O (4:1) and the mixture was heated at 65 °C for 24 h. The resulting solution was cooled and diluted with water and extracted trice with CH_2Cl_2. The organic layer was separated and dried ($MgSO_4$) and evaporated to give the solid crude product. The residue eluted from a column chromatography of silica gel with hexane/ethyl acetate (v/v= 4:1) to give the desired product 1,3-*alternate*-**3** (194 mg, 73%) as prisms. Mp 154–156°C. ^{1}H NMR (300 Hz, $CDCl_3$) δ 0.88 (18H, s, tBu), 1.08 (18H, s, tBu), 1.22 (6H, t, *J*=7.1 Hz, CH_2CH_3), 4.15 (4H, q, *J*=7.1 Hz, CH_2CH_3), 4.45 (4H, s, CH_2), 4.84 (4H, s, CH_2), 6.28 (4H, s, CH_2), 7.24 (4H, s, ArH), 7.28 (2H, s, Triazole-H), 7.33 (4H, s, ArH), 7.88 (2H, d, *J*=9.0 Hz, Pyrene-H), 7.99–8.23 (14H, m, Pyrene-H), 8.34 (2H, d, *J*=9.0 Hz, Pyrene-H). ^{13}C NMR (75 MHz, $CDCl_3$): 14.07, 22.59, 31.01, 33.82, 52.08, 60.43, 64.85, 67.60, 122.18, 123.22, 124.45, 124.85, 124.94, 125.62, 125.71, 126.21, 127.18, 127.25, 128.04, 128.23, 128.79, 129.07, 130.54, 131.13, 131.84, 131.96, 133.15, 144.59, 145.97, 146.00, 156.51, 157.20, 167.91. IR: ν_{max} (KBr)/cm^{-1} 2960,

2360, 1768, 1442, 1380, 1265, 1190, 1045. FABMS: *m/z* 1483.42 (M^+). Anal. calcd for $C_{88}H_{86}N_6O_8S_4$ (1483.92): C, 71.23; H, 5.84; N, 5.66. Found: C, 71.09; H, 5.70; N, 5.64.

3.4.2.5. 4-tert-Butyl-[1H-(1-pyrenylmethyl-(1,2,3-triazolyl)-4-methoxy) benzene (4)

A mixture of 4-*tert*-butyl-1-(propargyloxy)benzene (95 mg, 0.5 mmol) and **9** (140 mg, 1.1 mmol) in 20 mL THF/H_2O (4:1) and the mixture was heated at 65 °C for 24 h at the presence of CuI as catalyst. The resulting solution was cooled and diluted with water and extracted trice with CH_2Cl_2. The organic layer was separated and dried ($MgSO_4$) and evaporated to give the solid crude product. The residue eluted from a column chromatography of silica gel with hexane/ethyl acetate (6:1, v/v) to give the desired product **4** (134 mg, 60%) as pale yellow prisms. Mp 147–149°C. ^{1}H NMR (300 MHz, $CDCl_3$) δ 1.24 (9H, s, tBu), 5.07 (2H, s, CH_2), 6.25 (2H, s, CH_2), 6.82 (2H, d, *J*=5.4 Hz, ArH), 7.22 (2H, d, *J*=5.4 Hz, ArH), 7.37 (1H, s, Triazole-H), 7.94–8.25 (9H, m, Pyrene-H). ^{13}C NMR (75 MHz, $CDCl_3$) δ 31.41, 33.98, 52.42, 62.10, 114.19, 121.85, 124.42, 124.88 125.02, 125.79, 125.90, 126.15, 126.35, 126.61, 127.15, 127.62, 128.27, 129.03, 129.26, 130.51, 131.12, 132.10, 143.84, 155.88. IR: ν_{max} (KBr)/cm^{-1} 2954, 2360, 1768, 1442, 1380, 1265, 1190, 1045. *m/z* 445.26 (M^+). Anal. calcd for $C_{30}H_{27}N_3O$ (445.57): C, 80.87; H, 6.11; N, 9.43. Found: C, 80.62; H, 6.03; N, 9.36.

3.5 References

1. (a) de Silva, A. P.; Gunaratne, H. Q. N.; Gunnlaugsson, T.; Huxley, A. J. M.;McCoy, C. P.; Rademacher, J. T.; Rice, T. E. *Chem. Rev*. **1997**, *97*, 1515–1566. (b) Desvergne, J.-P.; Czarnik, A. W. *Chemosensors of Ion and Molecular Recognition; Dordrecht*, The Netherlands: Kluwer, 1997.
2. (a) Winnik, F. M. *Chem. Rev*. **1993**, *93*, 587–614. (b) Fabbrizzi, L.; Poggi, A.; *Chem. Soc. Rev.* **1995**, *24*, 197–202. (c) Suzuki, Y.; Morozumi, T.; Nakamura, H. *J. Phys. Chem. B*. **1998**, *102*, 7910–7917. (d) Yang, J.-S.; Lin, C.-S.; Hwang, C.-Y. *Org. Lett*. **2001**, *3*, 889–892. (e) Kim, J. S.; Choi, M. G.; Song, K.C.; No, K. T.; Ahn, S.; Chang, S.-K. *Org. Lett*. **2007**, *9*, 1129–1132.
3. (a) Böhmer, V. *Angew. Chem. Int. Ed. Engl*. **1995**, *24*, 713–745. (b) Ikeda, A., Shinkai, S. *Chem. Rev*. **1997**, *97*, 1713–1734. (c) Kim, J. S.; Quang, D. T. *Chem. Rev*.

2007, *107*, 3780–3799. (d) Leray, I.; Valeur, B. *Eur. J. Inorg. Chem*. **2009**, 3525–3535.

4. Diamond, D.; McKervey, M. A. *Chem. Soc. Rev*. **1996**, *25*, 15–24.
5. Gutsche, C. D. *Calixarenes Revisited: Monographs in Supramolecular Chemistry* (Ed.: J. F. Stoddart), The Royal Society of Chemistry, Cambridge, **1998**.
6. (a) Kumagai, J.; Hasegawa, M.; Miyanari, S.; Sugawa, Y.; Sato, Y.; Hori, T.; Ueda, S.; Kamiyama, H.; Miyano, S. *Tetrahedron Lett*. **1997**, *38*, 3971–3972. (b) Iki, N.; Kabuto, C.; Fukushima, T.; Kumagai, H.; Takeya, H.; Miyanari, S.; Miyashi, T.; Miyano, S. *Tetrahedron* **2000**, *56*, 1437–1443.
7. (a) Lhoták, P. *Eur. J. Org. Chem*. **2004**, 1675–1692. (b) Shokova, E. A.; Kovalev, V. V. *Russ. J. Org. Chem*. **2003**, *39*, 1–28. (b) Morohashi, N.; Narumi, F.; Iki, N.; Hattori, T., Miyano, S. *Chem. Rev*. **2006**, *106*, 5291–5316. (c) Csokai, V.; Grün, A .; Balázs, B.; Simon, A.; Tóth, G.; Bitter, I. *Tetrahedron* **2006**, *62*, 10215–10222. (d) Stoikov, I. I.; Yushkova, E. A.; Zhukov, A. Y.; Zharov, I.; Antipin, I. S.; Konovalov, A. I. *Tetrahedron* **2008**, *64*, 7489–7497. (e) Kumar, M.; Dhir, A.; Bhalla, V. *Tetrahedron* **2009**, *65*, 7510–7497.
8. (a) Ratte, H. T. *En*V*iron. Toxicol. Chem.* **1999**, *18*, 89–108. (b) Zhang, X. B.; Han, Z. X.; Fang, Z. H.; Shen, G. L.; Yu, R. Q. *Anal. Chim. Acta.* **2006**, *562*, 210–215.
9. McClure, D. S. *J. Chem. Phys*. **1952**, *20*, 682–686.
10. Varnes, A. W.; Dodson, R. B.; Whery, E. L. *J. Am. Chem. Soc*. **1972**, *94*, 946–950.
11. (a) Rurack, K.; Kollmannsberger, M.; Resch-Genger, U.; Daub, J. *J. Am. Chem. Soc*. **2000**, *122*, 968–96. (b) Kim, J. S.; Shon, O. J.; Rim, J. A.; Kim, S. K.; Y, J. *J. Org. Chem.* **2002**, *67*, 2348–2351. (c) Yang, R.-H.; Chan, W.-H.; Lee, A. W. M.; Xia, P.-F.; Zhang, H.-K.; Li, K. *J. Am. Chem. Soc.* **2003**, *125*, 2884–2885. (d) Coskun, A.; Akkaya, E. U. *J. Am. Chem. Soc.* **2005**, *127*, 10464–10465. (e) Iyoshi, S.; Taki, M.; Yamamoto,Y. *Inorg. Chem.* **2008**, *47*, 3946–3948. (f) Nolan, E. M.; Lippard, S. J. *Chem. Rev*. **2008**, *108*, 3443–3480. (g) Joseph, R.; Ramanujam, B.; Acharya, A.; Rao, C. P. *J. Org. Chem.* **2009**, *74*, 8181–8190. (h) Chatterjee, A.; Santra, M.; Won, N.; Kim, S.; Kim, K. J.; Kim, B. S.; Ahn, H. K. *J. Am. Chem. Soc.* **2009**, *131*, 2040–2041. (i) Wang, H.-H.; Xue, L.; Qian, Y.-Y.; Jiang, H. *Org. Lett.* **2010**, *12*, 292–295.

12. Rurack, K.; Resch-Genger, U.; Rettig, W. *J. Photochem. Photobiol, A* **1998**, *118*, 143–149.
13. Ni, X.-L.; Wang, S.; Zeng, X.; Tao, Z.; Yamato, T. *Org. Lett*. **2011**, *13*, 552–555.
14. Iki, N., Narumi, F., Fujimoto, T., Morohashi, N., Miyano, S. *J. Chem. Soc. Perkin Trans. 2* **1998**, 2745–2750.
15. (a) Broan, C. J. *Chem. Commun.* **1996**, 699–700; (b) Park, S.-Y.; Yoon, J.-H.; Hong, C.-S.; Souane, R., Kim, J.-S.; Matthews, S. E.; Vicens, J. *J. Org. Chem*. **2008**, *73*, 8212–8218.
16. (a) Chang, K.-C.; Su, I.-H.; Senthilvelan, A.; Chung, W.-S. *Org. Lett.* **2007**, *9*, 3363–3366. (b) Ojida, A.; Mito-oka, Y.; Inoue, M.-A.; Hamachi, I. *J. Am. Chem. Soc.* **2002**, *124*, 6256–6258. (c) Choi, M.; Kim, M.; Lee, K. D.; Han, K.-N.; Yoon, I.-A.; Chung, H.-J.; Yoon, J. *Org. Lett*. **2001**, *3*, 3455–3457.
17. Chae, M.-Y.; Cherian, X. M.; Czarnik, A. W. *J. Org. Chem.* **1993**, *58*, 5797–5801.
18. (a) Benesi, H. A.; Hildebrand, J. H. *J. Am. Chem. Soc.* **1949**, *71*, 2703–2707. (b) Stern, O; Volmer, M. *Phys. Z*. **1919**, *20*, 183–188.
19. Job, P. *Ann. Chim*. **1928**, *9*, 113–203.
20. Ikeda, A.; Tsuzuki, H.; Shinkai, S. *J. Chem. Soc., Perkin Trans. 2* **1994**, 2073–2080.
21. (a) Sýkona, J.; Himl, M.; Stibor, I.; Císařová, I.; Lhoták, P. *Tetrahedron* **2007**, *63*, 2244–2248. (b) Iki, N. *J. Incl. Phenom. Macrocyclic Chem*. **2009**, *64*, 1–13. (c) Kumar, M.; Kumar, R.; Bhalla, V. *Org. Lett*. **2011**, *13*, 366–369.
22. Ni, X.-L.; Tomiyasu, H.; Shimizu, T.; Pérez-Casas, C.; Zeng, X.; Yamato, T. *J. Incl. Phenom. Macrocyclic Chem*. **2010**, *68*, 99–108.

Chapter 4

Pyrene-Linked Triazole-Modified Homooxacalix[3]arene: A Unique C_3 Symmetry Ratiometric Fluorescent Chemosensor for Pb^{2+}

This chapter described a new type of fluorescent chemosensor based on homooxacalix[3]arene. The fluorescent sensor was highly selective for Pb^{2+} in comparison with other metal ions tested by enhancement of the monomer emission of pyrene. This results suggested that the C_3 symmetric structure of homooxacalix[3]arene has potential application in the development of a new ratiometric fluorescent chemosensor for heavy metal ions.

4.1 Introduction

The Pb^{2+} ion is one of the most toxic heavy metal ions and is responsible for a range of adverse environmental and health problems. A variety of symptoms have been attributed to lead poisoning, including memory loss, anemia, muscle paralysis, and, particularly, mental retardation of children.[1] Consequently, the selective signaling of Pb^{2+} is a very important topic in relation to the detection and treatment of this toxic metal ion in chemical and biological systems.[2] Among these detection approaches for the Pb^{2+} ion, fluorescence spectroscopy is widely used because of its high sensitivity, simple application, and low cost.

Calixarenes are ideal scaffolds or building blocks for the development of fluorescent receptors for molecular recognition via the incorporation of an appropriate sensory group. Therefore, many fluorescent chemosensors based on calixarenes, which show highly selective recognition of alkaline and alkaline-earth cations have been synthesized.[3] However, fluorescent sensors for heavy metal ions, particularly ratiometric receptors for lead,[4] have remained rare up to now because these metal ions are known to quench fluorescence emission via enhanced spin-orbital coupling,[5] energy or electron transfer.[6] Fluorescence quenching is not only disadvantageous for a high signal output during detection but is also undesirable for analytical purposes.[7] Thus, it is important that the recognition of Pb^{2+} by the chemosensor does not quench the fluorescence. On the other hand, homooxacalix[3]arene, which has a basic C_3-symmetric cavity and is related to both calixarenes and crown ethers, has attracted supramolecular chemists to make receptors for metal cations,[8] ammonium cations,[9] and fullerene derivatives.[10]

Additionally, click chemistry has attracted considerable attention recently and has been applied in a wide range of fields[11] for its efficiency, regioselectivity, and compatibility with reaction conditions. For example, Chung and Kim et al. have incorporated triazole rings onto tailored calix[4]arene scaffolds as receptors and fluorescent sensors for metal ions.[12] Furthermore, it is well known in coordination chemistry that the complexation of lead with a ligand containing at least three nitrogen donor atoms is favored by the activation of the inert pair on the Pb^{2+} ion, leading to a shortening of the Pb-N bond length and a much stronger covalent bonding.[13] Therefore, we hypothesized that suitably arranged functionalized ligand moieties containing nitrogen atoms attached to homooxacalix[3]arene should be a good

receptor candidate for lead ions. Therefore, with this in mind, we have synthesized compounds 1 and 2 and studied their cation-binding affinity.

4.2 Results and Discussion

The synthetic routes for fluorescent sensors **1** and **2** are described in Scheme 1. We

Scheme 1

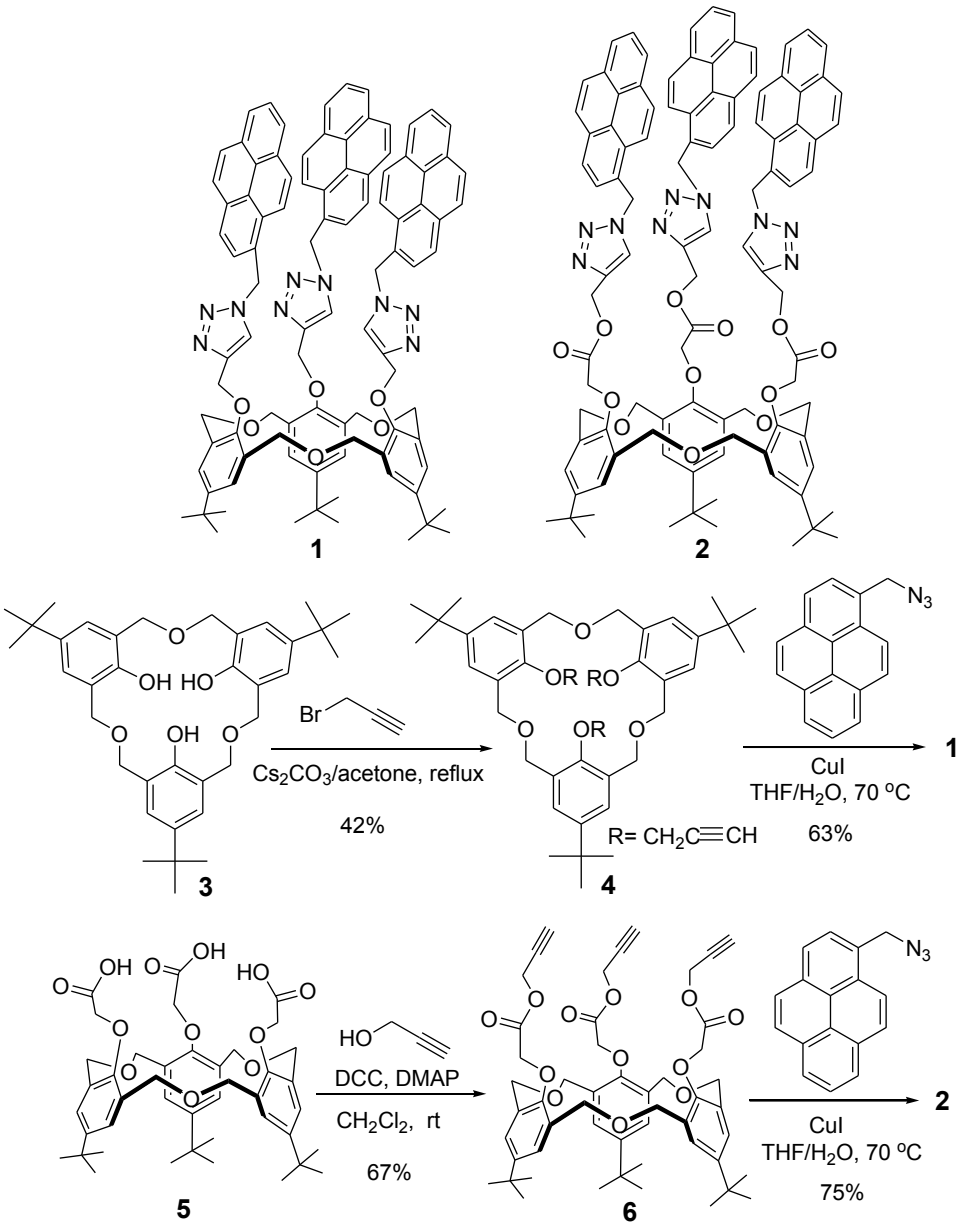

firstly synthesized **4** with 42% yield by the reaction of **3** and propargyl bromide in the presence Cs_2CO_3 in dry acetone solution. The ^1H NMR results suggested that compound **4** adopts a partial-cone structure (Figure 1a). Previously, Shinkai et al. established that

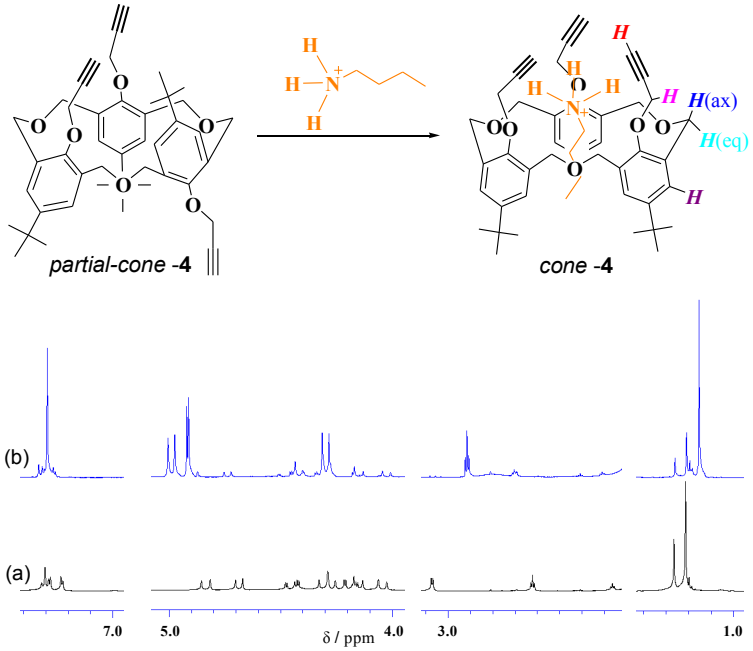

Figure 1. (a) Partial ^1H NMR spectra of **4** (4.0 mM) in a $CDCl_3/CD_3CN$ (10:1 v/v) solution and (b) in the presence of 1 equiv of *n*-$BuNH_3ClO_4$.

interconversion between conformers of **3**, which occurs by oxygen-through-the-annulus rotation, can be sterically allowed for methyl, ethyl, and propyl groups whereas it is inhibited for the butyl group.[14] However, the selective introduction of a propargyl group onto phenolic groups has not yet been accomplished. Thus, we first carried out the ^1H NMR titration experiment of **4** with *n*-$BuNH_3ClO_4$ in $CDCl_3/CD_3CN$ (10:1 v/v). The results indicated that the interconversion between cone and partial-cone conformation also takes place with a propargyl moiety on compound 4 (Figure 1). Most interestingly, the X-ray crystal structure of **4** (Figure 2) clearly revealed that there are two different conformations in the unit cell, and that one exhibits a classical partial-cone structure (Figure 2a) while the other exhibits an intermediate from partial-cone to cone structure (Figure 2b). Accordingly, fluorescent sensor 1 can be obtained from the reaction of **4** with 1-azidomethylpyrene under standard conditions

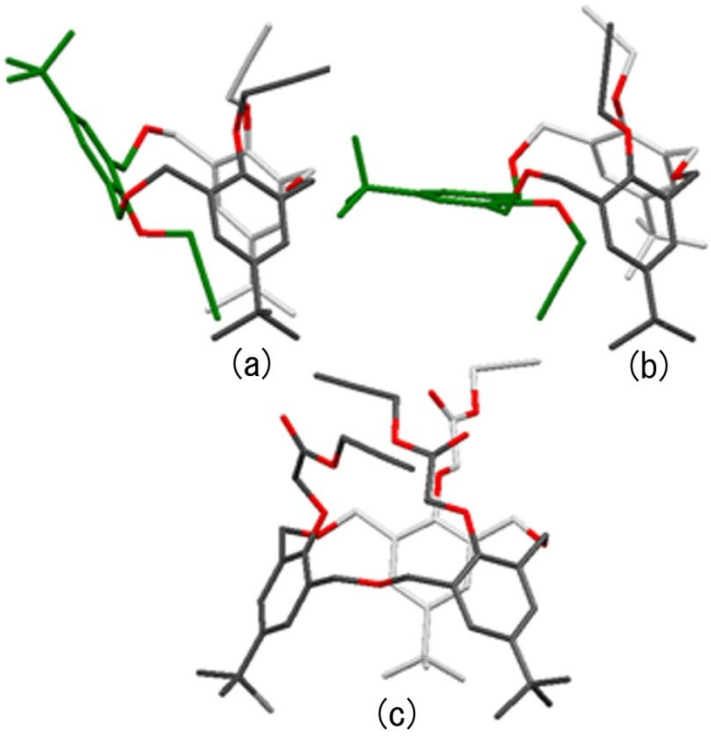

Figure 2. The X-ray structure of **4** (a and b) and **6** (c) with two different conformations in the unit cell, hydrogen atoms are omitted for clarity.

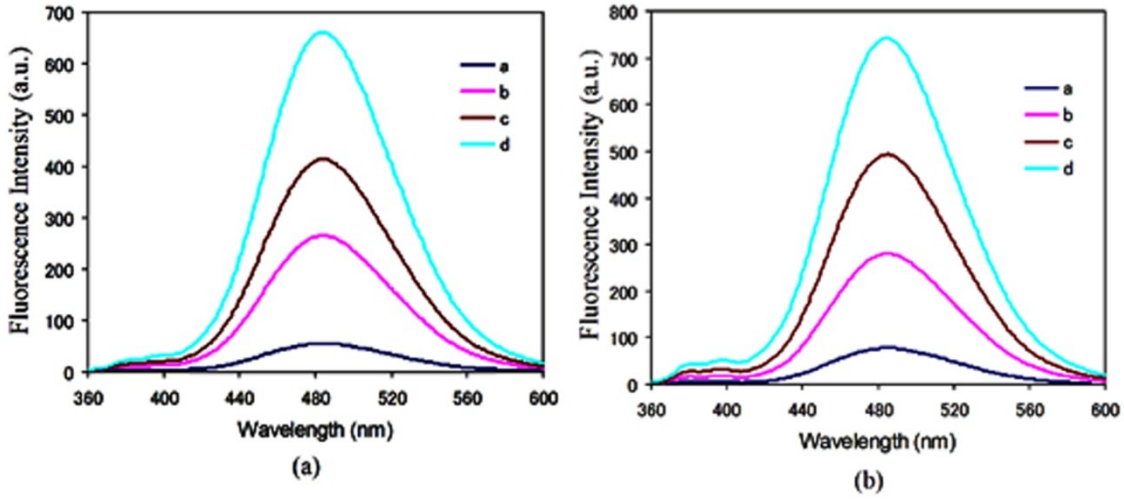

Figure 3. Fluorescence spectra of **1** (a) and **2** (b) with different concentrations in CH_3CN/CH_2Cl_2 (1000:1, v/v) (a = 0.1 μM, b = 0.5 μM, c = 1 μM, d = 2 μM).

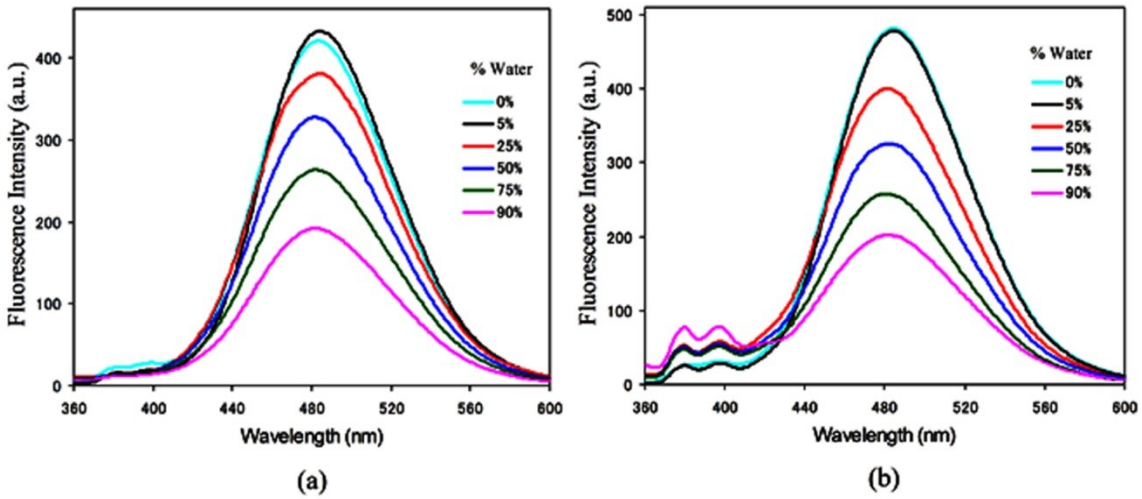

Figure 4. Effects of water composition on the fluorescence of **1** (a) and **2** (b) in aqueous organic solution. [**1**] = [**2**] = 1.0 μM at 298K.

for click chemistry with 63% yield of the cone conformation. A similar procedure was employed in the synthesis of chemosensor 2 from compound 5 in 75% yield.

Dilution experiments at different concentrations of **1** and **2** indicated that the excimer emission resulted from the intramolecular excimer, rather than the intermolecular excimer (Figure 3). Using of organic solvent was unavoidable due to limited solubility of **1** and **2** in water. So, the fluorescent spectra properties of **1** and **2** were evaluated in organic solvent systems and their aqueous solutions (Figure 4). In order to have a more optimized condition for the realization of the peak selectivity for the targeting cations, the effects on the fluorescence of **1** and **2** with various metal ions in the absence and presence of water were systematically investigated (Figures 5-9). As shown in Figure 5b, the selectivity monomer emission output signal of receptor **1** for Pb^{2+} is lower obviously compared to receptor **2**, and both receptors also still exhibited impressively recognition to Zn^{2+} by switching the monomer emission signal. However, from the competitive experiment for Pb^{2+}(Figure 6). It seems that the monomer emission peak of **2**•Pb^{2+} could be compromised if Hg^{2+}, Cu^{2+} or Cr^{3+} was present, that may be attributed to Hg^{2+} and Cu^{2+} very easily quenching the fluorescence of **2** in organic system (Figure 7a, and Figure 8a). Interestingly, when we carried out the fluorescent selective response of receptor **2** to Pb^{2+} by coexisting ions in the presence of small amount of water system (CH_3CN/H_2O/DMSO, 1000:50:1, v/v), the fluorescence titration experiment of Hg^{2+}, Cu^{2+} with receptor **2** in aqueous organic

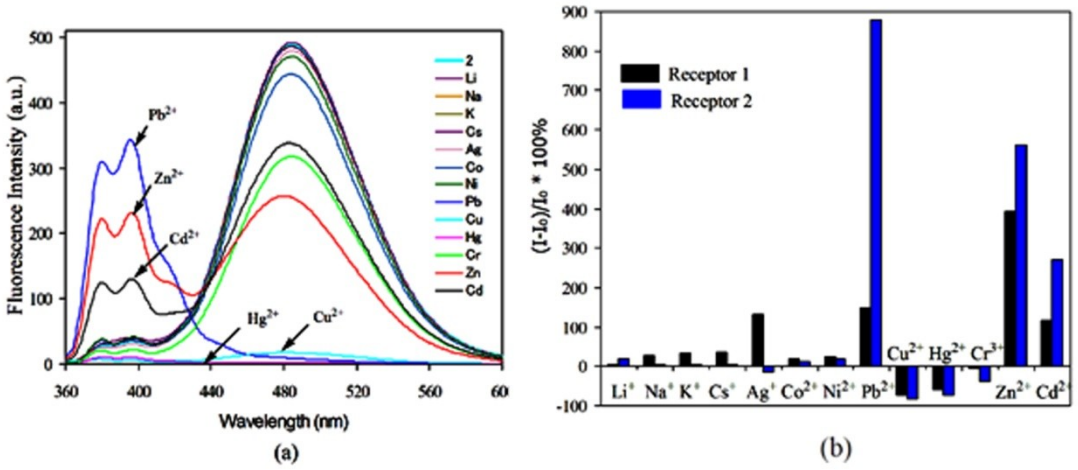

Figure 5. Fluorescence spectra of receptor **2** (a) and Fluorescence intensity changes ((I-I_o)/I_o× 100%) of receptors **1** and **2** (each of 1.0 μM) (b) in CH_3CN/CH_2Cl_2 (1000:1, v/v) at 298 K upon addition of various metal perchlorates (20 equiv). I_o is fluorescence emission intensity at 396 nm for free host **1** and **2,** and I is the fluorescent intensity after adding metal ions. λ_{ex} = 343 nm.

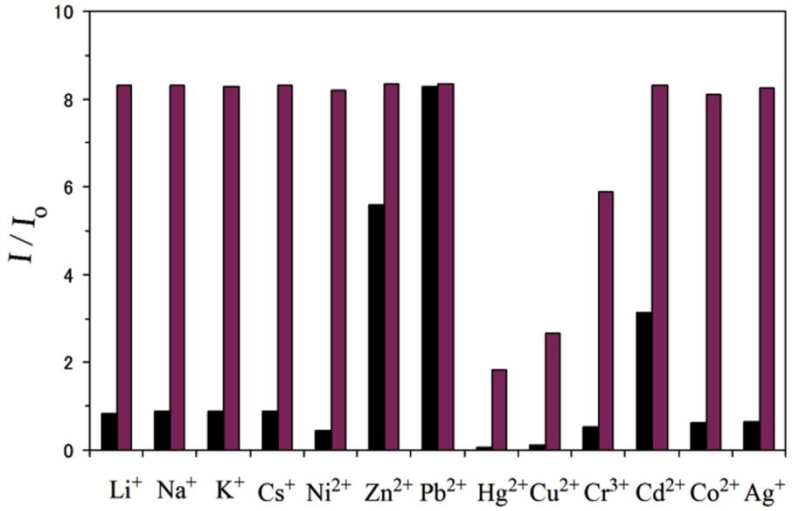

Figure 6. Fluorescence responses of **2** (1.0 μM) in CH_3CN/CH_2Cl_2 (v:v = 1000:1) to 20 μM tested metal ions (black bar) and to the mixture 20 μM other tested metal ions with 20 μM Pb^{2+} (red bar).

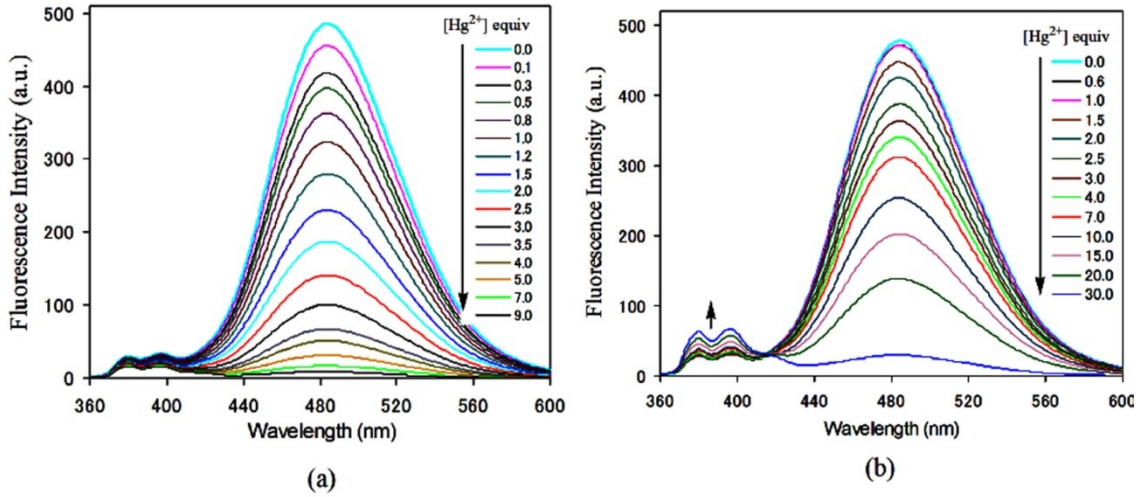

Figure 7. Fluorescence spectra of **2** (1.0 μM) upon addition of increasing concentration of Hg^{2+} in (a) CH_3CN/DMSO (1000:1, v/v) and (b) CH_3CN/H_2O/DMSO (1000:50:1, v/v) at 298K; λ_{ex} = 343 nm

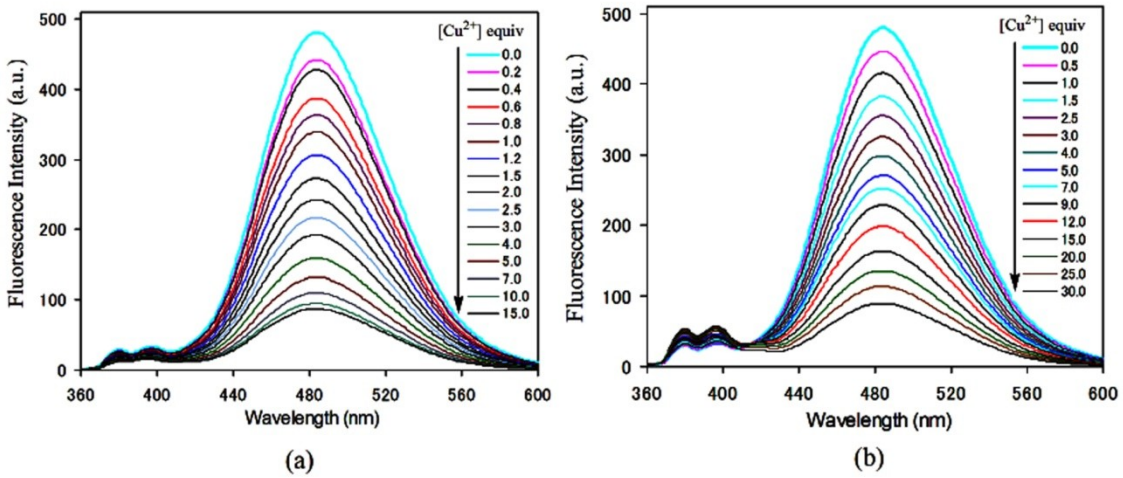

Figure 8. Fluorescence spectra of **2** (1.0 μM) upon addition of increasing concentration of Cu^{2+} in (a) CH_3CN/DMSO (1000:1, v/v) and (b) CH_3CN/H_2O/DMSO (1000:50:1, v/v) at 298K; λ_{ex} = 343 nm.

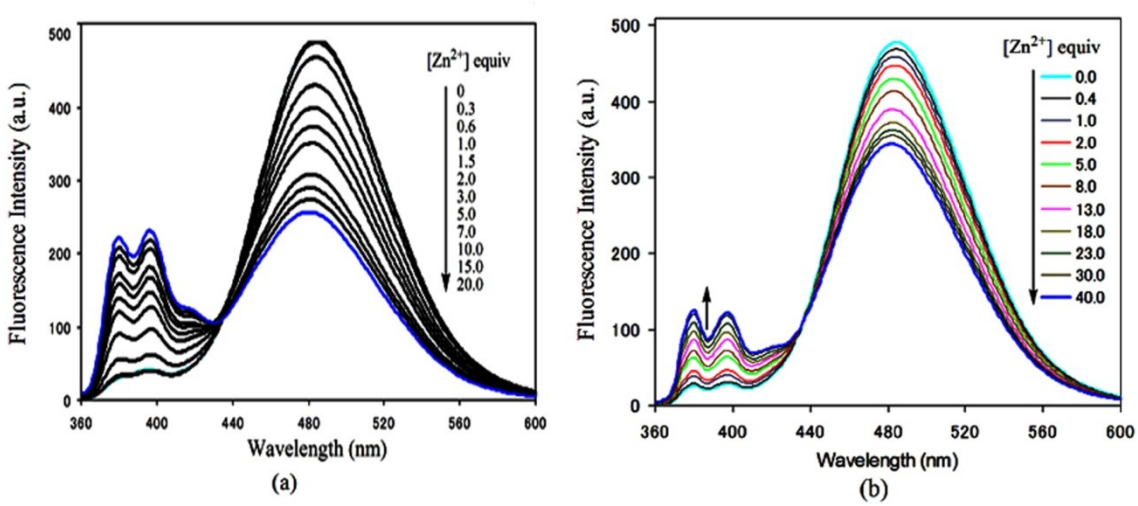

Figure 9. Fluorescence spectra of **2** (1.0 μM) upon addition of increasing concentration of Zn^{2+} (a) CH_3CN/DMSO (1000:1, v/v) and (b) in CH_3CN: H_2O: DMSO (1000:50:1, v/v) at 298K; λ_{ex} = 343 nm.

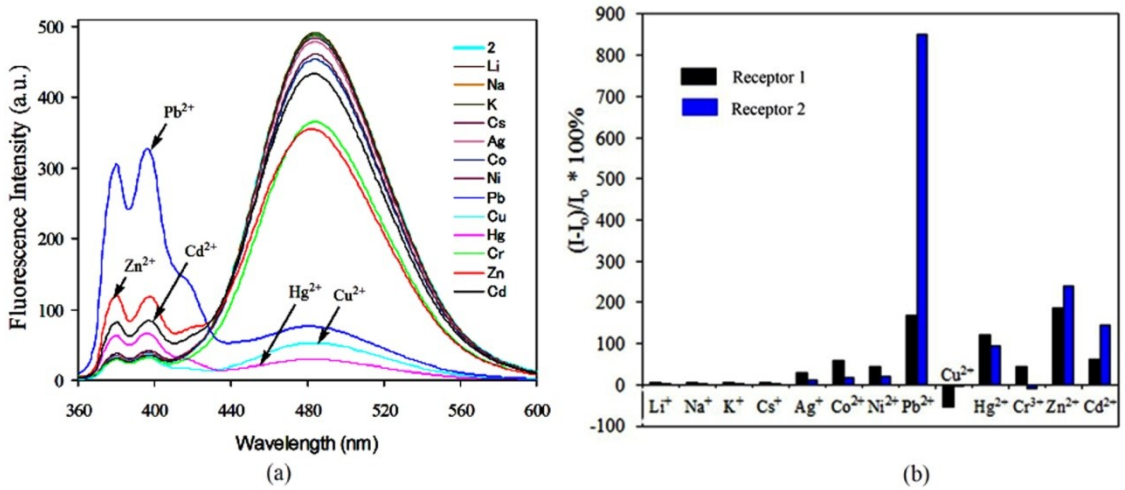

Figure 10. Fluorescence intensity changes receptor **2** (a) and (b) ((I-I_o)/I_o× 100) of receptors **1** and **2** (each of 1.0 μM) in CH_3CN/H_2O/DMSO (1000:50:1, v/v) at 298 K upon addition of various metal perchlorates (30 equiv). I_o is fluorescence emission intensity at 396 nm for free host **1** and **2**, and I is the fluorescent intensity after adding metal ions. λ_{ex} = 343 nm

solution (Figure 7b, and Figure 8b) indicates that these metal ions are not quenching the monomer emission of receptor **2**, and even have a slightly enhancement of monomer emission of both receptor **1** and **2** (Figure 10b). Moreover, at the same condition, as shown in

Figure 9, the selectivity output signal of the receptor **2** with Zn^{2+} have been extremly inhibited compared to in pure organic solvents. On the basis of these observations, the fluorescent behaviors of **1** and **2** toward metal ions were carried out in organic aqueous solution (CH_3CN/H_2O/DMSO, 1000:50:1, v/v).

Figure 10 shows the fluorescence intensity changes of the monomer emission for receptors **1** and **2** in the presence of various metal ions. As can be seen, among the metal ions tested, no significant spectral changes were observed upon addition of alkali metal ions; a much weaker response were given compared to Pb^{2+} at the same concentration for Ag^{+}, Co^{2+}, Ni^{2+}, Hg^{2+}, $Zn^{2+}$and Cd^{2+}, apart from Cu^{2+} where quenching was observed. The larger different fluorescence intensities caused by Pb^{2+} for receptors **1** and **2**, relative to their monomer ratios, suggest that receptor **2** has a much higher affinity and selectivity toward Pb^{2+} ion. This may be attributed to the greater flexibility of triazole moieties on receptor **2** enabling them to adopt the appropriate geometry for the binding of Pb^{2+} ion.

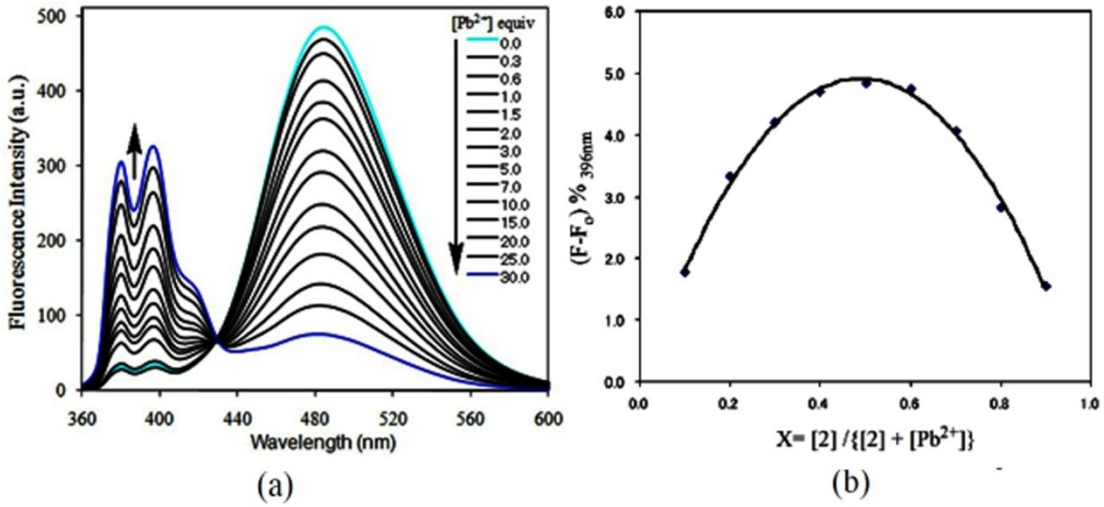

Figure 11. Fluorescence spectra of receptor **2** (1.0 μM) upon addition of increasing concentrations of $Pb(ClO_4)_2$ in CH_3CN/H_2O/DMSO (1000:50:1, v/v)(a) and (b) Job's plot of receptor **2** with Pb^{2+} at 298K . λ_{ex} = 343 nm.

The fluorescence sensing mechanisms of receptors **1** and **2** are attributed to pyrene moieties which form the fluorophore. These are appended to the calixarene scaffold by triazole groups to form a strong excimer. This results in a characteristic decrease of the excimer emission intensity and a concomitant increase of monomer emission intensity when

the triazole rings selectively bind to cations.[12c,15] Figure 11a shows the fluorescence spectra of receptor **2** by addition of increasing concentrations of Pb^{2+}.The fluorescence intensity of excimer emission of receptor **2** markedly decreased while the monomer emission intensity significantly increased and reached a plateau after adding about 30 equiv of Pb^{2+}. Meanwhile, a discernible isoemissive point was observed at 429 nm. The 1:1 complex of **2**•Pb^{2+} was confirmed by a Job plot[16] (Figure 11b). The association constant (K_a)[17] was determined to be 2.60×10^5 M^{-1} (error <10%). Similar fluorescence titration experiments were carried out for **1**•Pb^{2+}, **1**•Zn^{2+}, **1**•Hg^{2+}, **1**•Cu^{2+}, **2**•Hg^{2+}, **2**•Cu^{2+}, **2**•Cr^{3+} **2**•Zn^{2+} and **2**•Cd^{2+}, and related association constant were determined (Figure 12), respectively.

Table 1

Metal ions	Pb^{2+}	Cu^{2+}	Hg^{2+}	Zn^{2+}
K_a (M^{-1}) (organic)	1.92×10^5	1.2×10^5	2.22×10^5	8.5×10^4
K_a (M^{-1}) (organic & aqueous)	1.12×10^5	1.33×10^5	9.37×10^4	4.95×10^4

Table 2

Metal ions	Pb^{2+}	Cu^{2+}	Hg^{2+}	Cr^{3+}	Zn^{2+}	Cd^{2+}
K_a (M^{-1}) (organic)	7.64×10^5	6.65×10^5	5.86×10^5	3.85×10^4	9.51×10^4	3.79×10^4
K_a (M^{-1}) (organic & aqueous)	1.28×10^5	1.02×10^5	9.93×10^4	1.54×10^4	2.81×10^4	1.41×10^4

Figure 12. The associate constants (K_a) of receptors **1** (Table 1) and **2** (Table 2) with metal ions in organic solvent systems and their aqueous solutions.

To further investigate the selectivity for lead ions over other metal ions, interferences to the selective response of receptor **2** to Pb^{2+} by coexisting ions were evaluated (Figure 13), no significant interference in detection of Pb^{2+} were observed in the presence of other competitive cations. These results suggested that **2** can be used as a potential chemosensor for Pb^{2+} ion.

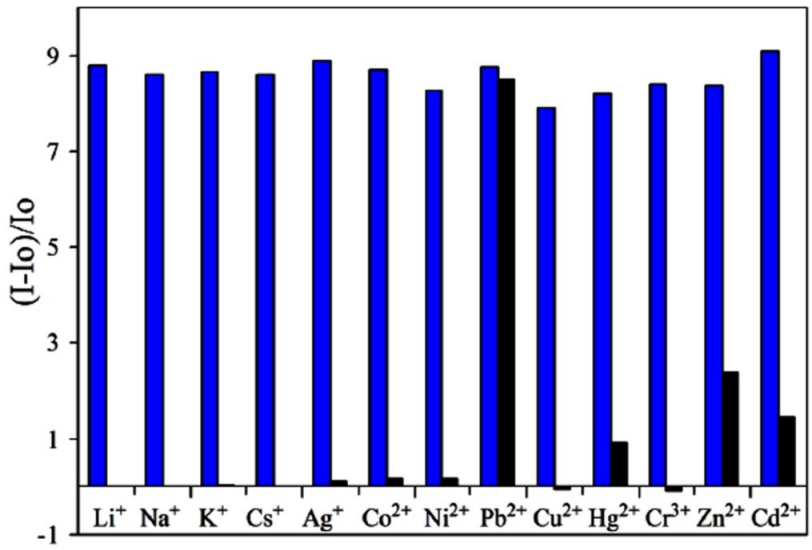

Figure 13. Fluorescence responses of **2** (1.0 μM) in CH_3CN: H_2O: DMSO (1000:50:1, v/v) to 30 μM various tested metal ions (black bar) and to the mixture 30 μM tested metal ions with 30 μM Pb^{2+} (blue bar). I_o is fluorescence emission intensity at 396 nm for free **2,** and I is the fluorescent intensity after adding metal ions.

To protect the fluorescence of an ionophore from being quenched by heavy atoms, several potential approaches are available:[18] i) insulating the fluorophore from the metal by a particular molecular spacer; ii) separating the metal from the fluorophore by placing the latter some distance from the metal binding site; and iii) isolating the metal from the fluorophore by introducing sufficient ionophore. It is believed that the fluorescence of ionophore with two triazole moieties incorporated onto a tailored calixarene scaffold can be strongly quenched by Pb^{2+}.[12] However, for receptors **1** and **2**, which depend on the C_3 symmetry of homooxacalix[3]arene, the three nitrogen-rich triazole ligands serve as an adequate electronic effects to isolate lead ion from pyrene moiety and maintain the fluorescence.

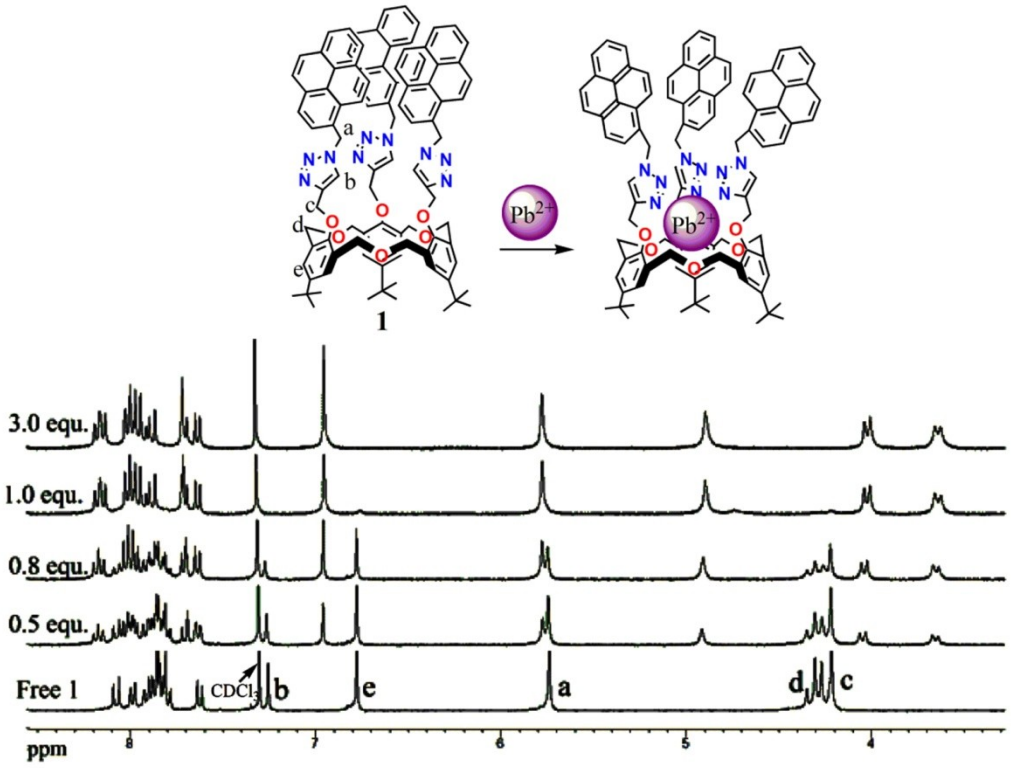

Figure 14. The plausible complexation of **1** for Pb^{2+} ion, and partial ^1H NMR (300 MHz) spectra of **1** (4.0 mM) in $CDCl_3/CD_3CN$ (v/v = 10:1) upon gradual addition of $Pb(ClO_4)_2$ at 298K.

To seek further more detailed information on the binding properties of receptors **1** and **2** with metal ions, ^1H NMR titration experiments were carried out in a mixture of $CDCl_3/CD_3CN$ (10:1, v/v). As shown in Figure 14, upon gradual addition of Pb^{2+} salt (0.5 equiv) to a solution of **1**, the resonances corresponding to the protons on receptor **1** were split into two sets of signals. Until in the presence 1 equiv of Pb^{2+}, the original proton signal disappeared (Figure 14). This result may be attributed to the complexed and uncomplexed of receptor **1** with Pb^{2+} is slower than the NMR time scale, therefore, free receptor **1** and complex **1**•Pb^{2+} are individually observed. Moreover, the significant ^1H NMR shifted signal for protons b, c, d and e indicated that Pb^{2+} ion is recognized by the nitrogen atoms of triazole ring and oxygen atoms in the macrocycle of receptor **1**.[8e] However, in the case of the titration experiments for complex **2**•Pb^{2+}, no significant chemical shift changes of the protons were observed, except for the triazole ring proton H_b and O*CH*$_2$-triazole linker H_c of receptor

2 (Figure 15). These observations suggested that only the nitrogen atoms in triazole moieties of receptor **2** participated to complex with Pb^{2+}.[19]

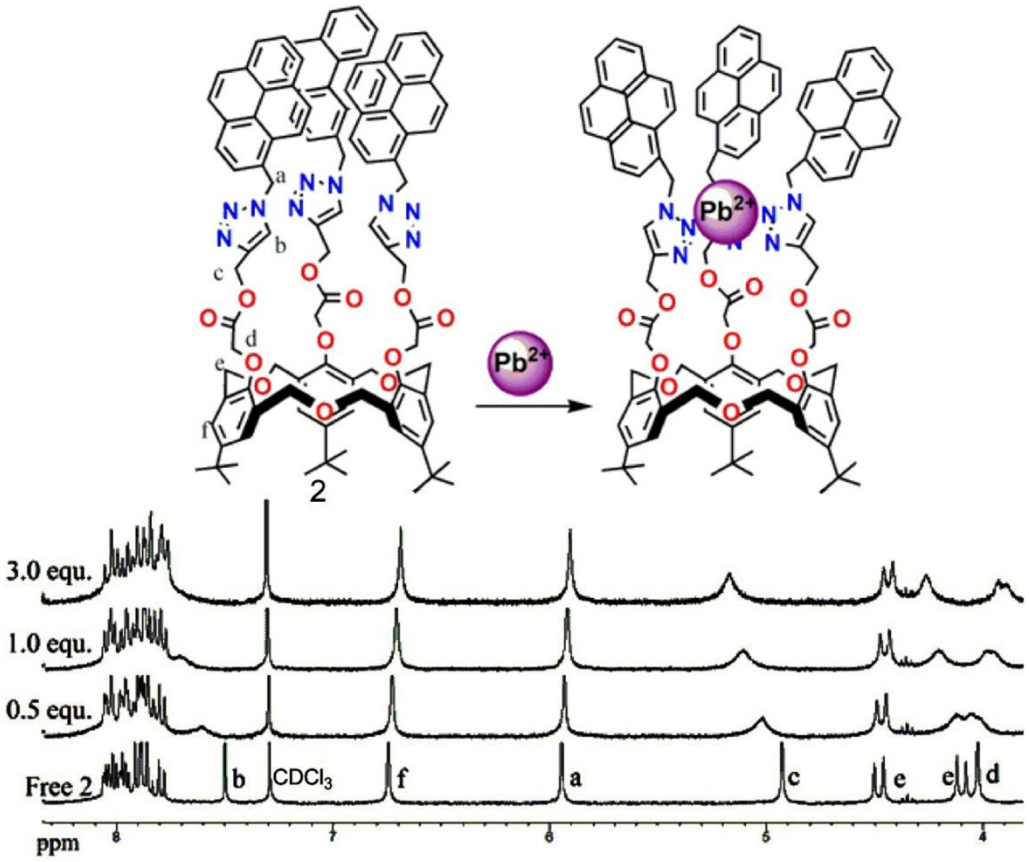

Figure 15. The plausible complexation of **2** for Pb^{2+} ion, and partial ^1H NMR (300 MHz) spectra of **2** (4.0 mM) in $CDCl_3/CD_3CN$ (v/v = 10:1) upon gradual addition of $Pb(ClO_4)_2$ at 298K.

4.3 Conclusions

In summary, we have prepared a new type of fluorescent chemosensor based on homooxacalix[3]arene that incorporates a sufficient ionophore to avoid fluorescence quenching by Pb^{2+}. It possesses a high affinity and selectivity for lead ions relative to most other competitive metal ions by enhancement of the monomer fluorescence emission of pyrene in organic aqueous solution. We expect that the present design strategy and the remarkable photophysical properties of this sensor will help to extend applications of fluorescent sensors for heavy metal ions.

4.4 Experimental Section

4.4.1 General methods: All reagents were purchased from Aldrich and were used without further purification. Melting points (Yanagimoto MP-S1) were uncorrected. Proton nuclear magnetic resonance (^{1}H NMR) spectra were recorded on a Nippon Denshi JEOL FT-300 spectrometer. Chemical shifts are reported as δ values (ppm) relative to internal Me_4Si. Mass spectra were obtained on a Nippon Denshi JMS-01SA-2 mass spectrometer at an ionization energy of 70 eV; *m/z* values reported include the parent ion peak. All the fluorescence spectra were recorded on JASCO FP-750 spectrometer. Elemental analyses were performed by Yanaco MT-5. Data of X-ray diffraction was collected on a Bruker Apex-2000 CCD diffractometer using graphite monochromated Mo Kα radiation (λ = 0.71073Å) with ω scan mode. Structural solution and full matrix least-squares refinement based on F^2 were performed with the SHELXS-97 and SHELXL-97 program package, respectively. All the non-hydrogen atoms were refined anisotropically. The hydrogen atoms were generated geometrically.

4.4.2 Materials

The preparations of compound **3**[1] and **5**[2] were obtained following the procedures reported in literature.

4.4.2.1. Preparation of compound 4: A solution of compound **3** (0.3 g, 0.52 mmol) and Cs_2CO_3 (1.69 g, 5.2 mmol) was refluxed for 1 h in dry acetone (15 ml). 3-bromo-1-propyne (propargyl bromide (0.62 g, 5.2 mmol) and dry acetone (10 ml) were added and the mixture refluxed for 18 h. The solvent was evaporated and the residue partitioned between 10% HCl and CH_2Cl_2. The organic layer was separated and dried ($MgSO_4$) and the solvents were evaporated. The residue was dried to afford **4** as a colorless oil (0.15 g, 42%) which was recrystallized from $CHCl_3$/hexane (1:3, v:v) to afford the desired product **4** as colourless prisms. Mp 106–108°C. ^{1}H NMR (300 MHz, $CDCl_3$) δ 1.29 (s, 18H, *t*Bu), 1.35 (s, 9H, *t*Bu), 1.98 (t, 1H, *J* = 2.4 Hz, acetylene-*H*), 2.41 (t, 2H, *J* = 2.4 Hz, acetylene-*H*), 2.87 (d, 2H, ArO-*CH*$_2$-acetylene), 4.32 (s, 4H, ArO-*CH*$_2$-acetylene), 4.1–5.0 (m, 12H, ether bridge), 7.27 (d, 2H, *J* = 2.4 Hz, Ar-*H*), 7.31 (s, 2H, *J* = 2.4 Hz, Ar*H*), 7.37 (s, 2H, Ar*H*). ^{13}C NMR (75 MHz, $CDCl_3$) δ 31.39, 31.46, 34.26, 34.39, 60.08, 61.74, 64.25, 66.50, 69.33, 73.82, 75.04,

79.47, 80.05, 126.57, 128.21, 128.45, 130.14, 130.71, 131.77, 146.81, 146.93, 151.99, 153.43. MS *m/z* 690 [M^+]. Anal. Calcd for $C_{45}H_{54}O_6$ (690.91): C, 78.23; H, 7.88; Found: C, 78.48; H, 7.65.

4.4.2.2. Preparation of compound 1: Copper iodide (10 mg) was added to compound **4** (120 mg, 0.17 mmol) and 1-azidomethylpyrene (143 mg, 0.56 mmol) in 20 mL mixture of THF/H_2O (v/v = 10:1) and the mixture was heated at 70 °C for 24 h. The resulting solution was cooled and extracted trice with $CHCl_3$. The organic layer was separated and dried ($MgSO_4$) and evaporated to give the solid crude product. The residue recrystallized from hexane/CH_2Cl_2 (3:1) to yield white solid (156 mg, 63%). Mp 139-141°C. ^{1}H NMR (300 MHz, $CDCl_3$) δ 0.97 (s, 27H, *t*Bu), 4.21 (s, 6H, ArO-*CH_2*- triazole). 4.29 (t, 12H, *J* = 9 Hz, ether bridge), 5.75 (s, 6H, triazole-*CH_2*-pyrene), 6.77 (s, 6H, Ar-*H*), 7.22 (s, 3H, triazole-*H*), 7.63 (d, 3H, *J* = 8.1, pyrene-*H*), 7.79-8.0 (m, 21H, pyrene-*H*), 8.08 (d, 3H, *J* = 9.3 Hz, pyrene-*H*). ^{13}C NMR (75 MHz, $CDCl_3$) δ 31.35, 34.09, 51.723, 66.78, 69.47, 121.91, 123.39, 124.14, 124.57, 124.67, 125.45, 125.52, 125.91, 126.01, 126.96, 127.27, 127.89, 128.60, 128.74, 130.24, 130.85, 130.90, 131.61, 146.18, 152.07. MS *m/z* 1462.68 [M^+]. Anal. Calcd for $C_{96}H_{87}N_9O_{12}$ (1462.77): C, 78.82; H, 5.99; N, 8.62; Found: C, 78.99; H, 6.14; N, 8.47.

4.4.2.3. Preparation of compound 6: To a 10 mL of CH_2Cl_2 were added compound **5** (300 mg, 0.4 mmol) and alcohol-propargyl (201.6 mg, 4.5 mmol). The mixture was stirred for 30 min at 0 °C (ice/water bath) under N_2. Then 1,3-dicyclohexylcarbodiimide (DCC) (741.6 mg, 4.5 mmol) and 4-(dimethylamino)-pyridine (DMAP) (90 mg, 0.75 mmol) were added, and the mixture was stirred for 30 min at 0 °C. The cooling bath was then removed and the solution was stirred at room temperature. After being stirred for 72 h, the reaction mixture was filtered to yield a clear filtrate and washed with water and brine. The organic layer was dried over $MgSO_4$, filtered, and evaporated, and the residue was washed with hexane and methanol to afford the white solid (232 mg, 67%). Mp 117-119°C. ^{1}H NMR (300 MHz, $CDCl_3$) δ 1.08 (s, 27H, *t*Bu), 2.53 (t, 3H, *J* = 3 Hz, acetylene-*H*), 4.50 (d, 6H, *J* = 12 Hz, ether bridge), 4.51 (s, 6H, ArO-*CH_2*-COO), 4.84(d, 6H, *J* = 2.5 Hz, COO-*CH_2*- acetylene), 4.89 (d, 6H, *J* = 12 Hz, ether bridge), 6.94 (s, 6H, Ar-*H*). ^{13}C NMR (75 MHz, $CDCl_3$) δ 31.43, 34.18, 52.41, 70.32, 70.57, 75.40, 126.68, 130.91, 146.50, 152.83, 168.93. MS *m/z*

865.41 [M^+]. Anal. Calcd for $C_{51}H_{60}O_{12}$ (865.01): C, 70.81; H, 6.99; Found: C, 70.74; H, 6.97.

4.4.2.4. Preparation of compound 2: Copper iodide (10 mg) was added to compound **6** (87.6 mg, 0.1mmol) and 1-azidomethylpyrene (87 mg, 0.32 mmol) in 20 mL mixture of THF/H_2O (v/v = 10:1) and the mixture was heated at 70 °C for 24 h. The resulting solution was cooled and extracted trice with $CHCl_3$. The organic layer was separated and dried ($MgSO_4$) and evaporated to give the crude product. The residue recrystallized from CH_2Cl_2 to yield a pale red solid (124 mg, 75.8%). Mp 128-129°C. ^{1}H NMR (300 MHz, $CDCl_3$) δ 1.01 (s, 27H, *t*Bu), 3.99 (s, 6H, ArO-*CH*$_2$-COO), 4.11(d, 6H, J = 12 Hz, ether bridge), 4.48 (d, 6H, J = 12 Hz, ether bridge), 4.91 (s, 6H, COO-*CH*$_2$-triazole), 5.92 (s, 6H, triazole-*CH*$_2$-pyrene), 6.74 (s, 6H, Ar-*H*), 7.46 (s, 3H, triazole-*H*), 7.78-8.21 (m, 27H, pyrene-*H*). ^{13}C NMR (75 MHz, $CDCl_3$) δ 31.37, 34.05, 52.08, 57.63, 70.06, 70.32, 121.74, 124.13, 124.76, 125.55, 125.67, 126.12, 126.54, 126.63, 126.98, 127.62, 128.06, 128.79, 128.96, 130.22, 130.72, 130.84, 131.85, 146.14, 152.77, 169.32. MS *m/z* 1636.56 [M^+]. Anal. Calcd for $C_{102}H_{93}N_9O_{12}$ (1636.88): C, 74.84; H, 5.73; N, 7.70; Found: C, 74.64; H, 5.66; N, 7.44.

Crystallographic Data for 4 and 6: Recrystallized from $CHCl_3$/Hexane (1:3). Crystal data: $C_{45}H_{54}O_6$; M = 690.88; crystal system: monoclinic; space group: P 21/n; a = 20.996(8) Å, b = 13.093(5) Å, c = 29.621(11) Å; α = 90.00°, β = 92.026(5)°, γ = 90.00°, V = 8138(5) Å^3; Z = 8; D_c = 1.128 g cm^{-3}; R_{int} = 0.0627, R [I > 2σ(I)]^a = 0.0808, wR [I > 2σ(I)]^b = 0.2234 for 5673 unique reflections. Compound **6**: Recrystallized from $CHCl_3$/Hexane (1:3). Crystal data: $C_{51}H_{60}O_{12}$; M = 864.99; crystal system: monoclinic; space group: P 21/c; a = 21.681(4) Å, b = 10.3225(17) Å, c = 21.136(4) Å; α = 90.00°, β = 94.411(5)°, γ = 90.00°, V = 4716.4(13) Å^3; Z = 4; D_c = 1.218 g cm^{-3}; R_{int} = 0.0630, R [I > 2σ(I)]^a = 0.0730, wR [I > 2σ(I)]^b = 0.1737 for 5740 unique reflections. Crystallographic data (excluding structure factors) for the structure reported in this paper have been deposited with the Cambridge Crystallographic Data Centre as supplementary publication No. CCDC–794146. CCDC–807566 Copies of the data can be obtained free of charge on application to CCDC, 12 Union Road, Cambridge CB2 1EZ, UK (fax: +44 1223/336 033; deposit@ccdc.cam.ac.uk).

4.5 References

1. Lin-Fu, J. S. Lead Poisoning, A Century of Discovery and Rediscovery. In *Human Lead Exposure*; Needleman, H. L., Ed.; Lewis Publishing: Boca Raton, FL, 1992.
2. (a) Deo, S.; Godwin, H. A. *J. Am. Chem. Soc*. **2000**, *122*, 174– 175. (b) Liu, J.; Lu, Y. *J. Am. Chem. Soc*. **2003**, *125*, 6642–6643. (c) Halouani, H.; Dumazet-Bonnamour, I.; Perrin, M.; Lamartine, R. *J. Org. Chem*. **2004**, *69*, 6521–6527. (d) Chen, P.; Greenberg, B.; Taghvi, S.; Romano, C.; van der Lelie, D.; He, C. *Angew. Chem., Int. Ed*. **2005**, *44*, 2715–2719. (e) Kwon, J. Y.; Jang, Y. J.; Lee, Y. J.; Kim, K. M.; Seo, M. S.; Nam, W.; Yoon, J. *J. Am. Chem. Soc*. **2005**, *124*, 10107–10111. (f) Kim, I.-K.; Dunkhorst, A.; Gilbert, J.; Bunz, U. H. F. *Macromolecules* **2005**, *38*, 4560–4562. (g) Zapata, F.; Caballero, A.; Espinosa, A.; Tárraga, A.; Molina, P. *Org. Lett*. **2008**, *10*, 41–44. (h) Ranyuk, E.; Douaihy, C. M.; Bessmertnykh, A.; Denat, F.; Averin, A.; Beletskaya, I.; Guilard, R. *Org. Lett*. **2009**, *11*, 987–990.
3. (a) Ji, H.-F.; Brown, G. M.; Dabestani, R. *Chem. Commun.* **1999**, 609–610. (b) Kim, J. S.; Noh, K. H.; Lee, S. H.; Kim, S. K.; Kim, S. K.; Yoon, J. *J. Org. Chem.* **2003**, *68*, 597–600. (c) Bu, J.-H.; Zheng, Q.-Y.; Chen, C.-F.; Huang, Z.-T. *Org. Lett*. **2004**, *6*, 3301–3303. (d) Kim, H. J.; Kim, J. S. *Tetrahedron Lett.* **2006**, *47*, 7051–7055. (e) Souchon, V.;. Leray, I.; Valeur, B. *Chem. Commun*. **2006**, 4224-4226. (f) Kim, J. S.; Quang, D. T. *Chem. Rev*. **2007**, 3780–3799.
4. (a) Metivier, R.; Leray, I.; Valeur, B. *Chem. Commun.* **2003**, 996 –997. (b) Metivier, R.; Leray, I.; Valeur, B. *Chem.–Eur. J.* **2004**, *10*, 4480–4490. (c) Kim, J. S.; Kim, H. J.; Kim, H. M.; Kim, S. H.; Lee, J. W.; Kim, S. K.; Cho, B. R. *J. Org. Chem*. **2006**, *71*, 8016–8022. (d) Kumar, M.; Babu, J. N.; Bhalla, V.; Kumar, R. *Sens. Actuat. B*. **2010**, *144*, 183–191.
5. McClure, D. S. *J. Chem. Phys.* **1952**, *20*, 682–686.
6. Varnes, A. W.; Dodson, R. B.; Whery, E. L. *J. Am. Chem. Soc.* **1972**, *94*, 946–950.
7. Rurack, K.; Resch-Genger U.; Rettig, W. *J. Photochem. Photobiol. A. Chem.* **1998**, *118*, 143–149.
8. (a) Yamato, T.; Haraguchi, M.; Nishikawa, J.; Ide, S.; Tsuzuki, H. *Can. J. Chem*. **1998**, *76*, 989–996. (b) Araki, K.; Hayashida, H. *Tetrahedron Lett*. **2000**, *41*, 1807–1810. (c) Yamato, T.; Zhang, F. L.; Tsuzuki, H.; Miura, Y. *Eur. J. Org. Chem*. **2001**, 1069–1075.

(d) Tsubaki, K.; Morimoto, T.; Otsubo, T.; Fuji, K. *Org. Lett*. **2002**, *4*, 2301–2304. (e) Marcos, P. M.; Ascenso, J. R.; Cragg, P. J. *Supramol. Chem*. **2007**, *19*, 199–206.

9. (a) Odashima, K.; Yagi, K.; Tohda, K.; Umezawa, Y. *Bioorg. Med. Chem. Lett.* **1999**, *9*, 2375–2378. (b) Ikeda, A.; Udzu, H.; Zhong, Z.; Shinkai, S.; Sakamoto, S.; Yamaguchi, K. *J. Am. Chem. Soc.* **2001**, *123*, 3872–3877. (c) Tsubaki, K.; Otsubo, T.; Morimoto, T.; Maruoka, H.; Furukawa, M.; Momose, Y.; Shang, M.; Fuji, K. *J. Org. Chem*. **2002**, *67*, 8151–8156.
10. (a) Tsubaki, K.; Tanaka, K.; Fuji, K.; Tanaka, K.; Kinoshita, T. *Chem. Commun.* **1998**, 895–896. (b) Atwood, J. L.; Barbour, L. J.; Nichols, P. J.; Raston, C. L.; Sandoval, C. A. *Chem.–Eur. J.* **1999**, *5*, 990–996. (c) Ikeda, A.; Hatano, T.; Shinkai, S.; Akiyama, T.; Yamada, S. *J. Am. Chem. Soc.* **2001**, *123*, 4855–4856.
11. (a) Angell, Y. L.; Burgess, K. *Chem. Soc. Rev.* **2007**, *36*, 1674–1689. (b) Moses, J. E.; Moorhouse, A. D. *Chem. Soc. Rev.* **2007**, *36*, 1249–1262.
12. (a) Chang, K.-C.; Su, I.-H.; Senthilvelan, A.; Chung, W.-S. *Org. Lett.* **2007**, *9*, 3363–3366. (b) Chang, K.-C.; Su, I.-H.; Lee, G.-H.; Chung, W.-S. *Tetrahedron Lett*. **2007**, *48*, 7274–7278. (c) Park, S. Y.; Yoon, J.; Hong, C. S.; Souane, R.; Kim, J. S.; Matthews, S. E.; Vicens, J. *J. Org. Chem.* **2008**, *73*, 8212–8218.
13. Hancock, R. D.; Martell, A. E. *Chem. Rev.* **1989**, *89*, 1875–1914.
14. (a) Araki, K.; Inada, K.; Otsuka, H., Shinkai, S. *Tetrahedron* **1993**, *49*, 9465–9478. (b) Araki, K.; Inada, K.; Shinkai, S. *Angew. Chem.*, *Int. Ed.* **1996**, *35*, 72–74.
15. Broan, C. J. *Chem. Commun.* **1996**, 699–700.
16. Job, P. *Ann. Chim.* **1928**, *9*, 113–203.
17. (a) Benesi, H. A.; Hildebrand, J. H. *J. Am. Chem. Soc*. **1949**, *71*, 2703–2707. (b) Connors, K. A. *Binding Constants*; Wiley: New York, 1987. (c) Stern, O; Volmer, M. *Phys. Z*. **1919**, *20*, 183–188.
18. (a) Leray, I.; Valeur, B. *Eur. J. Inorg. Chem*. **2009**, 3525–3535. (b) Xu, Z. C; Yoon, J.; Spring, D. R. *Chem. Commun.* **2010**, 2563–2565.
19. (a) Colasson, B.; Save, M.; Milko, P.; Roithová, J.; Schröder, D.; Reinaud, O. *Org. Lett.* **2007**, *9*, 4987–4990. (b) Marcos, P. M.; Ascenso, J. R.; Seguradu, M. A. P.; Bernardino, R. J; Cragg, P. J. *Tetrahedron* **2009**, *65*, 496–503.

Chapter 5

Ratiometric Fluorescent Receptors for Both Zn^{2+} and $H_2PO_4^-$ Ions Based on A Pyrenyl-Linked Triazole Modified Homooxacalix[3]arene: A Potential Molecular Traffic Signal with an R-S Latch Logic Circuit

*This chapter exhibited an interesting ratiometric detection signal output for targeting cations and anions through switching the excimer emission of pyrene from the "on-off" to the "off-on" type in neutral solution by using host receptor (**L**). ^1H NMR titration results suggested that the Zn^{2+} center of receptor **L**•Zn^{2+} provided an excellent pathway of organizing anion binding groups for optimal host–guest interactions. In addition, the fluorescence emission changes by the inputs of Zn^{2+} and $H_2PO_4^-$ ions can be envisioned as a combinational R-S latch logic circuit at the molecular level.*

5.1 Introduction

Ion recognition by artificial receptors has attracted increasing attention because of the important roles played by ions in both environment and biological systems.[1] For example, phosphate ions and their derivatives are not only noted for their important roles in signal transduction and energy storage in living systems,[2] but are also responsible for the eutrophication of waterways.[1] Accordingly, considerable effort has been paid to designing new chemosensors for the detection of phosphate ions and their derivatives over the last few decades,[3] including fluorescent chemosensors for the recognition of the dihydrogen phosphate anion.[4] However, due to fluorescence quenching, the dependence on organic solvents, or more specifically, the interference from other anions, there are still major challenges to be overcome in developing highly selective chemosensors for dihydrogen phosphate.

Generally, receptor interactions with anions are mainly based on the use of non-covalent interactions, such as Coulombic forces,[5] hydrogen bonding,[6] ion pair[7], π-stacking interactions,[8] or through coordinative interactions with metal ions included in the ligand.[9] The structural and geometrical flexibility of metal-ligand complexes can provide an excellent way of organizing anion binding groups for optimal host–guest interactions, even in the presence of a competitive aqueous solution.[10] Therefore, fluorescent sensors for anions based on metal-ligand complexes have appeared particularly attractive for supramolecular chemists due to their simplicity, high sensitivity, and high detection limits for trace chemicals detection.[11]

On the other hand, calixarenes are an important class of macrocyclic compounds and are ideal platforms for the development of cation, anion, and neutral molecule recognition.[12] For example, Reinaud and co-workers reported pioneering work on a Zn(II)-calix[6]arene complex as a favorable selective receptor for neutral coordinating guests through charge-dipole, hydrogen bonding, CH-π, and van der Waals interactions by combining a donor or acceptor site to the hydrophobic pocket.[13] Additionally, there has been intense interest recently in the design and synthesis of receptors and sensors based on 1,2,3-triazole derivatives.[14-17] For example, in calixarene chemistry, a copper catalyzed 1,2,3-triazole has been exploited by Zhao and co-workers to obtain water-soluble calix[4]arene derivatives.[14] More relevant to the work has been investigated by Chung and Kim *et al*. on the selective

binding of various metal cations by suitably functionalized with triazoles on calixarene scaffolds.[15-16] Moreover, amongst the different fluorogenic units, pyrene is one of the most useful tools due to its excimer-to-monomer emission (I_E/I_M) is very sensitive to conformation change,[18,19] Thus, utilizing the excimer *vs* monomer emission of the pyrene group as the ratiometric signal, a variety of "on-off" or "off-on" type of chemosensors have been successfully devised up to-date.[16,20,21]

More recently, Kumar and co-workers reported a series of interesting ratiometric fluorescent sensors for heavy metal ions based on calixarenes, which further can be exploited as logic gates at a molecular level.[22] Hence, given our work, these studies inspired us to use the complex **L** (Figure. 1) as a potential ion receptor and a logic circuit for molecular traffic signals based on binary logic. This can be accomplished through utilization of the unique fluorescent behavior of pyrenes based on the C_3-symmetric structure of the homooxacalix[3]arene. Against this background, we report here the fluorescent property of **L** and the selective fluorescent behavior toward targeting cations and anions by utilizing the ratiometric signal of the excimer/monomer emission (I_E/I_M) of the pyrene moiety from the "off" to the "on" .

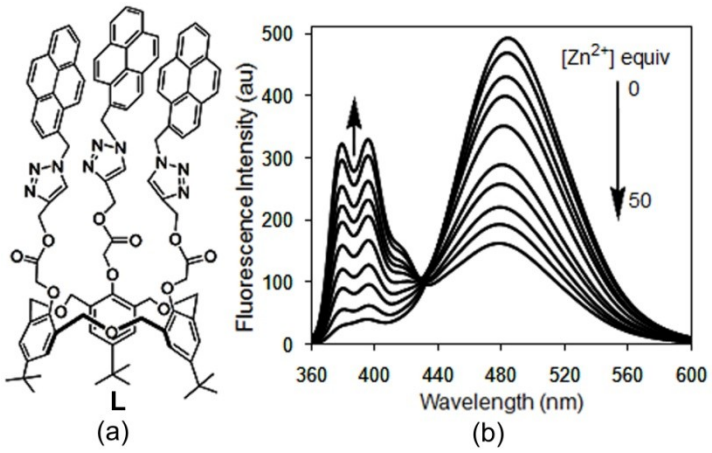

Figure 1. (a) Molecular structure of **L**. (b) Fluorescence spectra of **L** (1.0 μM) upon addition of increasing concentrations of $Zn(ClO_4)_2$ in CH_3CN/CH_2Cl_2 (1000:1, v/v) at 298K. λ_{ex} = 343 nm.

5.2 Results and Discussion

Host ligand (**L**) (Figure 1) was recently reported to have excellent affinity and was highly selective for the Pb^{2+} ion by enhancement of the monomer emission of pyrene in an organic/aqueous solution.[23] However, it should be noted that **L** also exhibits an impressive monomer signal output at larger equivalents of Zn^{2+} in pure organic solvents. The fluorescence spectra of **L** with increasing concentrations of Zn^{2+}, is depicted in Figure. 1b. It can be seen that both the monomer and excimer emissions of **L** appeared at the maximum emission wavelengths of 396 and 485 nm, respectively. The fluorescence intensity of the excimer emission of **L** gradually decreased ("on-off") and was accompanied by enhancement of the monomer emission as the concentration of Zn^{2+} increased in the CH_3CN/CH_2Cl_2 (1000:1, v/v). Meanwhile, a discernible isoemissive point was observed at 431 nm. A Job plot[23] for the binding between **L** and Zn^{2+} shows a 1:1 stoichiometry, and the association constant[23] of complex **L**•Zn^{2+} was determined to be 9.51 $\times 10^4$ M^{-1}. As mentioned in our previous work, the monomer emission of the complex **L**•Zn^{2+}could be strongly inhibited in an organic/aqueous solution. Therefore, in order to have more reasonable/optimal conditions for the recognition of peak selectivity for the targeting anions, the effects on the fluorescence

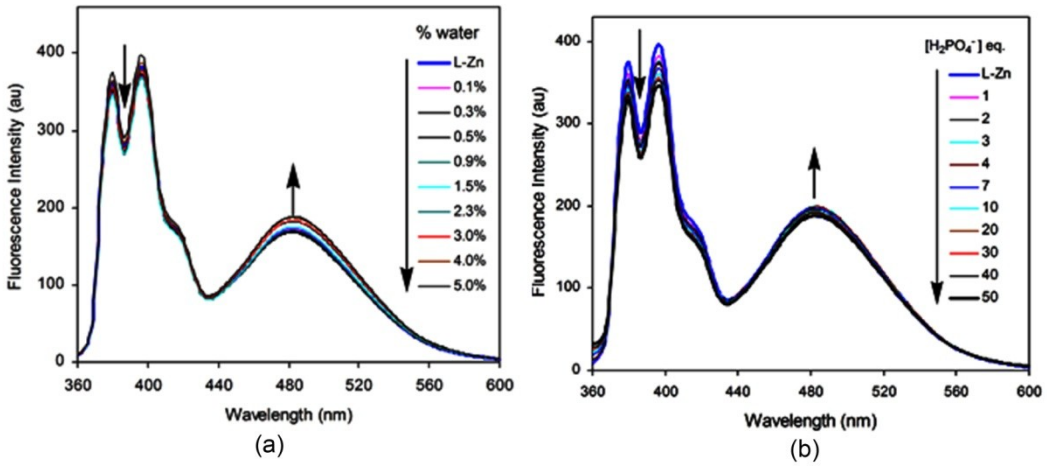

Figure 2. (a) Effects of different water content on the fluorescence of receptor **L**•Zn^{2+} (CH_3CN/CH_2Cl_2, 1000:1, v/v); (b) Fluorescence spectra of receptor **L**•Zn^{2+} in aqueous organic solution ($CH_3CN/CH_2Cl_2/H_2O$, 1000:1:50, v/v) upon addition of increasing concentrations of $TBAH_2PO_4$ in acetonitrile solution at 298 K. λ_{ex} = 343 nm.

of **L**•Zn^{2+} with various compositions of water were systematically evaluated (Figure 2). On the basis of these observations, the fluorescent behavior of **L**•Zn^{2+} toward anions was studied in the presence of small amounts of water, such as the environment of $CH_3CN/CH_2Cl_2/H_2O$ (1000:1:5, v/v).

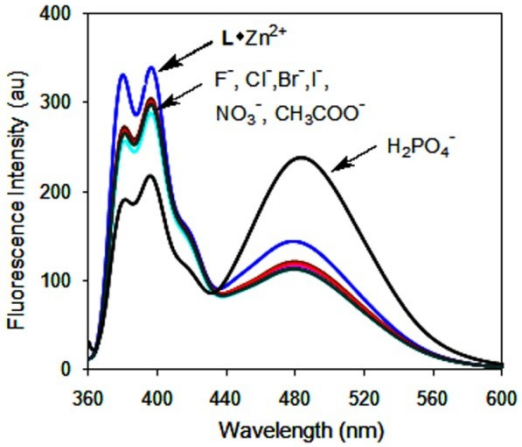

Figure 3. Fluorescence spectra of receptor **L**•Zn^{2+} in solution (CH_3CN/CH_2Cl_2, 1000:1, v/v) upon addition of various anions as their tetrabutylammonium salts in aqueous solution at 298 K. λ_{ex} = 343 nm.

The fluorescence intensity changes of the monomer and excimer emissions of **L**•Zn^{2+} ([**L**]/[Zn^{2+}] = 1:50, [**L**] = 1.0 μM) upon addition of various anions, *viz* F^-, Cl^-, Br^-, I^-, CH_3COO^-, NO_3^-, and $H_2PO_4^-$ (40 μM), determined as their tetrabutylammonium (TBA) salts in aqueous solution, are summarized in Figure 3. We found that upon excitation into the pyrene fluorophore at 343 nm, 67% enhancement of the excimer fluorescence intensity was observed upon addition of about 40 equiv of $H_2PO_4^-$ compared to that of only complex **L**•Zn^{2+}. Slight monomer and excimer emission quenching was observed upon interaction with the other tested anions (Figure 3). These results suggested that complex **L**•Zn^{2+} has a high selectivity for the $H_2PO_4^-$ anion by enhancement of the excimer emission of pyrene. The selectivity of **L**•Zn^{2+} for the $H_2PO_4^-$ over other anions can be attributed to the C_3 symmetric structure of **L**, and the strong electrostatic effects of Zn^{2+} to the phosphate unit.[3m, 10] In order to further evaluate the effect on the fluorescent selectivity for the $H_2PO_4^-$ anion in the absence and presence of Zn^{2+} cation, the fluorescence spectra of **L** upon addition of various

anions was carried out under the same conditions. The small fluorescence intensity changes of the monomer and excimer emissions indicated that the Zn^{2+}-center of receptor **L**•Zn^{2+} plays a key role in the selectivity for $H_2PO_4^-$ anion (Figure 4).

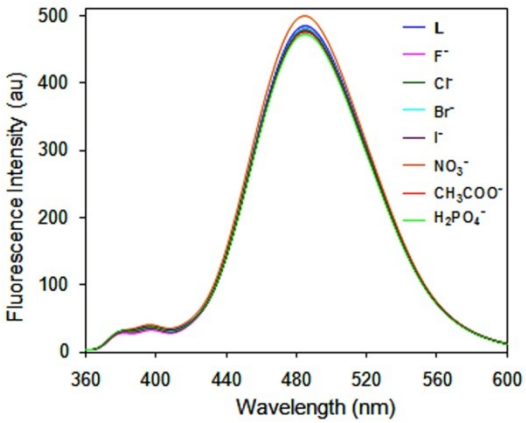

Figure 4. Fluorescence spectra of receptor **L** in solution (CH_3CN/CH_2Cl_2, 1000:1, v/v) upon addition of various anions as their tetrabutylammonium salts in aqueous solution at 298 K. λ_{ex} = 343 nm.

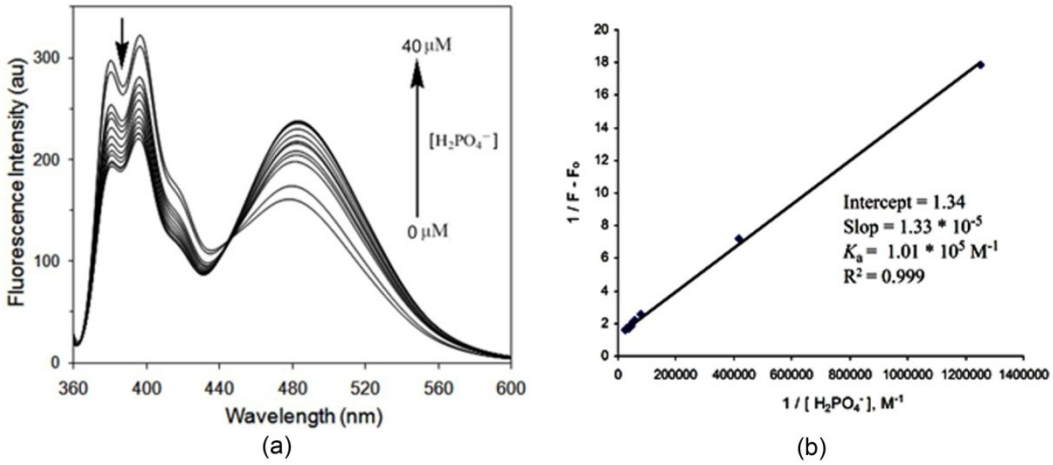

Figure 5. (a) Fluorescence spectra of receptor **L**•Zn^{2+} upon addition of increasing concentration of $TBAH_2PO_4$ in $CH_3CN/CH_2Cl_2/H_2O$ (1000:1:5, v/v); (b) Bensei-Hilderbrand plot of **L**•Zn^{2+} with varied concentrations $H_2PO_4^-$ at 298K. λ_{ex} = 343 nm.

Figure 5a illustrates the fluorescence titration experiments of receptor **L**•Zn^{2+} with the $H_2PO_4^-$ anion in neutral solution. No shift on the maximum of monomer and excimer

emissions of pyrene moiety were observed upon the addition of $H_2PO_4^-$ anion with excitation wavelength at 343 nm, However, when increasing concentrations of $H_2PO_4^-$ were added to the solution of **L**•Zn^{2+}, the fluorescence intensity of the monomer emission of pyrene gradually decreased and the accompanying excimer emission increased ("off-on"), and reached a plateau on adding about 40 equiv of $H_2PO_4^-$ anion. A discernible isoemissive point appeared at 447 nm. The association constant[24] of **L**•Zn^{2+} with $H_2PO_4^-$ was calculated to be 1.01×10^5 M^{-1} (Figure 5b). Interestingly, when addition of increasing concentrations of Zn^{2+} to the solution of **L**•$H_2PO_4^-$ (Figure 6a), which also have a similar selectivity signal output with the absence of $H_2PO_4^-$, and the association constant was determined to be 4.38×10^4 M^{-1} (Figure 6b). Thus, based on above observations, a multiple fluorescent chemosensor for Zn^{2+} ion and $H_2PO_4^-$ anion, which works by switching the ratiometric signal of I_{E485}/I_{M396} from the "off" (Figure 7a) to the "on" (Figure 7b) has been constructed and evaluated. The detection limit of the receptor was carried out using fluorescence intensity titration against various concentrations of Zn^{2+} ion and $H_2PO_4^-$ anion. Therefore, the detection limit reached 1.66×10^{-7} M for Zn^{2+} ion (Figure 8a) and 1.52×10^{-7} M for $H_2PO_4^-$ anion (Figure 8b), respectively.

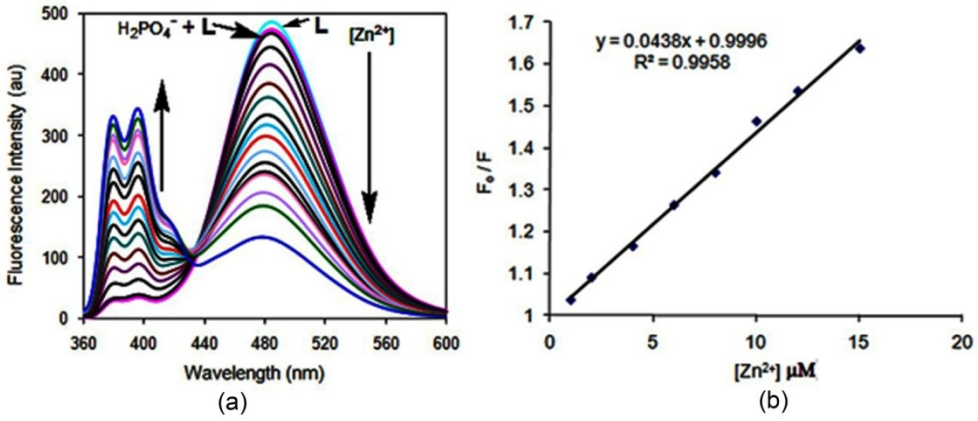

Figure 6. (a) Fluorescence spectra of **L**•$H_2PO_4^-$ ([**L**] = 1.0 μM, [$H_2PO_4^-$] = 40 μM) in CH_3CN/CH_2Cl_2 (1000:1, v/v) upon addition of increasing concentrations of Zn^{2+} (0-100 μM) in acetonitrile solution; (b) Stern–Volmer plot of **L**•$H_2PO_4^-$ with varied concentrations of Zn^{2+} at 298K.

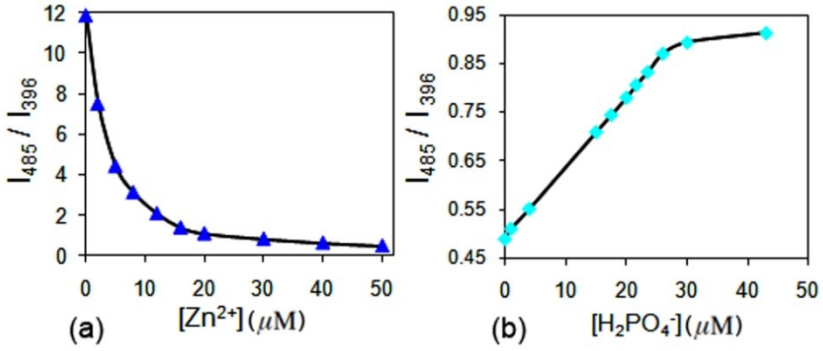

Figure 7. Ratiometric signal changes of I_{E485}/I_{M396}: (a) upon addition increasing concentrations of Zn^{2+} in **L** (1.0 μM) solution (CH_3CN/CH_2Cl_2, 1000:1, v/v); (b) upon addition increasing concentrations of $H_2PO_4^-$ in **L**•Zn^{2+} ([**L**]/[Zn^{2+}] = 1:50, [**L**] = 1.0 μM) solution ($CH_3CN/CH_2Cl_2/H_2O$, 1000:1:5, v/v) at 298K. λ_{ex} = 343 nm.

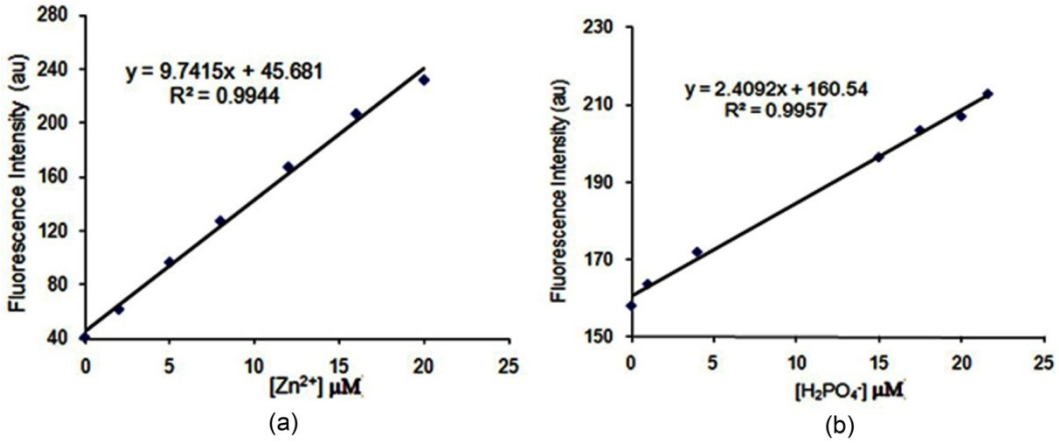

Figure 8. (a) Plot of fluorescence intensity change (396 nm) of **L** with varied concentrations of Zn^{2+}; (b) Plot of fluorescence intensity change (485 nm) of **L** with varied concentrations of $H_2PO_4^-$ at 298K. The limit of detection of Zn^{2+} and $H_2PO_4^-$ was calculated to be 1.66×10^{-7} M, 1.52×10^{-7} M , respectivity, by the formula (3σ/K).

To further evaluate the analytical application of the receptor **L**•Zn^{2+} as a probe for the $H_2PO_4^-$ anion, an estimation of the interference to the selective response of receptor **L**•Zn^{2+}

for $H_2PO_4^-$ was conducted in the presence of other anions (Figure 9). The fluorescence intensity was almost identical of that obtained in the absence of other anions, indicating that the receptor **L**•Zn^{2+} can be used as a selective chemosensor for the $H_2PO_4^-$ anion.

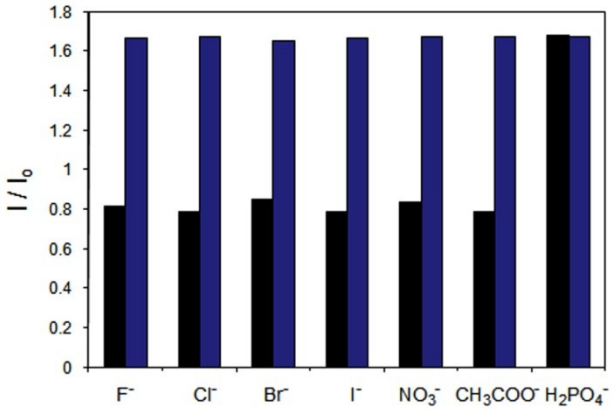

Figure 9. Fluorescence responses of receptor **L**•Zn^{2+} to 40 μM various tested anions (black bar) and to the mixture 40 μM tested anions with 40 μM $H_2PO_4^-$ (blue bar). I_o is fluorescence emission intensity at 485 nm for free receptor **L**•Zn^{2+}**,** and I is the fluorescent intensity after adding anions at 298 K. λ_{ex} = 343 nm.

In an effort to gain more detailed information on the interactions between **L**•Zn^{2+} and the $H_2PO_4^-$ anion, ^{1}H NMR spectroscopic studies were carried out in $CDCl_3/CD_3CN$ (10:1, v/v). The spectral differences are shown in Figure 10. In the presence of 1.0 equiv of Zn^{2+}, for example, the peak of the proton H_b on the triazole ring is shifted downfield by 0.05 ppm from δ 7.51 to 7.56 ppm, whereas the O*CH*$_2$-triazole linker proton H_c and the H_a proton proximal to the pyrene are shifted upfield by 0.17 ppm and 0.12 ppm, respectively. Compared to the complex **L**•Pb^{2+},[23] these spectral changes especially the smaller downfield chemical shift of triazole proton H_b suggest that the Zn^{2+} ion of the complex **L**•Zn^{2+} may be located in the negative cavity formed by the nitrogen-rich triazole ligand and the carbonyl group. These results are also fully in line with the fluorescence spectra changes (Figure 1b), which were observed for the complex **L**•Zn^{2+}. In particular, the coordination force of the Zn^{2+} ion would prevent the three pyrene moieties from maintaining π-π stacking for the excimer emission,

and instead leads to a concomitant increase of the monomer emission of the pyrene in the fluorescence spectra. However, as increasing concentrations of $TBAH_2PO_4$ were added to the solution of **L**•Zn^{2+}, it was noted that the peak for proton H_b undergoes a larger downfield

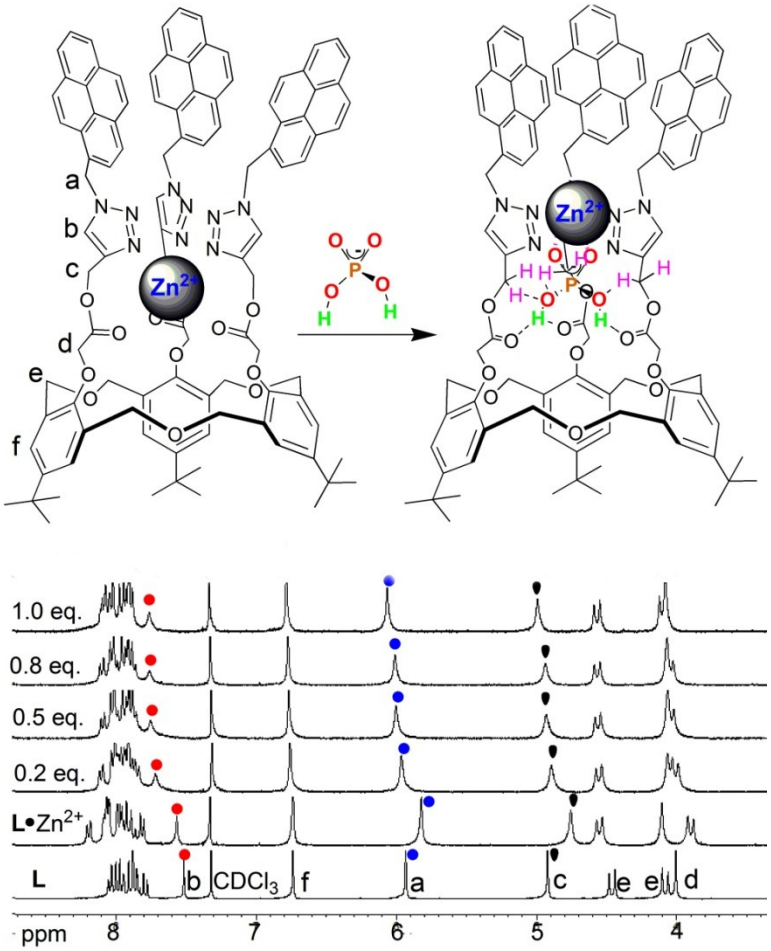

Figure 10. The proposed structure of **L**•Zn^{2+} for $H_2PO_4^-$ anion, and partial ^1H NMR spectra of **L** (5.0 mM), **L**•Zn^{2+} (1.0 eq.), and increasing concentrations of $H_2PO_4^-$ anion in $CDCl_3/CD_3CN$ (10:1, v/v) at 298 K.

shift compared to that for **L**•Zn^{2+} ($\Delta\delta$ = 0.16 ppm), suggesting that maybe only the nitrogen atoms of the three triazole groups of **L** are involved in binding with Zn^{2+} in the presence of $H_2PO_4^-$ anion.[25] The protons H_c exhibit a gradual downfield shift rather than an upfield shift ($\Delta\delta$ = 0.19 ppm), which can be attributed to hydrogen binding of H_c with the oxygen atoms of $H_2PO_4^-$ anion.[26] The downfield chemical shift of the proton H_a ($\Delta\delta$ = 0.18 ppm) is due to

its proximity to the pyrene excimer moiety. These results suggested that the receptor **L**•Zn^{2+} and the $H_2PO_4^-$ anion not only have strong coordination and electrostatic interactions, but also have strong hydrogen bonding interactions. As a result, the ratiometric signal of I_{E485}/I_{M396} of complex **L**•Zn^{2+} changes from the "off" to the "on" upon addition of increasing concentrations of $H_2PO_4^-$ ion, which can be characterized as decreasing the monomer emission with a concomitant increase of the excimer emission of the pyrene moiety. The 1:1 ratio of receptor **L**•Zn^{2+} with $H_2PO_4^-$ was confirmed by ^{1}H NMR titration curves (Figure 11).

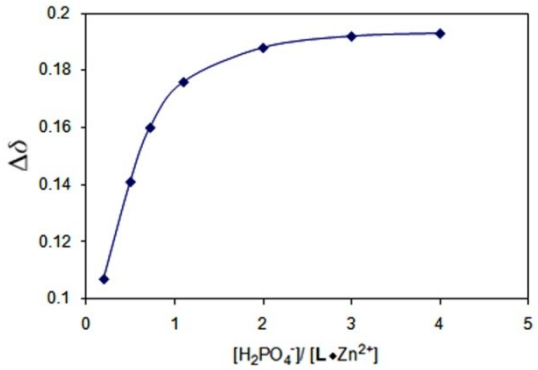

Figure 11. ^{1}H NMR titration curves showing 1:1 ration of $H_2PO_4^-$ with **L**•Zn^{2+} based on chemical shift changes in the O*CH*$_2$-triazole and *CH*$_2$–pyrene signals of receptor **L**•Zn^{2+}.

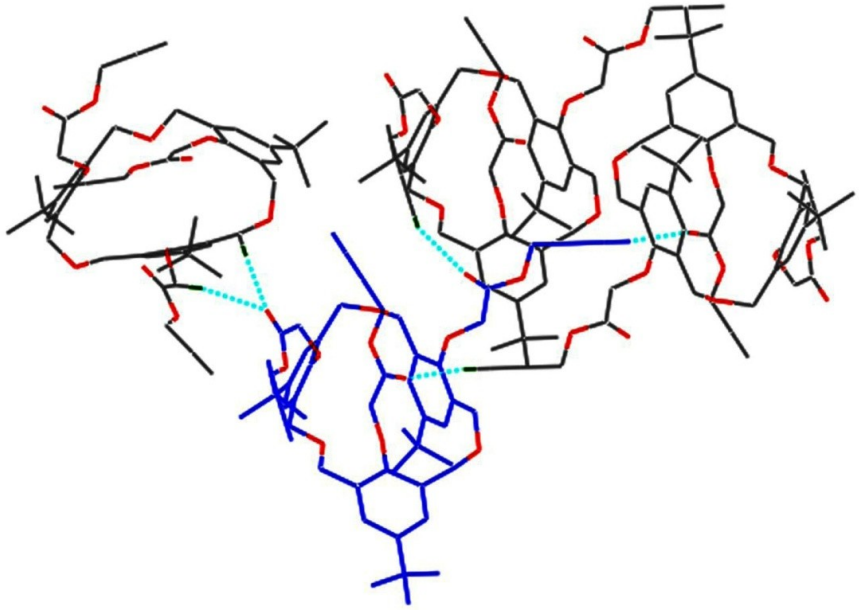

Figure 12. Intermolecular hydrogen binding between the protons and the carbonyl group in the X-ray structure of homooxacalix[3]arene-triacid-(O-propargyl).

Basically, in the design of anion receptors based on multiple hydrogen bonds, it is necessary to use complementary acceptor and donor patterns. In the host compound **L**, although some potential suitably hydrogen bonds acceptor (carbonyl) and donor (methylene proton H_c) were attached (Figure 12), the result of Figure 4 indicated that these anion binding sites do not selectively recognize anions efficiently in the absence of Zn^{2+} ion, and the ^1H NMR titration experimental results further suggested that the Zn^{2+}-center of receptor **L**•Zn^{2+} provides an excellent pathway of organizing anion binding groups for optimal host–guest interactions in the present system.

As mentioned previously, there is considerable current interest in the development of supramolecular system which can behave as molecular logic gates.[27-33] These systems convert the chemically encoded information as input and optical signals as output, such as absorptions, fluorescence and redox potential in response to a particular input, which results in the development of molecular level electronic and photonic devices for information processing and computation.[27] According to these observations, we can utilize the present system here to develop a simple but efficient logic circuit for a molecular traffic signal[33] with the help of binary logic based on an INHIBIT and OR gate by using Zn^{2+} and $H_2PO_4^-$ ions as the chemical inputs.

The two chemical inputs of Zn^{2+} and $H_2PO_4^-$ ions are designated as *Input* A and *Input* B, respectively, and considered as "1" when they are present and "0" if they are absent. Binary digits (*1* or *0*) can be used to represent the two states "On or Off" of each signal (Table 1). The output signals were measured as fluorescence emissions at 396 nm and 485 nm of the

Input A Zn^{2+}	*Input* B $H_2PO_4^-$	*Output* 1 396 nm	*Output* 2 485 nm
0	0	0	1
1	0	1	0
0	1	0	1
1	1	0	1

Table 1. Truth table for memory unit for two input signals *Input* A and *Input* B, where 1 and 0 indicate On and Off siganl; *Out* 1: monomer emission at 396 nm; *Out* 2: excimer emission at 485 nm.

receptor **L**, respectively, being "1" when fluorescence emission is high and "0" when fluorescence emission is low. The input and output strings of reversible "On-Off" switches with combination of Zn^{2+} and $H_2PO_4^-$ ions, are illustrated in truth table 1. The truth table values for output 1 at 396 nm give an INHIBIT logic gate, which is a combination of an AND gate with a NOT logic function at one of its inputs (Figure 13a). The truth table values for output 2 at 485 nm display different communication of input signals, the sequential logic circuit of excimer emission representing the Set/Reset element corresponds to the memory device (Figure 13a). The memory unit can be demonstrated in the feedback loop (Figure 13b) in which one of the device acts as input.

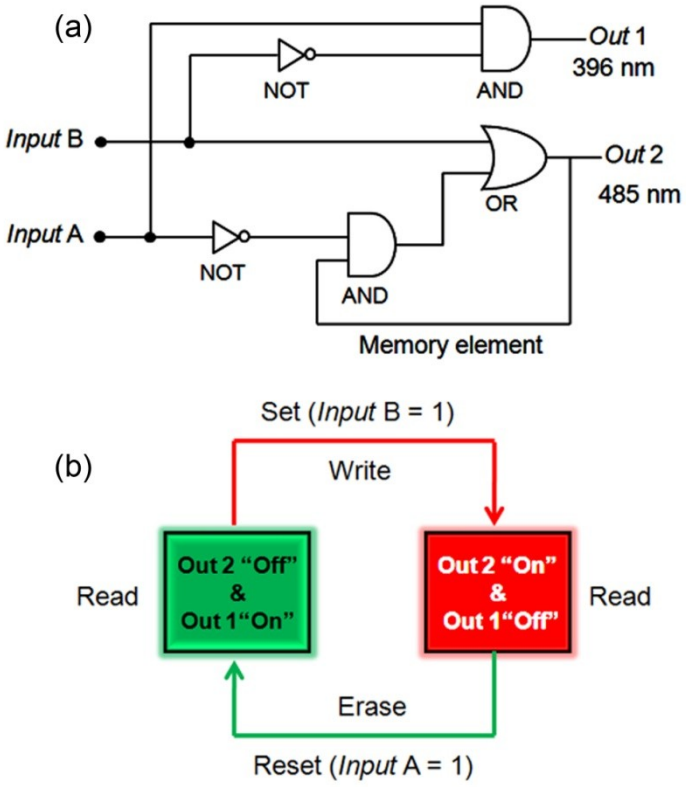

Figure 13. (a) Sequential logic circuit with the memory unit; (b) feedback loop with reversible logic operations for memory element with "Write-Read-Erase-Read" functions.

This behavior is extensively used in microprocessor for memory elements of integrated logic circuits. The sequential logic operations are presented by two inputs: Reset (*Input* A) and Set (*Input* B) (R-S Latch Logic circuit)[33,34] as a function of memory element. The

reversible and reconfigurable sequences of Set/Reset logic operations in a feedback loop demonstrate the memory feature of a "Write-Read-Erase" system with the output signals at the excimer and monomer emissions (Figure 13b). For the first input sequence, the addition of input A (Zn^{2+}) followed by input B ($H_2PO_4^-$) leads to increased fluorescence emission of the excimer at 485 nm (Figure 5a) and output 2 was "1" (On state), the stored information was "written" by the Set input. On reversal of the input sequence, the addition of input B ($H_2PO_4^-$) followed by input A (Zn^{2+}) gave a quenched fluorescence emission of the excimer at 485 nm (Figure 6a) and output 2 was "0" (Off state), and the stored information was "erased" by the Reset input.

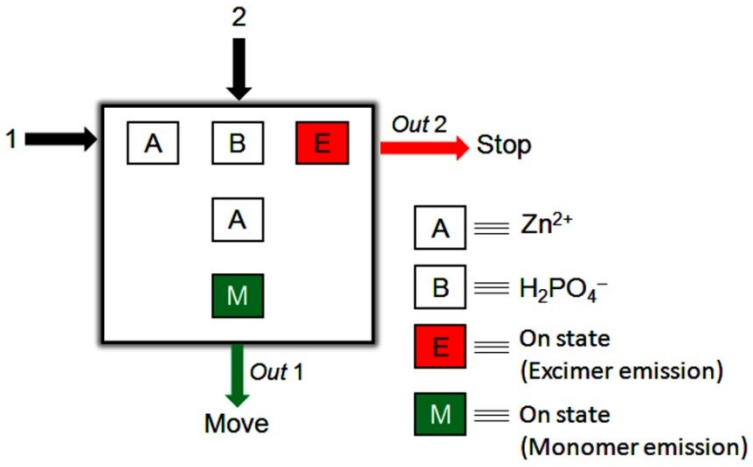

Figure 14. A sequence dependent traffic signal color based on R-S Latch Logic circuit.

With the above analysis, it should be noted that a simple but efficient logic circuit for molecular traffic signal could be constructed. For the first input sequence (Figure 14, 1), "A" followed by "B" give excimer emission "On" at 485 nm (*Out* 2, read), which can be designed as a red signal, and controls the traffic to stop. When the input sequence is reversed (Figure 14, 2), namely, the first input is "B" and then "A", fluorescence emission at 396 nm for monomer is "On" (*Out* 1, read). Thus, this sequence can be designed as a green signal to direct the traffic to move.

5.3 Conclusions

In summary, we have developed a new type of fluorescent sensor based on a pyrene-linked triazole-modified homooxacalix[3]arene with a C_3 symmetric structure, which displayed ratiometric selectivity for Zn^{2+} and $H_2PO_4^-$ ions in neutral solution. This system exhibited a novel detection signal output for targeting cations and anions through switching of the excimer emission of pyrene from the "on-off" to the "off-on" type. Thus, it is believed that this receptor will have a role to play in the sensing, detection, and recognition of Zn^{2+} and $H_2PO_4^-$ ions. In addition, a simple but efficient logic circuit for a molecular traffic signal in the help of binary logic based on an INHIBIT and OR gate by using Zn^{2+} and $H_2PO_4^-$ ions as chemical inputs has been constructed and evaluated. Further investigations of this strategy are currently ongoing.

5.4 Experimental Section

General. All melting points (Yanagimoto MP-S1) are uncorrected. NMR spectra were determined at 300 MHz with a Nippon Denshi JEOL FT-300 spectrometer using Me4Si as an internal reference: *J* values are given in Hertz. All the fluorescence spectra were recorded on a JASCO FP-750 spectrometer. Mass spectra were obtained on a Nippon Denshi JMS-01SG-2 mass spectrometer at ionization energy of 70 eV using a direct inlet system through GLC. Elemental analyses were performed by Yanaco MT-5.

Zn^{2+} titration of L solution determined by fluorescence. The fluorescent titration experiment of **L** was investigated by adding increasing concentrations of $Zn(ClO_4)_2$ (50 μL) (3 mM in CH_3CN solution) to 3 mL of **L** solution (1.0 μM in CH_3CN/CH_2Cl_2, 1000:1, v/v) in a cuvette. The spectra were recorded immediately after mixing. The excitation wavelength was 343 nm.

Selective fluorescent response of L•Zn^{2+} to various anions. The fluorescent response of **L**•Zn^{2+} to different anions was investigated by addition of 50 μL $Zn(ClO_4)_2$ (3.0 mM in CH_3CN) to 3 mL of **L** solution (1.0 μM in CH_3CN/CH_2Cl_2, 1000:1, v/v) in a cuvette over 1 h. The experiment was then further carried out by addition of 20 μL anion aqueous solution (6.0 mM) to the **L**•Zn^{2+} solution. The fluorescence spectra were recorded immediately after mixing. The excitation wavelength was 343 nm.

$H_2PO_4^-$ titration of L•Zn^{2+} solution determined by fluorescence spectra. The fluorescent response of **L**•Zn^{2+} was investigated by addition of 50 μL $Zn(ClO_4)_2$ (3.0 mM in CH_3CN solution) to 3 mL of **L** solution (1.0 μM in CH_3CN/CH_2Cl_2, 1000:1, v/v) in a cuvette over 1 h. Then the experiment was further carried out by addition of increasing concentrations of $TBAH_2PO_4$ (20 μL) aqueous solution (6.0 mM) to the **L**•Zn^{2+} solution. The fluorescence spectra were recorded immediately after mixing. The excitation wavelength was 343 nm.

Water titration of L•Zn^{2+} solution determined by fluorescence spectra. The fluorescent response of **L**•Zn^{2+} was investigated by addition of 50 μL $Zn(ClO_4)_2$ (3.0 mM in CH_3CN) to 3 mL of **L** solution (1.0 μM in CH_3CN/CH_2Cl_2, 1000:1, v/v) in a cuvette over 1 h. Then the experiment was further carried out by addition of increasing compositions of aqueous solution to the **L**•Zn^{2+} solution. The fluorescence spectra were recorded immediately after mixing. The excitation wavelength was 343 nm.

$H_2PO_4^-$ titration of L•Zn^{2+} in organic aqueous solution determined by fluorescence spectra. Based on the obtained solution of **L**•Zn^{2+} with 5% water composition in a cuvette. Further experiment was carried out by addition of increasing concentrations of $TBAH_2PO_4$ (25 μL) in acetonitrile solution (6.0 mM). The fluorescence spectra were recorded immediately after mixing. The excitation wavelength was 343 nm.

Selective fluorescent response of L to various anions. The fluorescent titration experiment of **L** (1.0 μM in CH_3CN/CH_2Cl_2, 1000:1, v/v) was investigated by addition of 20 μL anion aqueous solution (6.0 mM). The spectra were recorded immediately after mixing. The excitation wavelength was 343 nm.

^{1}H NMR titration experiments of L, L•Zn^{2+}, and L•Zn^{2+} with $H_2PO_4^-$. The ^{1}H NMR titration experiment was investigated by addition 10 μL of $Zn(ClO_4)_2$ (2.5×10^{-1} M) to the solution of **L** ($CDCl_3/CD_3CN$, 11:1, v/v) (5×10^{-3} M) in NMR tube (490 μL). Then further experiment was carried out by addition of increasing concentrations of $TBAH_2PO_4$ in acetonitrile solution (2.5×10^{-1} M). The spectra were recorded after mixing and the temperature of the NMR probe was kept constant at 298K.

5.5 References

1. (a) Schmidtchen, F. P.; Berger, M. *Chem. Rev.* **1997**, *97*, 1609–1646. (b) Beer, P. D.; Gale, P. A. *Angew. Chem., Int. Ed.* **2001**, *40*, 486–516. (c) Yoon, J.; Kim, S. K.; Singh, N. J.; Kim, K. S. *Chem. Soc. Rev.* **2006**, *35*, 355–360. (d) Steed, J. W. *Chem. Commun.* **2006**, 2637–2649. (e) Gale, P. A. *Chem. Commun.* **2011**, 82–86.
2. (a) Scenger, W. *Principles of Nucleic Acid Structure,* Springer, New York, 1998. (b) Lee, D. H.; Kim, S. Y.; Hong, J. *Angew. Chem., Int. Ed.* **2004**, *43*, 4777–4780. (c) Katayev, E. A.; Ustynyuk, Y. A.; Sessler, J. L. *Coord. Chem. Rev*. **2006**, *250*, 3004–3037.
3. (a) Lee, D. H.; Lee, H. Y.; Lee, K. H.; Hong, J. I. *Chem. Commun.* **2001**, 1188–1189. (b) Han, M. S.; Kim, D. H. *Angew. Chem., Int. Ed.* **2002**, *41*, 3809–3811. (c) Liao, J.-H.; Chen, C.-T.; Fang, J.-M. *Org. Lett.* **2002**, *4*, 561–564. (d) Ojida, A.; Mito-oka, Y.; Inoue, M.; Hamachi, I. *J. Am. Chem. Soc.* **2002**, *124*, 6256–6258. (e) Tobey, S. L.; Anslyn, E. V. *Org. Lett.* **2003**, *5*, 2029–2031. (f) Lee, D. H.; Im, J. H.; Son, S. U.; Chung, Y. K.; Hong, J.-I. *J. Am. Chem. Soc.* **2003**, *125*, 7752–7753. (g) Piatek, P.; Jurczak, J. *Chem. Commun.* **2002**, 2450–2451. (h) Quinlan, E.; Matthews, S. E.; Gunnlaugsson, T. *J. Org. Chem.* **2007**, *72*, 7497–7503. (i) Lin, Z.; Chen, H. C.; Sun, S.-S.; Hsu, C. P.; Chow, T. J. *Tetrahedron* **2009**, *65*, 5216–5221. (j) Chen, K.-H.; Liao, J.-H.; Chan, H.-Y.; Fang, J.-M. *J. Org. Chem.* **2009**, *74,* 895–898. (k) Yoo, J.; Kim, M.-S.; Hong, S.-J.; Sessler, J. L.; Lee, C.-H. *J. Org. Chem.* **2009**, *74,* 1065–1069. (l) Khatua, S.; Choi, S. H.; Lee, J.; Kim, K.; Do, Y.; Churchill, D. G. *Inorg. Chem.* **2009**, *48*, 2993–2999. (m) Kim, S. K.; Lee, D. H.; Hong, J. I.; Yoon, J. *Acc. Chem. Res*. **2009**, *42*, 23–31. (n) Zeng, Z.; Spiccia, L. *Chem.–Eur. J*. **2009**, *15*, 12941–12944.
4. (a) Gunnlaugsson, T.; Davis, A. P.; Glynn, M. *Chem. Commun.* **2001**, 2556–2557. (b) Yoon, J.; Kim, S. K.; Singh, N. J.; Lee, J. W.; Yang, Y. J.; Chellappan, K.; Kim, K. S. *J. Org. Chem.* **2004**, *69*, 581–583. (c) Zhou, L.-L.; Sun, H.; Li, H.-P.; Wan, H.; Zhang, X.-H.; Wu, S.-K.; Lee, S. T. *Org. Lett.* **2004**, *6*, 1071–1074. (d) Chen, Q.-Y.; Chen, C.-F. *Eur. J. Org. Chem.* **2005**, 2468–2472. (e) Guo, L.; Wang, Q.-L.; Jiang, Q.-Q.; Jiang, Q.-J.; Jiang, Y.-B. *J. Org. Chem.* **2007**, *72,* 9947–9953. (f) Caltagirone, C.; Gale, P. A.; Hiscock, J. R.; Brooks, S. J.; Hursthouse, M. B.; Light, M. E. *Chem. Commun.* **2008**, 3007–3009. (g) Huang, X.-H.; He, Y.-B.; Hu, C.-G.; Chen, Z.-H. *Eur. J. Org. Chem.* **2009**, 1549–1553. (h) Bejger, C.; Park, J. S.; Silver, E. S.; Sessler, J. L. *Chem. Commun.* **2010**, 7745–7747. (i) Alfonso, M.; Espinosa, A.; Tárraga, A.; Molina, P. *Org. Lett.* **2011**, *13*, 2078–2081.

5. (a) Vance, D. H.; Czarnik, A. W. *J. Am. Chem. Soc.* **1994**, *116*, 9397–9398. (b) Niikura, K.; Metzger, A.; Anslyn, E. V. *J. Am. Chem. Soc*. **1998**, *120*, 8533–8534. (c) Carcía-España, E.; Díaz, P. J.; Llinares, M.; Bianchi, A. *Coord. Chem. Rev*. **2006**, *250*, 2952–2986.
6. (a) Anzenbacher, P.; Jursikova, K.; Lynch, V. M.; Gale, P. A.; Sessler, J. L. *J. Am. Chem. Soc.* **1999**, *121*, 11020–11021. (b) Anzenbacher Jr, P.; Jursikova, K.; Sessler, J. L. *J. Am. Chem. Soc.* **2000**, *122*, 9350–9351. (c) Bowman-James, K. *Acc. Chem. Res*. **2005**, *38*, 671–678. (d) Lin, C.; Simov, V.; Drueckhammer, D. G. *J. Org. Chem.*, **2007**, *72*, 1742–1746.
7. Kim, S. K.; Sessler, J. L. *Chem. Soc. Rev.* **2010**, *39*, 3784–3809.
8. (a) Cho, H. K.; Lee, D. H.; Hong, J.-I. *Chem. Commun.* **2005**, 1690–1692. (b) Lee, H. N.; Xu, Z.; Kim, S. K.; Swamy, K. M. K.; Kim, Y.; Kim, S.-J.; Yoon, J. *J. Am. Chem. Soc.* **2007**, *129*, 3828–3829.
9. Steed, J. W. *Chem. Soc. Rev.* **2009**, *38*, 506–519.
10. O'Neil, E. J.; Smith, B. D. *Coord. Chem. Rev.* **2006**, 250, 3068–3080.
11. Czarnik, A. W. *Fluorescent Chemosensors for Ion and Molecule Recognition*, American Chemical Society, Washington, DC, 1993.
12. (a) Ikeda, A.; Shinkai, S. *Chem. Rev*. **1997**, *97*, 1713–1734. (b) Kim, J. S. Quan, D. T. *Chem. Rev.* **2007**, *107*, 3780–3799. (c) Darbost, U.; Rager, M.-N.; Petit, S.; Jabin, I.; Reinaud, O. *J. Am. Chem. Soc.* **2005**, *127*, 8517–8525. (d) Marcos, P. M.; Ascenso, J. R.; Seguradu, M. A. P.; Bernardino, R. J.; Cragg, P. J. *Tetrahedron* **2009**, *65*, 496–503. (e) Leray, I.; Valeur, B. *Eur. J. Inorg. Chem*. **2009**, 3525–3535.
13. Sénèque, O.; Rager, M.-N.; Giorgi, M.; Prangé, T.; Tomas, A.; Reinaud, O. *J. Am. Chem. Soc.* **2005**, *127*, 14833–14840.
14. Ryu, E.-H.; Zhao, Y. *Org. Lett.* **2005**, *7*, 1035–1037.
15. (a) Chang, K.-C.; Su, I.-H.; Lee, G.-H.; Chung, W.-S. *Tetrahedron Lett.* **2007**, *48*, 7274–7278. (b) Chang, K.-C.; Su, I.-H. Senthilvelan, A., Chung, W.-S. *Org. Lett.* **2007**, *9*, 3363–3366.
16. Park, S-Y.; Yoon, J-H.; Hong, C-S.; Souane, R.; Kim, J.-S. Matthews, S. E., Vicens, J. *J. Org. Chem.* **2008**, *73*, 8212–8218.
17. (a) Colasson, B.; Save, M.; Milko, P.; Roithová, J.; Schröder, D.; Reinaud, O. *Org. Lett*. **2007**, *9*, 4987–4990. (b) Morales-Sanfrutos, J.; Ortega-Muñoz, M.; Lopez-Jaramillo, J.; Hernandez-Mateo, F.; Santoyo-Gonzalez, F. *J. Org. Chem*. **2008**, *73*, 7768–7771. (c) Zhan,

J.; Tian, D.; Li, H. *New J. Chem.* **2009**, *33*, 725–728. (d) Pathak, R. K.; Ibrahim, S. M.; Rao, C. P. *Tetrahedron Lett*. **2009**, *50*, 2730–2734. (e) Kim, S. H.; Choi, H. S.; Kim, J.; Lee, S. J.; Quang, D. T.; Kim, J. S. *Org. Lett*. **2010**, *12*, 560–563. (f) Hsieh, Y.-C.; Chir, J.-L.; Wu, H.-H; Guo, C.-Q.; Wu, A.-T. *Tetrahedron Lett*. **2010**, *51*, 109–111.

18. Valeur, B.; Bourson, J.; Pouget, J.; Czarnik, A. W. *Fluorescent Chemosensors for Ion and Molecule Recognition*; ACS Symposium Series 538; American Chemical Society: Washington, DC, 1993.
19. (a) McClure, D. S. *J. Chem. Phys.* **1952**, *20*, 682–686. (b) Varnes, A. W.; Dodson, R. B.; Whery, E. L. *J. Am. Chem. Soc.* **1972**, *94*, 946–950.
20. (a) Moon, S. Y.; Youn, N. J.; Park, S. M.; Chang, S. K. *J. Org. Chem.* **2005**, *70*, 2394–2397. (b) Lee, S. H.; Kim, S. H.; Kim, S. K.; Jung, J. H.; Kim, J. S. *J. Org. Chem.* **2005**, *70*, 9288–9295. (c) Schazmann, B.; Alhashimy, N.; Diamond, D. *J. Am. Chem. Soc.* **2006**, *128*, 8607–8614. (d) Park, S. M.; Kim, M. H.; Choe, J. I.; No, K. T.; Chang, S. K. *J. Org. Chem.* **2007**, *72*, 3550–3553.
21. (a)Yang, J. S.; Lin, C. S.; Hwang, C. Y. *Org. Lett.* **2001**, *3*, 889–892. (b) Strauss, J. Daub, J. *Org. Lett*. **2002**, *4*, 683–686. (c) Martínez, R.; Espinosa, A.; Tárraga, A.; Molina, P. *Org. Lett.* **2005**, *7*, 5869–5872. (d) Cho, H. K.; Lee, D. H.; Hong, J.-I. *Chem. Commun*. **2005**, 1690–1692. (e) Ma, L.-J.; Liu, Y.-F.; Wu, Y. *Chem. Commun*. **2006**, 2702–2704. (f) Kim, H. J.; Hong, J.; Hong, A.; Ham, S.; Lee, J. H.; Kim, J. S. *Org. Lett*. **2008**, *10*, 1963–1966. (g) Romero, T.; Caballero, A.; Tárraga, A.; Molina, P. *Org. Lett*. **2009**, *11*, 3466–3469. (h) Jung, H. S.; Park, M.; Han, D. Y.; Kim, E.; Lee, C.; Ham, S.; Kim, J. S. *Org. Lett*. **2009**, *11*, 3378–3381. (i) Hung, H.-C.; Cheng, C.-W.; Ho, I.-T.; Chung, W. S. *Tetrahedron. Lett.* **2009**, *50*, 302–305. (j) Hung, H. C.; Cheng, C. W.; Wang, Y. Y.; Chen, Y. J.; Chung, W. S. *Eur. J. Org. Chem.* **2009**, 6360–6366. (k) Zhou, Y.; Zhu, C.-Y.; Gao, X.-S.; You, X.-Y.; Yao, C. *Org. Lett*. **2010**, *12*, 2566–2569.
22. Dhir, A.; Bhalla, V.; Kumar, M. *Org. Lett.* **2008**, *10*, 4891–4894. (b) Dhir, A.; Bhalla, V.; Kumar, M. *Tetrahedron Lett.* **2008**, *49*, 4227–4230. (c) Kumar, M.; Kumar, R.; Bhalla, V. *Org. Lett.* **2011**, *13*, 366–369.
23. Ni, X.-L.; Wang, S.; Zeng, X.; Tao, Z.; Yamato, T. *Org. Lett*. **2011**, *13*, 552–555.
24. Benesi, H. A.; Hildebrand, J. H. *J. Am. Chem. Soc.* **1949**, *71*, 2703–2707.

25. (a) Colasson, B.; Save, M.; Milko, P.; Roithová, J.; Schröder, D.; Reinaud, O. *Org. Lett*. **2007**, *9*, 4987–4990. (b) Huang, S.; Clark, R. J.; Zhu, L. *Org. Lett*. **2007**, *9*, 4999–5002.
26. (a) Kim, S. K.; Singh, N. J.; Kim, S. J.; Kim, H. G.; Kim, J. K.; Lee, J. W.; Kim, K. S.; Yoon, J. *Org. Lett.* **2003**, *5*, 2083–2086. (b) Kumar, A.; Pandey, P. S. *Org. Lett.* **2008**, *10*, 165–168.
27. (a) Balzini, V.; Venturi, M.; Credi, A. Ed. *Molecular Devices and Machines. A Journey into the Nano world*; Wiley-VCH: Wienheim, 2003. (b) de Silva, A. P.; McClenaghan, N. D. *Chem. –Eur. J.* **2004**, *10*, 574–586. (c) Szacilowski, K. *Chem. Rev.* **2008**, *108*, 3481–3548. (d) Ozlem, S.; Akkaya, E. U. *J. Am. Chem. Soc.* **2009**, *131*, 48–49.
28. Lee, J. W.; Park, S. Y.; Cho, B.-K.; Kim, J. S. *Tetrahedron Lett.* **2007**, *48*, 2541–2546. (b) Joseph, R.; Ramanujam, B.; Acharya, A.; Rao, C. P. *J. Org. Chem.* **2009**, *74*, 8181–8190. (c) Chang, K.-C.; Su, I.-H.;. Wang, Y.-Y; Chung, W.-S. *Eur. J. Org. Chem.* **2010***,* 4700–4704.
29. (a) Zhou, W. D.; Li, J. B.; He, X. R.; Li, C. H.; Lv, J.; Li, Y. L.; Wang, S.; Liu, H. B.; Zhu, D. B. *Chem.–Eur. J*. **2008**, *14*, 754–763. (b) Katz, E.; Willner, I. *Angew. Chem., Int. Ed*. **2005**, *44*, 4791–4794.
30. (a) Raymo, F. M.; Alvarado, R. J.; Giordani, S.; Cejas, M. A. *J. Am. Chem. Soc*. **2003**, *125*, 2361–2364. (b) Baron, R.; Onopriyenko, A.; Katz, E.; Lioubashevski, O.; Willner, I.; Wang, S.; Tian, H. *Chem. Commun.* **2006**, 2147–2149.
31. (a) Andreasson, J.; Straight, S. D.; Bandyopadhyay, S.; Mitchell, R. H.; Moore, T. A.; Moore, A. L.; Gust, D. *J. Phys. Chem. C* **2007**, *111*, 14274–14278. (b) Perez-Inestrosa, E.; Montenegro, J. M.; Collado, D.; Suau, R. *Chem. Commun*. **2008**, 1085–1087.
32. (a) Margulies, D.; Felder, C. E.; Melman, G.; Shanzer, A. *J. Am. Chem. Soc*. **2007**, *129*, 347–354. (b) Kumar, M.; Dhir, A.; Bhalla, V. *Org. Lett*. **2009**, *12*, 2567–2570.
33. Kumar, M.; Dhir, A.; Bhalla, V. *Chem. Commun*. **2010**, 6744–6746.
34. Ruiter, G.; Tartavosky, E.; Oded, N.; Van der Boom, M. E. *Angew. Chem., Int. Ed.*, **2010**, *49*, 169–172.
35. Mastsumoto, H.; Nishio, S.; Takeshita, M.; Shinkai, S. *Tetrahedron*. **1995**, *51*, 4647–4654. (b) Yamato, T.; Zhang, F. L.; Tsuzuki, H.; Miura, Y. *Eur. J. Org. Chem*. **2001**, 1069–1075.

Summary

Calixarenes are an important class of macrocyclic compounds and are ideal platforms for the development of cation, anion, and neutral molecule recognition. For example, a series of work on metal ligand-calixarene complex as a favorable selective receptor for neutral coordinating guests through charge-dipole, hydrogen bonding, CH-π, and van der Waals interactions by combining a donor or acceptor site to the hydrophobic pocket.

On the other hand, Cations and anions recognition by artificial receptors has attracted increasing attention because of the important roles played by ions in both environment and biological systems. Among of metal ions, Heavy metal ions are of great attention, not only due to the fact that some heavy metal ions play important roles in living systems, but also for they are very toxic and hence capable of causing serious environmental and health problems. Therefore, the development of increasingly selective and sensitive methods for the determination of heavy metal ions is currently receiving considerable attention. Many approaches such as atomic absorption, ICP atomic emission, UV-vis absorption, and fluorescence spectroscopy have been employed to detect low limits. Among these methods, fluorescence spectroscopy is widely used because of its high sensitivity, facile operation, and low cost. Furthermore, the photophysical properties of a fluorophore can be easily tuned using a range of routes: charge transfer, electron transfer, energy transfer, the influence of the heavy metal ions, and the destabilization of nonemissive n-π^* excited states.

Fluorescent chemosensors for anions and cations have proven popular, but those for many heavy metal ions such as Pb(II), Hg(II), Fe(III), Cu(II), and Ag(I) present challenges because these cations often act as fluorescence quenchers due to reverse PET or heavy atom effect. Such as Cu(II) is a typical ion that causes the chemosensor to decrease fluorescent emissions due to quenching of the fluorescence by mechanisms inherent to the paramagnetic species. Such decreased emissions are impractical for analytical purposes because of their low signal outputs upon complexation.

Thus, against this background, several kinds of fluorescent chemosensors for heavy metal ions and anions were designed and synthesized based on calixarene in this dissertation. The sensitivity and selectivity properties of these receptors to the target analyte were carefully evaluated.

In chapter 1, a shortly review of the recently development of fluorescent receptors for cations and anions based on calixarene. While many prospects of fluorescent receptors for ions by utilizing the unique topology of calixarenes, which enabling them to encapsulate many different gust, have been demonstrated. Such as fluorescent recognition for cations: Cu^{2+}, Pb^{2+}, Hg^{2+}, Zn^{2+} and anions: F^{-}, Cl^{-}, $H_2PO_4^{-}$ and so on. However, it should be noted that there are relativity few example of receptors for ions with ratiometric enhancement of fluorescence. Because fluorescence quenching is not only disadvantageous for a high signal output during detection but is also undesirable for analytical purposes.

With this in mind, in chapter 2, 1,3-*alternate*-1,2,3-triazole based on thiacalix-[4]arene, 1,3-*alternate*-**1** and **2** have been synthesized, due to click chemistry has attracted considerable attention recently and has been applied in a wide range of fields for its efficiency, regioselectivity, compatibility with reaction conditions and especially for its ions binding ability. 1,3-*alternate*-**1** have been first determined by means of X-ray analysis, which suggested that the nitrogen atom N3 on triazole ring can act as hydrogen bond acceptors in the self-assembly of a supramolecular structure. The fluorescence spectra changes of 1,3-*alternate*-**2** indicated that the thiacalix[4]arene bearing 1,2,3-triazole groups was highly selective for Ag^{+} in comparison with other tested metal ions by enhancement of the monomer emission of pyrene. The ^{1}H NMR results indicated that Ag^{+} can be selectively recognized by the triazole moieties on the receptors **1** and **2** together with the ionophoricity cavity formed by the two inverted benzene rings and sulfur atoms of the thiacalix[4]arene.

Following the same interest, in chapter 3, thiacalix-[4]arene based 1,3-*alternate*-**3** and mono triazole attached reference compound **4** have been further obtained. The fluorescence spectra changes suggested that chemosensors **3** was highly selective for Ag^{+} over other metal ions by enhancing the monomer emission of pyrene in neutral solution same as receptor **2**. Other heavy metal ions, such as Cu^{2+}, and Hg^{2+} quench both the monomer and excimer emission of pyrene acutely. However, the fluorescent intensity of compound **4** was not obviously changed upon addition of Ag^{+} ion and other metal ions, except in the cases of Hg^{2+}, and Cu^{2+} ions, where acute quenching was observed. These results indicated that the fluorescent sensitive and selective binding of Ag^{+} ion requires the coordination of two triazole rings.

In chapter 4, A new type of fluorescent chemosensor based on pyrene-linked triazole-

modified homooxacalix[3]arene **1** and **2** were developed. The fluorescent sensor **2** was highly selective for Pb^{2+} in comparison with other metal ions tested by enhancement of the monomer emission of pyrene by utilizing the C_3 symmetric structure of homooxacalix[3]arene. This provided sufficient ionophore to avoid fluorescence quenching by Pb^{2+}. The ^1H NMR results suggested that Pb^{2+} ion is recognized by the nitrogen atoms of triazole ring and oxygen atoms in the macrocycle of receptor **1**, However, in the case of complex **2**•Pb^{2+}, no significant chemical shift changes of the protons were observed, except for the triazole ring proton, these observations indicated that only the nitrogen atoms in triazole moieties of receptor **2** participated to complex with Pb^{2+}.

In chapter 5, following the experimental results of chapter 4, with the unique structure of fluorescent receptor **2**, we utilized complex **2**•Zn^{2+} as a receptor for recognition of $H_2PO_4^-$. This system exhibited an interesting ratiometric detection signal output for $H_2PO_4^-$ through switching the excimer emission of pyrene from the "on-off" to the "off-on" type in neutral solution. Fluorescence spectra and ^1H NMR titration results suggested that the Zn^{2+} center of receptor **2**•Zn^{2+} provided an excellent pathway of organizing anion binding groups for optimal host–guest interactions. It is thus believed that this receptor has potential application in sensing, detection, and recognition of both Zn^{2+} and $H_2PO_4^-$ ions with different optical signals. Furthermore, the fluorescence emission changes by the inputs of Zn^{2+} and $H_2PO_4^-$ ions can be envisioned as a combinational R-S latch logic circuit at the molecular level.

In summary, several kinds of fluorescent chemosensors for heavy metal ions and anions were designed and synthesized based on the unique topology of thiacalix[4]arene and homooxacalix[3]arene. Both novel structures provided sufficient ionophore to avoid fluorescence quenching by heavy metal ions. We expect that the present design strategy and the remarkable photophysical properties of these chemosensors will help to extend applications of fluorescent sensors based on calixarenes for heavy metal ions and anions.

Publications

1. Synthesis and heteronuclear inclusion properties of a novel thiacalix[4]arene-based hard-soft receptor with 1,3-*alternate* conformation
   X.-L. Ni, H. Tomiyasu, T. Shimizu, C. Pérez-Casas, X. Zeng and T. Yamato
   J. Incl. Phenom. Macrocyclic Chem. **2010**, *68*, 99–108.

2. Heteroditopic receptors tris(2-pyridylamide) derivatives derived from hexahomo trioxacalix[3]arene triacetic acid
   M. Takimoto, **X.-L. Ni**, S. Rahman, X. Zeng and T. Yamato
   J. Incl. Phenom. Macrocyclic Chem. **2011**, *70*, 69–80.

3. Pyrene-linked triazole-modified homooxacalix[3]arene: a unique C_3 symmetry ratiometric fluorescent chemosensor for Pb^{2+}
   X.-L. Ni, S. Wang, X. Zeng and T. Yamato
   Org. Lett. **2011**, *13*, 552–555.

4. Synthesis and evaluation of a novel pyrenyl-appended triazole-based thiacalix[4]arene as fluorescent sensor for Ag^{+} ion.
   X.-L. Ni, X. Zeng, C. Redshaw and T. Yamato
   Tetrahedron **2011***, 67*, 3248–3253.

5. Ratiometric fluorescent receptors for both Zn^{2+} and $H_2PO_4^{-}$ ions based on a pyrenyl-linked triazole modified homooxacalix[3]arene: a potential molecular traffic signal with an R-S latch logic circuit
   X.-L. Ni, X. Zeng, C. Redshaw and T. Yamato
   J. Org. Chem. **2011**, *76*, 5696–5702.

6. Synthesis, structure and inclusion properties of *cone*-tris{[(5′-methyl-2,2′-bipyridyl)-5-yl]oxycarbonylmethoxy}hexahomotrioxacalix[3]arene
   X.-L. Ni, M. Takimoto, X. Zeng and T. Yamato
   J. Inclusion Phenom. Macrocyclic Chem. in press.

7. Synthesis, crystal structure and complexation behaviour of a thiacalix[4]arene bearing 1,2,3-triazole groups
   X.-L. Ni, X. Zeng, C. Redshaw and T. Yamato
   Supra. Chem. in press.

8. Novel ion-pair receptors based on hexahomotrioxacalix[3]arene derivatives
   X.-L. Ni, X. Zeng, D. L. Hughes, C. Redshaw and T. Yamato
   Org. Biomol. Chem. in press.